

**324**

# **SAG-TENSION CALCULATION METHODS FOR OVERHEAD LINES**

**Task Force  
B2.12.3**

**June 2007**



# Sag-Tension Calculation Methods for Overhead Lines

## Task Force B2.12.3

Convenor of WG B2.12:	D. Douglass (United States)
Secretary of WG B2.12:	M. Gaudry (France)
Task Force 3 Leader	D. Douglass (United States)
Task Force 3 Secretary	S. Hoffmann (United Kingdom)

H. Argasinska (Poland), K. Bakic (Slovenia), Anand Goel (Canada), S. Hodgkinson (Australia), S. Hoffmann (United Kingdom), J. Iglesias Diaz (Spain), F. Jakl (Slovenia), D. Lee (Korea), T. Kikuta (Japan), Ryuzo Kimata (Japan), F. Massaro (Italy), A. Maxwell (Sweden), G. Mirosevic (Croatia), D. Muftic (South Africa), Y. Ojala (Finland), R. Puffer (Germany), J. Reding (United States), B. Risse (Belgium), T.O.Seppa (United States), R. Stephen (South Africa), S. Ueda (Brazil), L. Varga (Hungary)

Former Members of WG B2.12 who contributed to this brochure:  
Y. Motlis (Canada, deceased), V. Morgan (Australia)

Other members of Study Committee B2 who participated in the writing, editing, and reviewing of this document are:

WG B2.11 – C. B. Rawlins (United States), D. Havard (Canada), K. Papailiou (Switzerland)  
WG B2.6 – J. Rogier (Belgium)

Designated Study Committee B2 Reviewers  
G. Brennan (Australia), J. Peralta (Portugal)

Study Committee B2 Members  
P. Riisio (Finland), E. Ghannoum (Canada), C. Hardy (Canada), P. Meyere (Canada)

Members of IEEE Subcommittee 15.11 Towers, Poles, and Conductors who contributed:  
Neal Schmidt (US), Rea Berryman (US), Steve Barrett (Canada), Alain Peyrot (US)

**Copyright © 2007**

*“Ownership of a CIGRE publication, whether in paper form or on electronic support only infers right of use for personal purposes. Are prohibited, except if explicitly agreed by CIGRE, total or partial reproduction of the publication for use other than personal and transfer to a third party; hence circulation on any intranet or other company network is forbidden”.*

**Disclaimer notice**

*“CIGRE gives no warranty or assurance about the contents of this publication, nor does it accept any responsibility, as to the accuracy or exhaustiveness of the information. All implied warranties and conditions are excluded to the maximum extent permitted by law”.*

**N° ISBN : 978-2-85873-010-0**

Table of Contents

List of Figures ..... iii

List of Tables ..... v

EXECUTIVE SUMMARY ..... i

    Introduction ..... i

    The Catenary Equation ..... ii

    Mechanical Coupling of Spans ..... iii

    Conductor Tension Limits ..... iv

    Conductor Elongation – Elastic, Plastic, and Thermal ..... iv

    Sag-tension Calculation Methods ..... v

    Parameter Sensitivity ..... v

    Conclusions ..... vi

ABSTRACT ..... 1

KEY WORDS ..... 1

DEFINITIONS ..... 2

TERMS ..... 5

1.0 INTRODUCTION ..... 7

    1.1 Conductor Naming Convention ..... 7

    1.2 The Catenary Clearance Envelope ..... 7

2.0 THE CATENARY ..... 10

    2.1 Catenary and parabolic solutions for sag in level spans ..... 10

    2.2 Total Conductor Length ..... 12

    2.3 Conductor Slack ..... 12

    2.4 Total and Horizontal Tension ..... 14

    2.5 Engineering accuracy of sag calculations ..... 16

    2.6 Effect of change in conductor loading per unit length ..... 17

    2.7 Inclined spans ..... 18

3.0 MODELING MECHANICALLY COUPLED SPANS ..... 21

    3.1 Mechanical Equilibrium at Suspension Points ..... 22

    3.2 Ruling Span Sag-tension Calculations ..... 26

4.0 CONDUCTOR TENSION LIMITS ..... 28

    4.1 Conductor tension limits under high ice and wind loading ..... 28

    4.2 Avoiding Aeolian Vibration Fatigue ..... 29

5.0 CONDUCTOR ELONGATION - ELASTIC, PLASTIC, AND THERMAL ..... 31

    5.1 Overview of Conductor Elongation Models ..... 31

    5.2 Linear Thermal and Elastic Elongation ..... 34

        5.2.1 Linear Elastic Strain - All Aluminium Conductors ..... 34

        5.2.2 Linear Thermal Strain – All Aluminium Conductor ..... 36

        5.2.3 Linear Elastic Strain - Non-Homogeneous ACSR (A1/Syz) Conductors ..... 37

        5.2.4 Linear Thermal Strain - Non-Homogeneous A1/S1x Conductor ..... 38

    5.3 Simplified Plastic Elongation (SPE) Model ..... 39

    5.4 Experimentally Measured “Plastic” Elongation of Stranded Conductors ..... 43

        5.4.1 Stress-strain testing of stranded conductors ..... 43

        5.4.2 Plastic elongation under initial high loading ..... 47

        5.4.3 Long-time “Metallurgical” Creep - Plastic Elongation for Persistent Moderate Loading ..... 49

5.4.4	Long-time Creep Plastic Elongation with non-homogeneous stranded conductors .....	53
5.4.5	Summing Plastic Elongation.....	53
6.0	SAG-TENSION CALCULATION METHODS .....	54
6.1	Sag-tension for A1 Conductor with LE (Linear Elongation) Model .....	56
6.2	Sag-tension for A1/S1A Conductor at high temperature with Simplified Plastic Elongation (SPE) Model.....	58
6.3	Sag-tension Calculation with Experimental Plastic Elongation (EPE) Model .....	61
6.3.1	Maximum conductor tension with the EPE model .....	61
6.3.2	Final sag-tension accounting for aluminum creep with the EPE model...	63
6.3.3	Calculating Final sag-tension at high temperature with EPE model .....	65
7.0	CONDUCTOR PARAMETER STUDIES .....	68
7.1	Conductor Weight.....	68
7.2	Elastic Elongation.....	69
7.3	Plastic Elongation .....	70
7.4	Thermal elongation .....	71
7.5	Errors at elevated temperature .....	73
7.6	Thermal elongation at low temperature. ....	74
8.0	References.....	75

## List of Figures

Figure 1 - Catenary variation with conductor temperature, ice & wind loads, and time after installation where $T_{max}$ is the maximum conductor temperature. ....	i
Figure 2 – Conductor Stress (H/A) and Sag (D) vs. %Slack ( $100*(L-S)/S$ ) where $L$ =conductor length and $S$ =Span length based on the catenary equations.....	iii
Figure 3 - Conductor elongation diagram.....	iv
Figure 4 - Influence of variation in the coefficient of thermal elongation on high temperature sag.....	vi
Figure 5 – Catenary variation with conductor temperature, ice & wind loads, and time after installation where $T_{max}$ is the maximum conductor temperature. ....	8
Figure 6 - The Catenary Curve for Level Spans.....	10
Figure 7 – Catenary Stress (H/A) and Sag (D) vs. %Slack ( $100*(L-S)/S$ ) for Bare Drake ACSR in a 300 m span at a tension of 20% RTS (69.5 MPa) at 15C.....	14
Figure 8 - Comparison of catenary $y(x)$ and difference between exact and parabolic approximate solution as a function of $x$ for ACSR Drake at a tension of 28020 N..	16
Figure 9 - Heavy radial ice buildup on a relatively small bare overhead conductor. ....	18
Figure 10 - Sag-tension for inclined spans. ....	19
Figure 11 - Typical strain angle structure used to terminate a transmission line section.	21
Figure 12 - Typical suspension structure.....	22
Figure 13 - Conductor Tension Variation with Temperature for 250m and 350m "Dead end" Spans of Drake A1/S1A (ACSR) installed to 35 kN at 15°C.....	23
Figure 14 - Moment Forces acting on a ceramic, glass, or composite Insulator Suspension String.....	24
Figure 15 – Unbalanced horizontal tension vs. horizontal deflection for a 1.8m long Insulator String weighing 890N supporting a 300m weight-span of Drake ACSR..	25
Figure 16 - Elongation diagram of stranded conductor in a catenary.....	33
Figure 17 - Assumed linear stress-strain behavior of a 402-A1-37 Arbutus conductor with and without plastic elongation. ....	36
Figure 18 – “Knee-point temperature” as affected by creep elongation of aluminium strands.....	42
Figure 19 – Typical stress-strain test results with 1-hour initial curve drawn and both initial and final modulus shown.....	44
Figure 20- Stress-strain curve for 37 strand A1 conductor.....	45
Figure 21 - Raw data from a stress-strain test of A1/Syz conductor.....	46
Figure 22 - Raw data for a stress-strain test performed on the steel core alone for the A1/Syz conductor whose composite test results are shown in Figure 21.....	46
Figure 23 - Initial plastic strain as a function of tension.....	48
Figure 24 - Creep elongation curves resulting from a series of tests at different tension levels, all at room temperature.....	50
Figure 25 - Creep elongation curves for A3 stranded conductor.....	51
Figure 26 - Graphical determination of creep elongation for a 37 strand all aluminium stranded conductor at a constant tension equal to 20% of the RTS over 10 years. ...	52
Figure 27 - Sag-tension calculation for A1 conductor with High wind loading.....	58
Figure 28 - Sag-tension at High Temperature with SPE model for Drake ACSR in 300 m span.....	60

Figure 29 - Sag-tension calculations of maximum, loaded conductor tension illustrating the effect of plastic elongation ..... 62

Figure 30 – Application of Experimental Plastic Elongation method in calculating aluminum and steel core component stresses for initial installation of Drake ACSR at 20%RTS and 15°C. .... 64

Figure 31 - Application of Experimental Plastic Elongation method in calculating aluminum and steel core component stresses after 10 years of creep elongation at 15°C for Drake ACSR initially installed at 20%RTS. .... 65

Figure 32 - Conductor Sag-tension calculation for high temperature after 10yr creep elongation at 15C. .... 66

Figure 33 - Sensitivity of Sag-tension calculations to variation in conductor weight per unit length. .... 69

Figure 34 - Sensitivity of Sag-tension calculations to variation in conductor elastic modulus ..... 70

Figure 35 - Sensitivity of Sag-tension calculations to variation in plastic elongation of Aluminum. .... 71

Figure 36 - Sensitivity of Sag-tension calculations to variation in thermal elongation rate. .... 72

## List of Tables

Table 1 - Examples of Conductor Naming Methods .....	7
Table 2 - Sag & Vertical force in a 300 m inclined span with Drake ACSR at H = 28000 N.....	20
Table 3 – Resultant Force between 250m and 350m dead-end spans of ACSR Drake at 100°C.....	25
Table 4 - Comparison of sag-tension for two spans which are mechanically independent, perfectly coupled, and coupled with actual tension inequality.....	27
Table 5 – Sag-tension for maximum ice and wind load and for high temperature shown as a function of initial stringing tension for a 300m span of Drake ACSR.....	28
Table 6 - H/w limits on unloaded conductor tension - Drake ACSR in a 300 m span. ....	30
Table 7 - Typical Linear Elastic Modulus for All Aluminium Conductors.....	35
Table 8 - List of Conductor Final Modulus Values .....	38
Table 9 – Maximum excess sag (m) due to the built-in aluminium stress posited by Rawlins, at temperatures above the kneepoint, as estimated with the Alcoa SAG10 computer program.....	43
Table 10 - Initial settling and one-hour creep strain as a function of conductor type and stress from Harvey & Larson.....	48
Table 11 - Stress-strain data from IEC 1597 Table 3 .....	49
Table 12 - Typical Sag-tension Calculation Results where the permanent elongation of the aluminum strands is determined by the maximum wind and ice load rather than by metallurgical creep at everyday temperature.....	54
Table 13 - Characteristics of 37-strand A1 and 26/7 strand A1/Sxy .....	56
Table 14 - "Knee-point temperatures" of A1/S1 (ACSR) as a function of stranding and span length determined by the Alcoa graphical method. All conductors have an aluminium strand area of 403 mm <sup>2</sup> . .....	67
Table 15 - Table of Basic Sag-tension Sensitivities .....	73
Table 16 - Various high temperature sag errors.....	73



## EXECUTIVE SUMMARY

This technical brochure specifies and explains the primary elements of the sag-tension calculation process, a process which is essential to the design and construction of overhead lines. The various mathematical tools and conductor data considered herein are used to predict sag and tension of catenaries at the full range of conductor temperatures and ice and wind loads that occur over the rather long life of an overhead power line. The goal of the document is not to develop a unique or "best" calculation method, but to describe the overall process and explain the common calculation methods.

### Introduction

Historically, for most overhead transmission lines, the sag of conductors (or tension) is measured at the time of construction when the line is not energized. At the time of installation, the conductors are at a temperature of 10°C to 35°C and tensioned to no more than 10% to 30% of their rated tensile strength. Once the line is constructed, the phase conductors may be subject to high temperatures during periods of high electrical loading and both the lightning shield wires and phase conductors must remain intact during high ice and wind load events for an expected useful life of 40 years or more. Under all foreseeable conditions, the conductors must not break under high tension, fatigue under persistent wind-induced motions, nor sag such that minimum electrical clearances are compromised.

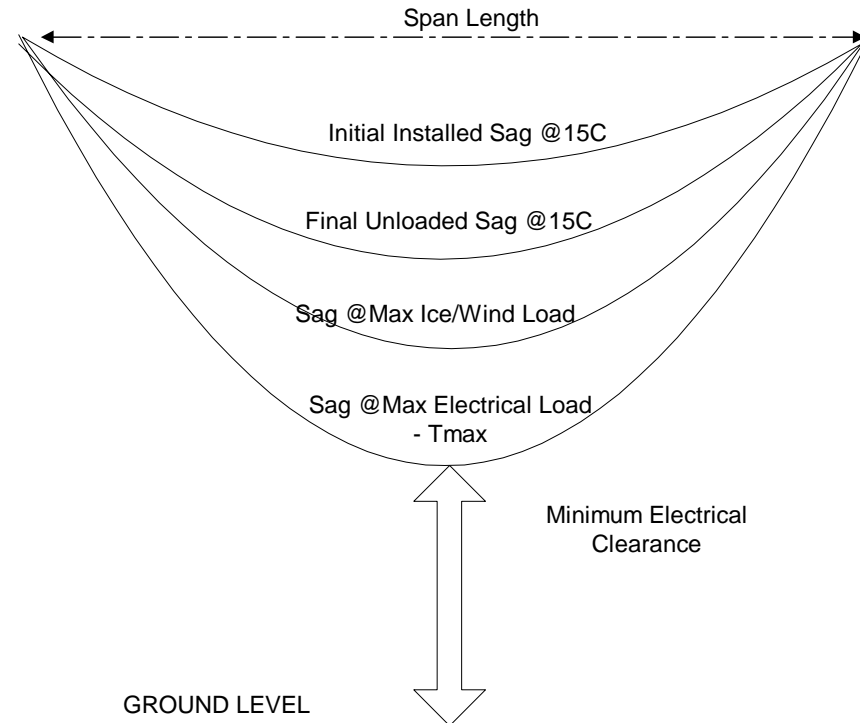


Figure 1 - Catenary variation with conductor temperature, ice & wind loads, and time after installation where Tmax is the maximum conductor temperature.

To assure that these conditions are met over the life of the line, the engineer must specify initial measured (i.e. stringing) sags, based upon the following "sag-tension" calculations:

- Sags and tensions after plastic elongation of the conductor due to occasional severe ice and/or wind loads and to long-term creep elongation of aluminium strand layers under normal everyday tension (difference in sag between the Initial and Final Sag at 15°C in Figure 1).
- Sags and tensions for all foreseen temperatures, over the life of the line, including those (above 50°C) which may result from high electrical current loads (See sag at maximum electrical load in Figure 1).
- The maximum conductor tension under ice and wind loads which “strain” structures (i.e. dead-end and angle) must withstand and the corresponding maximum sag which must not infringe on minimum electrical clearances.
- Conductor tensions during the coldest periods of winter to allow for sufficient self-damping to prevent aeolian vibration-induced fatigue over the life of the line.

### ***The Catenary Equation***

The catenary equations (both exact and approximate) are examined for both level and inclined spans. The various relationships between sag, tension (horizontal and total), weight per unit length, and span length are studied and explained. The concept of “slack” (difference in length between conductor and span) is defined and an important discussion of limits on calculation accuracy is included.

Both approximate “parabolic” equations and the exact hyperbolic catenary equations are explained. The catenary constant (tension divided by weight per unit length) is shown to be an essential parameter of these equations.

Figure 2 shows a typical relationship between sag, conductor tension, and “slack”, calculated with the catenary equation. As explained in the brochure, an increase in any or all of the components of conductor elongation (e.g. thermal, elastic, and plastic) leads to greater sag and reduced tension.

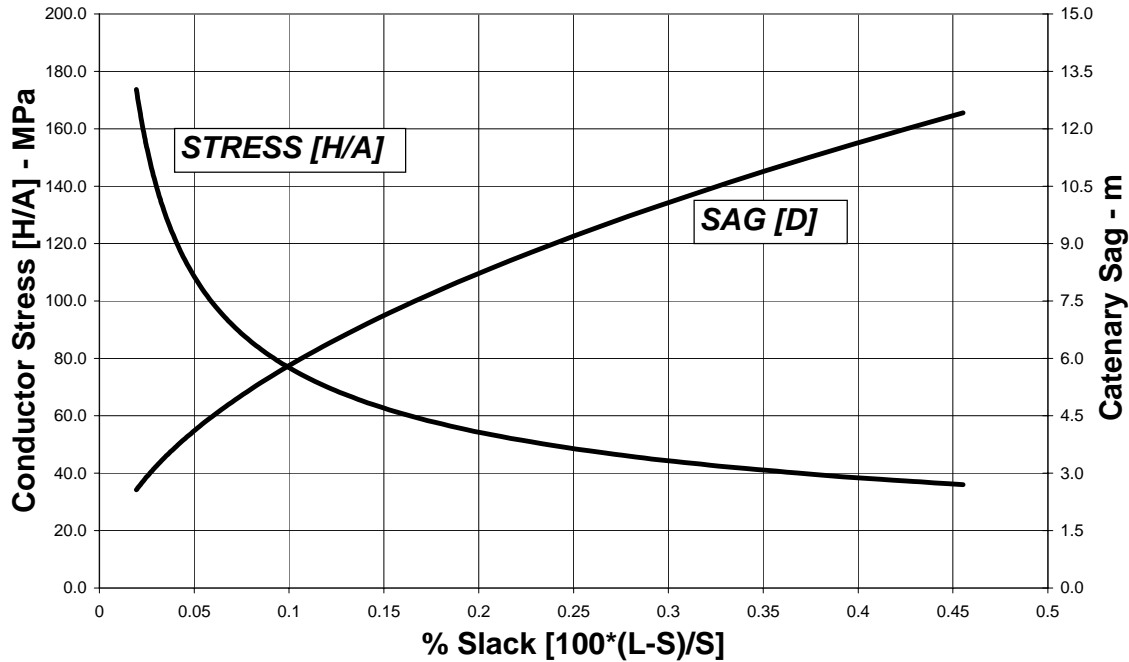


Figure 2 – Conductor Stress (H/A) and Sag (D) vs. %Slack ( $100*(L-S)/S$ ) where L=conductor length and S=Span length based on the catenary equations.

### ***Mechanical Coupling of Spans***

Transmission lines are usually comprised of multiple line sections. Each line section is terminated at each end by a strain structure that allows no longitudinal movement of the conductor attachment points and that the terminating insulator strings experience the full tension of the conductors. Tangent suspension structures are used within the line section to support the conductors. At suspension structures, the insulators and hardware used to support the conductors are usually free to move both transversely and longitudinally to the line and any modest difference in conductor tension between adjacent spans is equalized by small movements of the bottom of the insulator strings.

This tension equalization between suspension spans works reasonably well for modest changes in conductor temperature and small differences in ice and wind loading. The brochure explains how this simplifies the sagging of conductor during construction and stringing and in simplifying sag-tension calculations with the assumption of a “ruling” or “equivalent” span.

The discussion of slack, and the sensitivity of tension and sag to it, is applied to demonstrate how tension equalization at suspension supports occurs and under what conditions errors in calculation become significant. The physical understanding of the ruling span concept, as described in the brochure, is helpful in identifying those line design situations where it should not be used.

**Conductor Tension Limits**

Sag-tension calculations are normally performed with multiple constraints on tension and sag. For example, the maximum tension under a specified wind and ice load condition may be limited to 50% of rated strength and the conductor tension under everyday conditions may be limited to a tension over weight per unit length value of 1000 meters.

The brochure describes the purpose of various tension limits and recommends references that provide guidance in setting specific values.

**Conductor Elongation – Elastic, Plastic, and Thermal**

The most important differences in sag-tension calculation methods involve the modeling of conductor elongation due to changes in tension, temperature and time. In the simplest elongation model ("Linear Elongation"), plastic elongation is ignored, and conductor elongation under tension is assumed elastic. In a somewhat more sophisticated model ("Simplified Plastic Elongation"), plastic elongation is represented by a typical value based on experience. In the most accurate conductor elongation model ("Experimental Plastic Elongation"), plastic elongation is calculated based upon experimental laboratory conductor test data. In this experimental plastic elongation model, plastic increases in the conductor length are calculated (including initial strand deformation and settling, worst-case ice/wind load events, and long-time "creep" elongation due to sustained normal tension) based upon line design assumptions and historical field data.

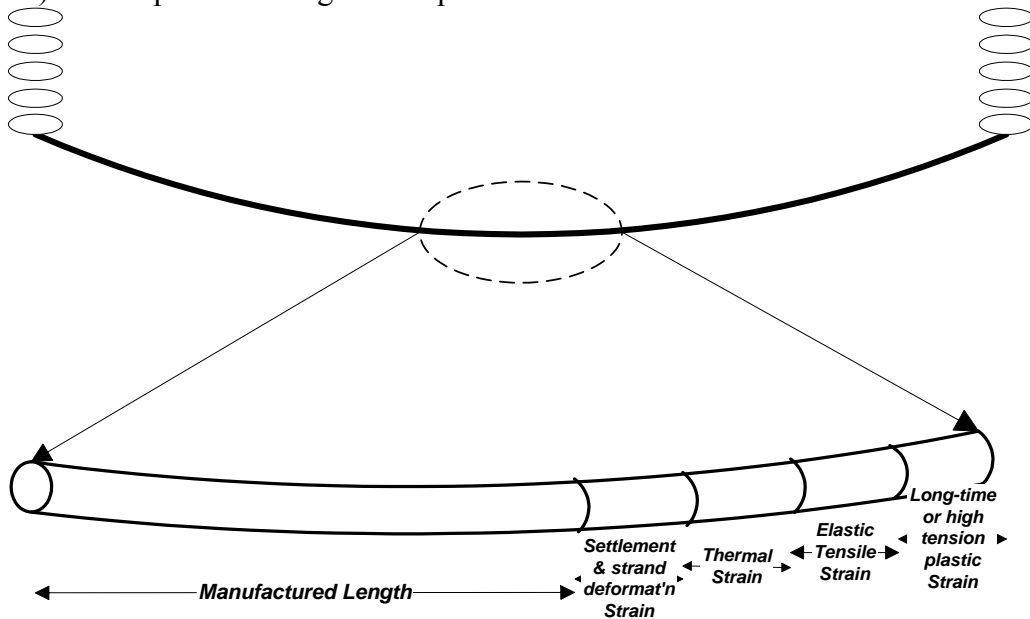


Figure 3 - Conductor elongation diagram.

The linear elongation model is simple to understand and allows algebraic solutions to sag-tension conditions but, by ignoring plastic conductor elongation, structure tension loads are over-estimated and conductor sag under both high wind/ice loading and at high electrical current levels, can be underestimated.

As discussed in the brochure, the Experimental Plastic Elongation model has several advantages: (a) it yields realistic structure tension loads; (b) calculation of high temperature sags with ACSR (A1/SA1) is more accurate; and (c) the plastic elongation of the conductor can be calculated based on assumed loading events rather than using a typical value based on experience.

### ***Sag-tension Calculation Methods***

The brochure acknowledges the widespread use of numerical solutions to sag-tension calculations but uses graphical representations to provide the reader with insight concerning the advantages and limitations of calculation methods of varying complexity. In this discussion, the conductor elongation models are used in combination with the catenary equation to determine sag-tension values for typical high temperature and ice/wind loading events. The sag-tension solutions presented in this chapter illustrate how plastic and thermal elongation, influence the tension distribution between aluminum layers and steel core in ACSR (A1/SA1).

In this section, typical sag-tension calculation results are discussed. The usual meaning of initial and final conditions is explained and their calculation demonstrated for the different conductor elongation models. The interaction of the steel core and aluminum layers under high tension and high temperature conditions is demonstrated graphically.

### ***Parameter Sensitivity***

In the final section of the brochure, some insight is provided into the influence of various key parameters used in sag-tension calculations. For example, variation in the thermal elongation coefficient of a stranded aluminum conductor can have considerable influence on the sags calculated for a line at high conductor temperatures. As shown in Figure 4, the sag at 100°C (9.7 m) increases by 200 and 500 mm when the coefficient of thermal expansion is increased by 10% and 30%, respectively.

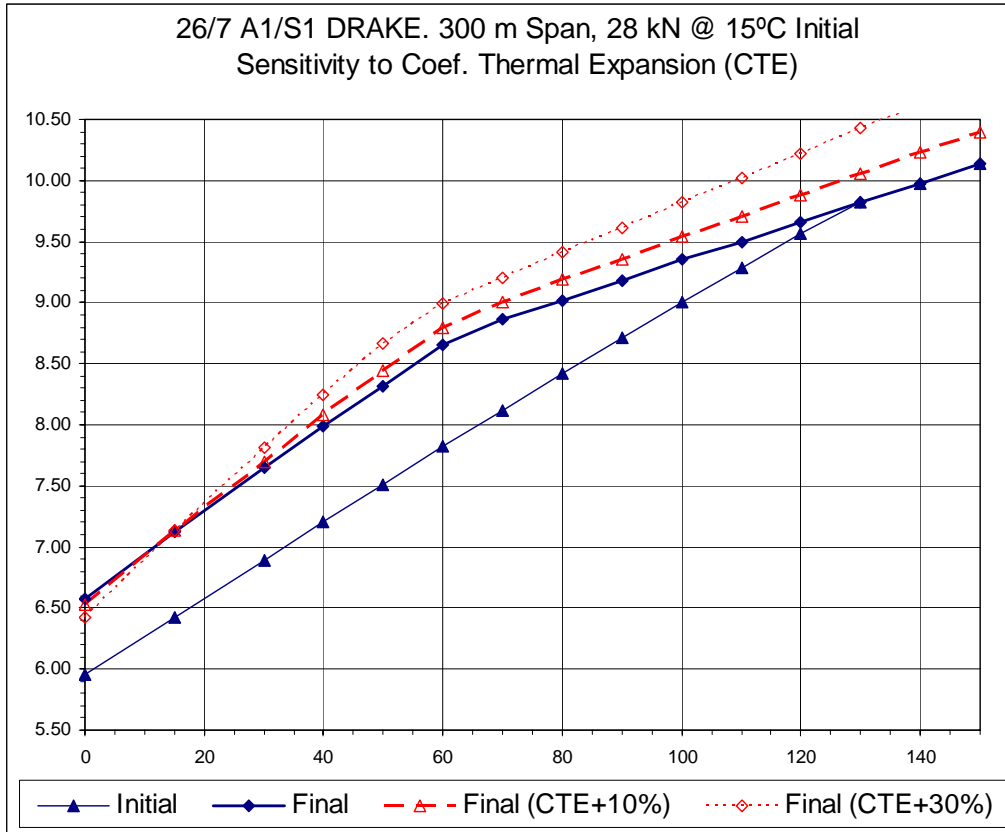


Figure 4 - Influence of variation in the coefficient of thermal elongation on high temperature sag.

It is clear from the discussion that, even with very careful laboratory tests and modern calculation methods, sag calculation errors cannot be less than 100 to 200 mm and are generally considerably greater.

### Conclusions

The sag-tension calculation process, with both exact and approximate catenary equations, is described in some detail. Three conductor elongation models are defined and the more complex, experimentally based model is recommended because its use allows the line designer to estimate both high temperature sags and maximum structure tension loads with superior accuracy.

Given the prevalence of numerical calculation tools, there is little need to use the approximate catenary equations or the simplified elastic conductor elongation models but the ruling span assumption of tension equalization between spans appears to be sufficiently accurate to be used in many new line designs.

Regardless of the calculation technique and conductor elongation model selected, it is concluded that there continues to be a need for sufficient clearance buffers in the design of new lines and the uprating of existing lines because of uncertainties in modeling the load sequence and detailed mechanical behavior of bare stranded overhead conductors.

## **ABSTRACT**

This brochure identifies and describes the most essential elements of the sag-tension calculation process and the various mathematical and experimental methods used to predict sag and tension of catenaries over the whole range of conductor temperatures and ice and wind loads that may occur over the life of a line. The goal is not to develop a unique calculation method, but to explain the overall process and identify the alternative modeling methods that are available.

Calculating the sag of conductors as a function of temperature and ice/wind loads and calculating the tension that these conductors exert on supporting structures is an essential part of the process of designing overhead power lines. The engineer is provided with a basic explanation of the sag-tension calculation methods that are in common use throughout the world and with a physical understanding of the processes and mathematical relationships that underlie these methods.

## **KEY WORDS**

AAC (Ax) - All Aluminium Conductor, ACSR (A1/Syz) - Aluminium Conductor Steel Reinforced, Creep Plastic Elongation, Electrical Clearance, Elastic Elongation, Plastic Elongation, Thermal Elongation, Initial Plastic Elongation, Knee-point Temperature, Manufactured Conductor Length, Maximum Allowable Conductor Temperature, Rated Tensile Strength (RTS), Ruling (Equivalent) Span, Stress-strain Curves, Thermal Rating, Weight per unit length, Weight Span, Wind Span.

## DEFINITIONS

AAAC (Ax) - All Aluminium Alloy Conductor (the x identifies the type of aluminium ally).

AAC (Ax) - All Aluminium Conductor (the x identifies the type of aluminium ally).

ACAR (A1/Ay) - Aluminium Conductor Alloy Reinforced (the y identifies the type of aluminium alloy used for the core wires).

ACSR (A1/Syz) - Aluminium Conductor Steel Reinforced (y represents the type of steel and z represents the class of zinc coating on the steel core wires).

Ampacity - The maximum constant line current which will satisfy the design, security and safety criteria of a particular line on which the conductor is installed. In this brochure, ampacity has the same meaning as "steady-state thermal rating."

Annealing - The process wherein the tensile strength of copper or aluminium wires is reduced at sustained high temperatures, usually above 75°C and 90°C respectively.

ASTM - American Society for Testing and Materials.

Creep Elongation – see Elongation, Plastic

Design Loading Plastic Elongation – see Elongation, Plastic

EC (grade aluminium) – "Electrical Conductor" grade aluminium also called A1 or 1350-H19 alloy.

EHS (S3) Steel Wires - Extra High Strength steel wires for ACSR (A1/S3y).

EDS (Everyday Stress) – The tension or stress that a conductor normally experiences for most of its service life, typically at a conductor temperature of 0°C to 25°C without wind or ice.

Electrical Clearance - The distance between energized conductors and other objects such as conductors, structures, buildings, and earth. Minimum clearances are usually specified by regulations.

Elongation, Elastic – Bare overhead conductors elongate under tension, increasing in length with increasing tension and decreasing in length with decreasing tension. Elastic elongation of conductor is "spring-like". The conductor returns to its original length (unloaded length) when tension is removed.

Elongation, Plastic – Aluminum strands and, to a much lesser extent, steel strands, used in bare overhead conductors, undergo plastic (i.e. permanent) elongation as the result of



tension applied over time. Initial plastic conductor elongation includes “strand settlement and deformation” which occurs during stringing and sagging (Initial Plastic Elongation), plastic elongation which occurs during relatively brief, high tensile-load events, and long-time “metallurgical creep” elongation which occurs at everyday tension levels over the life of the line. Metallurgical creep of aluminum is accelerated at sustained high temperatures (above 20°C). The components of plastic elongation are not additive (e.g. the plastic elongation rate at high tension is less after the line has been in place for 10 years than when the line is first installed).

Elongation, Thermal - Bare overhead conductors will expand or contract with changes in temperature. The rate of expansion or contraction is dependent on the conductor material and magnitude of temperature change. For ACSR conductors, the differential rates of expansion also shift tensile load between the aluminum strands and steel core.

HS Steel (S2) - High Strength steel core wires for ACSR (A1/S2y).

I.A.C.S. or IACS - International Annealed Copper Standard.

IEC - International Electrotechnical Commission.

Initial Plastic Elongation – see Elongation, Plastic

Knee-point Temperature - The conductor temperature above which the aluminium strands of an ACSR (A1/S1A) conductor have no tension or go into compression.

Manufactured Conductor Length – The conductor manufactured length as wound onto a reel with little or no tension. Normally, for ACSR, the manufactured lengths of the aluminum layers and the steel core are assumed to be the same (at zero tension) under everyday temperatures of 15 to 20°C.

Maximum Allowable Conductor Temperature - The highest conductor temperature at which an overhead power line can be safely operated (Also referred to as the line “design” or “templating” temperature).

Rated Tensile Strength (RTS) - The calculated value of composite conductor tensile strength, which indicates the minimum test value for stranded bare conductor. Similar terms include Ultimate Tensile Strength (UTS), Rated Breaking Strength (RBS), and Calculated Breaking Load (CBL).

Ruling (Equivalent) Span - A hypothetical, equivalent level span length where the variation of tension with conductor temperature or ice and wind load is the same as in a series of contiguous suspension spans with perfect tension equalization between spans.

Stress-strain Curves – These are plots of the complex relationships between mechanical tensile stress and conductor elongation. In the simplest case, these curves are

approximated as linear but are commonly modeled by non-linear, higher order polynomials.

Thermal Rating – This is the maximum electrical current that can be carried in an overhead transmission line (same meaning as ampacity) without exceeding the Maximum Allowable Conductor Temperature.

TW conductor - A bare overhead stranded conductor wherein the aluminium strands are trapezoidal in cross-section.

Up-rating - The process by which the thermal rating of an overhead power line is increased. While this term may also be used to refer to an increase in the operating voltage of an existing line, in this brochure the term is limited to an increase in the allowable current.

Weight per unit length - This brochure generally uses conductor weight per unit length. Mass per unit length can be obtained by dividing the weight by the acceleration of gravity (approximately  $9.81 \text{ m/sec}^2$ ).

Weight Span – The horizontal distance between the lowest points of a conductor on either side of the structure support.

Wind Span – The sum of half the distances from a conductor support point to each of the adjacent support points.

Worst-case weather conditions (for line rating calculation) - Weather conditions which yield the maximum or near maximum value of conductor temperature for a given line current.

## TERMS

$\alpha_A$  - Aluminium coefficient of linear thermal elongation,  $^{\circ}\text{C}^{-1}$

$\alpha_S$  - Steel coefficient of linear thermal elongation,  $^{\circ}\text{C}^{-1}$

$\alpha_{AS}$  - Composite aluminium-steel coefficient of linear thermal elongation,  $^{\circ}\text{C}^{-1}$

$\epsilon_{AS}$  - The strain in all the strands of an ACSR conductor.

$\epsilon_A$  - The strain in the aluminium strands of a stranded conductor (AAC, ACSR, etc.).

$\epsilon_{CA}$  - Total plastic elongation of aluminum strands, .

$\epsilon_S$  - The strain in the steel core of an ACSR conductor.

$\epsilon$  - The total strain in any conductor including both plastic, thermal, and elastic strains,  $\mu\text{s}$ .

$A$  - Conductor cross-sectional area,  $\text{mm}^2$

$A_A$  - Cross sectional area of aluminium strands,  $\text{mm}^2$

$A_S$  - Cross sectional area of steel strands,  $\text{mm}^2$

$A_{AS}$  - Total cross-sectional area,  $\text{mm}^2$

$D$  - Conductor sag, m

$E$  - Modulus of elasticity of the conductor, GPa

$E_A$  - Modulus of elasticity of aluminium, GPa

$E_S$  - Modulus of elasticity of steel, GPa

$E_{AS}$  - Modulus of elasticity of aluminium-steel composite, GPa

$H$  - The horizontal component of tension in the conductor, N

$h$  - The vertical distance between support point elevations, m

$H_A$  - The horizontal component of the tension in the aluminium strands of an aluminum conductor (AAC, ACSR, etc.).

$H_{AS}$  - The total horizontal tension in an ACSR conductor

$H_S$  - The horizontal component of the tension in the steel core of an ACSR conductor.

$L$  – Length of conductor between supports, m

$L_H$  - Length of conductor under horizontal tension  $H$ , m

$L_{REF}$  - Reference length of conductor under horizontal tension for no ice or wind load at everyday temperature  $H_{REF}$ , m

$S$  – Span length, m

$x$  – Horizontal distance from conductor low point to supporting structure, m

$w$  – Conductor weight per unit length, N/m

$T$  – Total or support tension in the conductor, N

# 1.0 INTRODUCTION

The goal of sag-tension calculations is to predict the catenary sags and the conductor tensions under all design conditions of conductor temperature and ice and/or wind loads. Maximum conductor tension is an important factor in structure design. Maximum conductor sag largely determines structure heights and locations in order to maintain electrical clearances throughout the life of the line. Thus both the mechanical and electrical integrity of an overhead transmission or distribution line is directly dependent on the accuracy of sag-tension calculations.

Sag-tension calculations are necessary when transmission lines are initially designed or if they are subsequently modified. While there are a number of different methods available, used by engineers in different countries, this technical brochure is intended to explain the most common methods and to provide a clear description of the most important assumptions underlying the common methods. This is especially important when many utilities are no longer able to support in-house experts in the subject and when new types of conductors are becoming commercially available.

Furthermore, given the trends in many countries toward deregulation of utilities, increased utilization of existing assets, and the often fierce opposition to building new lines, there is a need for increased accuracy in such calculations to avoid the possibility of electrical clearance violations.

## 1.1 Conductor Naming Convention

Naming and identifying bare stranded overhead conductors can be confusing due to different practices used by various utilities. This document will use both common conductor names (e.g. “403mm<sup>2</sup> 26/7 Drake ACSR”) and IEC conductor designations (e.g. 403-A1/S1A-26/7) [1][2]. In either case, the designated area (e.g. 403) is that of the conductive material in square mm. Some examples of common and IEC conductor names are listed in Table 1.

Table 1 - Examples of Conductor Naming Methods

IEC Conductor Designation	Common conductor designations
403-A1/S1A-54/7	403mm <sup>2</sup> ACSR 54/7 (Condor)
523-A1/S1A-42/7	523mm <sup>2</sup> ACSR 42/7 (Snowbird)
403-A1/S1A-26/7	403mm <sup>2</sup> ACSR 26/7 (Drake)
685-A1-61	685mm <sup>2</sup> , 61 strand, AAC (Columbine)

## 1.2 The Catenary Clearance Envelope

The energized conductors of transmission and distribution lines must be installed in a manner that minimizes the possibility of injury to people, flashovers to other conductors, and to inanimate objects such as buildings, whether below or adjacent to the line. Self-supporting overhead conductors elongate with time, with increasing temperature and with ice and wind loads; any such conductor elongation increases the sag of the conductor which may decrease the clearance to objects or people. Under all foreseeable conditions, despite the effects of weather and variations in electrical loading, the line’s conductors

must remain at safe distances from people, other conductors, vehicles, buildings, and any other reasonably anticipated activities.

To ensure safe minimum electrical clearances under all conditions, the height and lateral position of the conductor between support points must be calculated for all wind, ice and temperature conditions which the conductor may experience. These calculations are commonly referred to as "sag-tension" calculations and are the subject of this brochure.

Transmission line supporting structures are typically spaced a few hundred meters apart. This distance between supports is called the span length. Under most conditions, the flexural and torsional rigidity of stranded conductors can be neglected. Hence, the only conductor stresses that affect the sag between the conductor support points are axial tensile stresses along the wires.

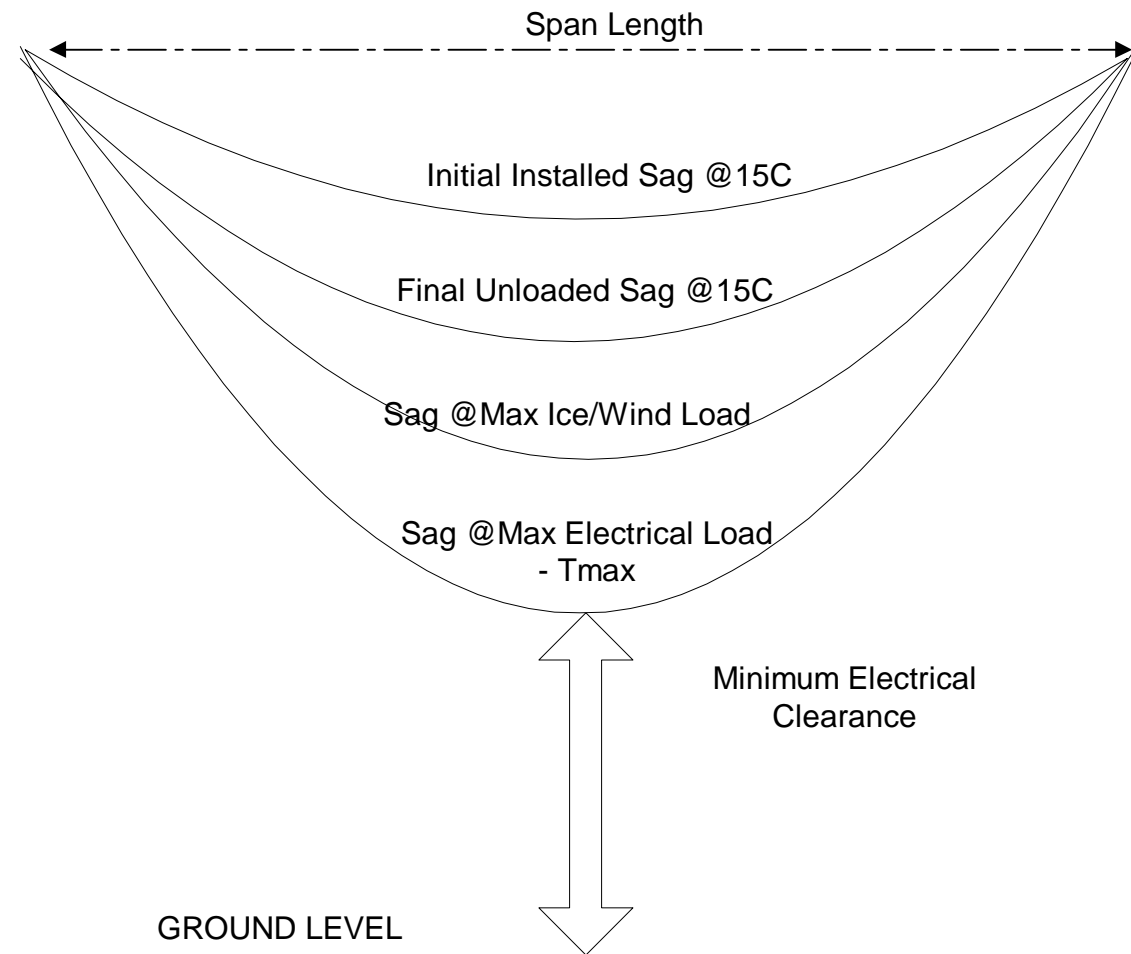


Figure 5 – Catenary variation with conductor temperature, ice & wind loads, and time after installation where  $T_{max}$  is the maximum conductor temperature.

It has been mathematically demonstrated that a suspended bare cable, when subjected to uniform loading per unit length, takes the form of a catenary between support points. The shape of the catenary curve, changes with temperature (thermal elongation), ice and wind

loading (design loading plastic elongation), and time (creep plastic elongation), as shown in Figure 5.

## 2.0 THE CATENARY

The shape of a catenary is a function of the conductor weight per unit length,  $w$ , and the horizontal component of tension,  $H$ . The sag of the conductor,  $D$ , is a function of these parameters, the span length,  $S$ , and the difference in elevation between the span support points.

### 2.1 Catenary and parabolic solutions for sag in level spans

Conductor sag and span length are illustrated in Figure 6 for a level span. More detail is provided in [3,4,5,6,7,8,9]

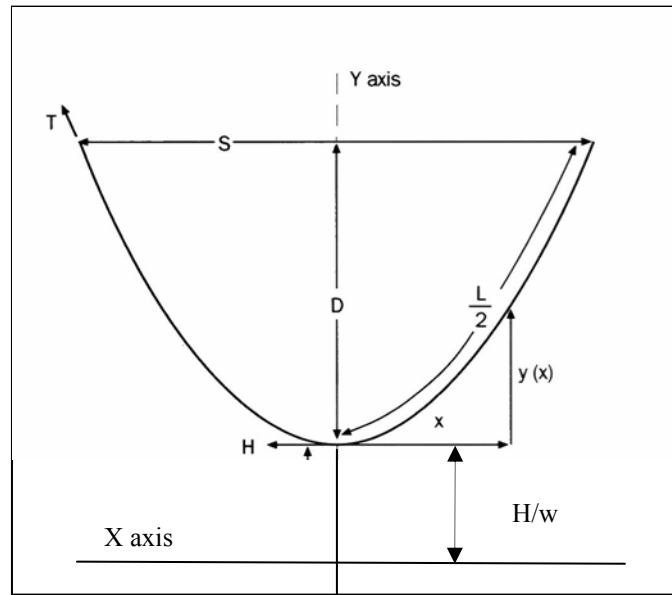


Figure 6 - The Catenary Curve for Level Spans

The catenary equation for a conductor between supports at equal heights or at different heights is the same. It is expressed in terms of the horizontal distance,  $x$ , from the vertex (or low point) of the catenary to a point on the catenary which is  $y(x)$  above the vertex. The catenary equation is given by:

$$y(x) = \frac{H}{w} \cdot \left[ \cosh\left(\frac{w \cdot x}{H}\right) - 1 \right] \cong \frac{w \cdot x^2}{2 \cdot H} \quad (1)$$

The expression on the right side of equation (1) is an approximate parabolic equation based upon the first term of the MacLaurin expansion of the hyperbolic cosine. The approximate parabolic equation is valid as long as  $x^2 w^2 / 12H^2 \ll 1$ .



For a level span, the low point is in the center, and the sag,  $D$ , is found by substituting  $x = S/2$  in the preceding equations. The exact catenary and approximate parabolic equations for sag become the following:

$$D = \frac{H}{w} \cdot \left\{ \cosh\left(\frac{w \cdot S}{2 \cdot H}\right) - 1 \right\} \cong \frac{w \cdot S^2}{8 \cdot H} \quad (2)$$

The approximate parabolic equation (2) is valid as long as  $w^2 S^2 / 48 H^2 \ll 1$ . Hence, it is usually not valid for long, steep, nor deep spans such as may be found in river, lake or fjord crossings. On the other hand, one can readily see the relationship between sag, tension, weight per unit length and span length in the approximate equation (e.g. Sag,  $D$ , is proportional to the square of the span length,  $S$ ).

The ratio,  $H/w$ , which appears in all of the preceding equations, is commonly referred to as the catenary constant or catenary parameter. An increase in the catenary constant causes the catenary curve to become shallower and the sag to decrease. Although it varies with conductor temperature, ice and wind loading, and time, the catenary constant typically has a value in the range of 500-2000 m for most transmission line catenaries under most conditions.

The following sample calculations are made using 403mm<sup>2</sup>, 26/7 ACSR (403-A1/S1A 26/7) "Drake" conductor. If not otherwise specified, the properties of the conductor, the assumed span length, and the horizontal component of tension,  $H$ , are:

1. Aluminium area = 402.8 mm<sup>2</sup>
2. Total area (aluminium and steel core) = 468.5 mm<sup>2</sup>
3. Weight per unit length = 15.97 N/m
4. RTS = 140 kN
5. Span length = 300 m
6. Horizontal component of tension = 20% of RTS = 28 kN.
7. Conductor temperature = 15°C

Under these conditions the sag of the span, according to equation 2, is:

$$D = \frac{28000}{15.97} \cdot \left\{ \cosh\left[\frac{15.97 \cdot 300}{2 \cdot 28000}\right] - 1 \right\} = 6.420m$$

Using the approximate parabolic equation, the sag is:

$$D = \frac{15.97 \cdot 300^2}{8 \cdot 28000} = 6.417m$$

In this particular case, the difference in calculated sag is only 3 mm. Since it is unlikely that the sag can be measured with an accuracy of less than 100 mm, the difference is negligible.

The horizontal component of tension,  $H$ , is the same at all points within the catenary. The total conductor tension is equal to  $H$  at the point in the catenary where the conductor slope is horizontal (for a level span, this is the midpoint of the span) but, as shown in section 2.4, the total tension increases as one approaches the support points.

## 2.2 Total Conductor Length.

Application of calculus to the catenary equation allows the determination of conductor length,  $L(x)$ , measured along the conductor from the low point of the catenary in either direction as a function of  $x$ .

The equation for conductor length between supports is:

$$L(x) = \frac{H}{w} \cdot \sinh\left(\frac{w \cdot x}{H}\right) \cong x \cdot \left(1 + \frac{x^2 \cdot w^2}{6 \cdot H^2}\right) \quad (3)$$

For a level span, the conductor length corresponding to half of the total conductor length is at the span's midpoint ( $X = S/2$ ), thus:

$$L = 2 \cdot L(x = \frac{S}{2}) = \left(\frac{2 \cdot H}{w}\right) \cdot \sinh\left(\frac{S \cdot w}{2 \cdot H}\right) \cong S \cdot \left(1 + \frac{S^2 \cdot w^2}{24 \cdot H^2}\right) \quad (4)$$

The parabolic equation for the total conductor length can also be expressed as a function of sag,  $D$ , by substitution of the sag parabolic equation (2):

$$L \cong S + \frac{8 \cdot D^2}{3 \cdot S} \quad (5)$$

For the example calculation, the exact total conductor length is:

$$L = \left(\frac{2 \cdot 28000}{15.97}\right) \cdot \sinh\left(\frac{300 \cdot 15.97}{2 \cdot 28000}\right) = 300.366 \text{ m}$$

The parabolic approximation gives the same conductor length of 300.366 m. Note that the total conductor length is only 0.366 m (about 0.1%) longer than the horizontal span length of 300 m.

## 2.3 Conductor Slack

Conductor slack is the difference between the total conductor length,  $L$ , and the chord distance between supports. For a level span the distance between supports is the span length,  $S$ . Equating and rearranging the preceding exact equations for  $L$  and  $S$ , the slack ( $L-S$ ) for the example problem is:

$$L - S = \left(\frac{2 \cdot H}{w}\right) \cdot \sinh\left(\frac{w \cdot S}{2 \cdot H}\right) - S \quad (7)$$

While slack has units of length, it may also be expressed as a percentage of the span length. In the preceding example calculation, the exact length of the conductor was found to be 300.366 m and the slack is 0.366 m (i.e. 0.122 % of the span length).

As noted previously, the parabolic (approximate) equations offer some additional insight into the interaction of slack, span length, and tension that the exact equations do not. For a level span:

$$L - S \cong S^3 \cdot \left( \frac{w^2}{24 \cdot H^2} \right) \cong D^2 \cdot \left( \frac{8}{3 \cdot S} \right) \quad (8)$$

From this equation, one can see that slack is approximately proportional to the 3<sup>rd</sup> power of span length. Thus for a series of suspension spans having the same horizontal tension, H, the slack of a 400 m span is eight times as large as the slack in a 200 m span. As shown later in this brochure, the cubic dependence of slack on span length is the reason sag-tension behavior of multiple suspension spans is largely determined by the longest spans.

The approximate equation for slack can also be inverted to obtain equations showing the dependence of sag, D, and tension, H, upon slack, L-S:

$$D \cong \sqrt{\frac{3 \cdot S \cdot (L - S)}{8}}$$

$$H \cong \frac{w \cdot S}{2} \cdot \sqrt{\frac{S}{6 \cdot (L - S)}}$$

Clearly, as the slack of the span becomes very small, the conductor sag approaches zero and the tension becomes very large.

To illustrate the impact of small changes in slack on tension and sag, consider the preceding 300 m level span example of Drake, 403mm<sup>2</sup>, 26/7 ACSR (403-A1/S1A-26/7) conductor with 0.366m of slack. If only 100 mm is added to the total conductor length, the sag and tension are approximately equal to:

$$D = \sqrt{\frac{3 \cdot 300 \cdot (0.366 + 0.1)}{8}} = 7.241 \text{ m}$$

$$H = \frac{15.97 \cdot 300}{2} \sqrt{\frac{300}{6 \cdot (0.366 + 0.1)}} = 24.8 \text{ kN}$$

Ignoring for the moment any change in length with tension in this example, adding 100 mm to the conductor length yields an 800 mm change in sag and a 13 % reduction in tension (3.2 kN). The *slack* concept is thus very useful in explaining how very small changes in conductor length – such as those caused by thermal, elastic or plastic elongation, have major effects on the sag of overhead line spans.

Given span length, S, and conductor weight per unit length, w, the exact catenary relationship between slack (and length) and horizontal tension, H, is found with equation (7) and the exact relationship between sag and tension is found with equation (2). For the sample problem described previously, with a span length of 300 m, the bare Drake

A1/S1A conductor is installed with a horizontal tension component of 28 kN which equals a conductor stress of 69.5 MPa given the conductor crosssectional area of 402.9 mm<sup>2</sup> and corresponds to a sag of 6.4 m. The variation of sag and conductor stress with % slack (100 \* slack) is shown in Figure 7.

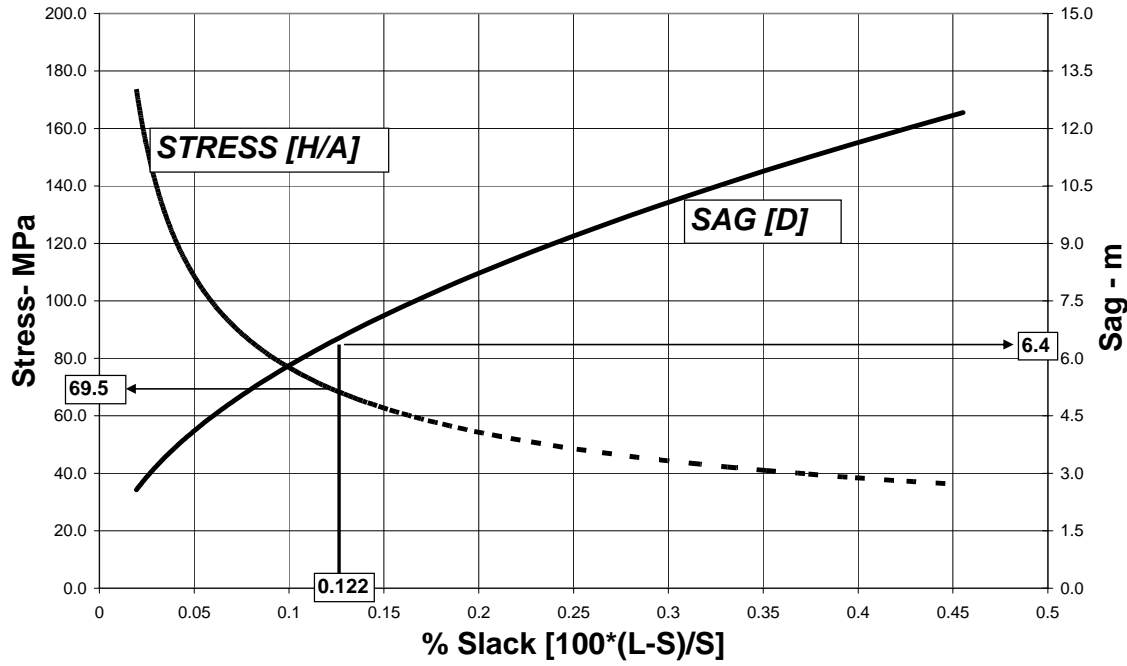


Figure 7 – Catenary Stress (H/A) and Sag (D) vs. %Slack (100\*(L-S)/S) for Bare Drake ACSR in a 300 m span at a tension of 20% RTS (69.5 MPa) at 15C

Looking to later discussions in this brochure, note the following about this plot:

1. Any increase in conductor length (% slack) yields a reduction in stress and an increase in sag.
2. A similar pair of curves can be plotted for other conductor weights per unit length due to ice and wind pressure.
3. Conductor plastic, elastic and thermal elongation curves can be plotted with the same horizontal axis if it is noted that marginal change in % slack ((L-S)/S) is essentially the same as marginal change in % elongation ((L-Lo)/Lo).

## 2.4 Total and Horizontal Tension

As noted previously, at the low point of the catenary, the conductor tension is equal to the horizontal component of tension. At every other location within the span, including the end supports, the total conductor tension is greater than the horizontal component.

For a level span, at the supports, the vertical component of tension is equal to half the weight of the conductor:

$$V = w \cdot L / 2 = H \cdot \sinh \left[ \frac{w \cdot S}{2 \cdot H} \right]$$

At the end supports, the total tension is the vector sum of the horizontal and vertical tension components:

$$T^2 = H^2 + \left( \frac{w \cdot L}{2} \right)^2$$

Substituting the equation for length, L, from section 2.2, and taking the square root of both sides of this equation, we obtain:

$$T = H \cdot \sqrt{1 + \sinh^2 \left( \frac{w \cdot S}{2 \cdot H} \right)} = H \cdot \cosh \left( \frac{w \cdot S}{2 \cdot H} \right)$$

To relate the total tension to the sag in this level span, the equation can be rearranged as:

$$T = H + H \cosh \left( \frac{w \cdot S}{2 \cdot H} \right) - H$$

$$T = H + w \cdot \left( \frac{H}{w} \cosh \left( \frac{w \cdot S}{2 \cdot H} \right) - \frac{H}{w} \right)$$

Substituting equation (2) for sag, we have:

$$T = H + w \cdot D$$

Given the conditions in the preceding example calculation for a 300 m level span of 403-A1/S1A-26/7 (ACSR) “Drake”, the total conductor tension at the attachment points, T, is 28.0 kN and exceeds the horizontal component of tension H by only 102 N (0.36%)

$$T = 28000 + 15.97 * 6.420 = 28000N + 102N$$

The approximate (“parabolic”) catenary curve equations are useful for order of magnitude checks and provide more insight into the physics of sag-tension (e.g. sag is dependent on the square of span length) but there is little advantage to their use in numerical calculations. For most cases, except those of long and deep catenaries, the difference between the exact and approximate solutions is small. As shown in Figure 8, the difference in calculated catenary position, y(x), as a function of x is quite small for horizontal distances up to about 300 m (equivalent to a level span of 600m). For a 500 m horizontal distance (1000 m level span), however, the sag error is about 0.5 m.

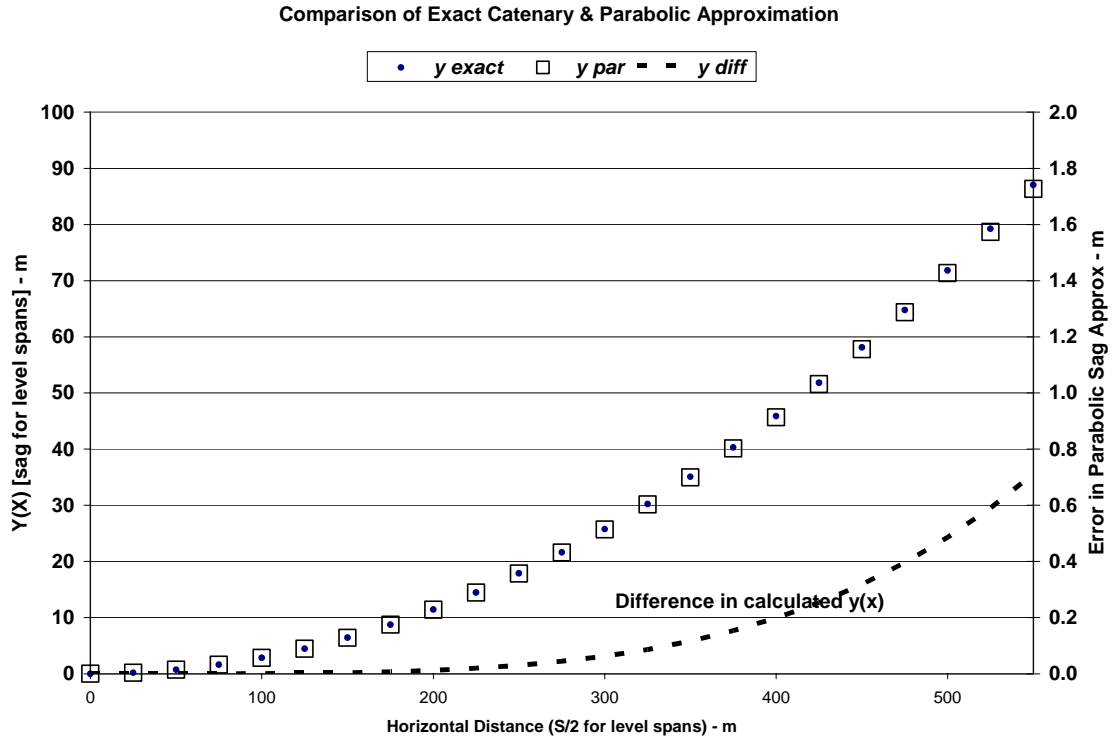


Figure 8 - Comparison of catenary  $y(x)$  and difference between exact and parabolic approximate solution as a function of  $x$  for ACSR Drake at a tension of 28020 N.

## 2.5 Engineering accuracy of sag calculations

In practical line design engineering, several factors limit the accuracies that can be achieved in sag calculations, unless extraordinary measures are taken to correct seemingly minor error sources. Some of the basic error sources include:

1. **Uncertain weight of the conductor** - The nominal values for conductor weight corresponds to the minimum acceptable weight. In reality, the weight of the conductor typically exceeds the nominal value by 0.2% to 0.6%. During a conductor's life, the conductor's mass typically increases slightly by tarnishing effects. Also, the weight of a wet conductor can exceed the dry-weight by 1.5% to 2.5%.
2. **End of span effects** - The catenary equations assume that the conductor is fully flexible. If the bending stiffness of the conductor is taken into account, the actual sag in spans supported in suspension clamps is found to be less than that of catenary calculations. If the ends of the span in the prior example consist of 30 cm long suspension clamps, the effect of the suspension clamp and the bending stiffness changes the length of the effective catenary to 299.37 m and reduces the sag from 6.41 m to 6.38 m, i.e. a reduction of 0.4%. If the suspension clamps are

equipped with armor rods, the sag reduces to 6.35 m, i.e. a reduction of 0.9%.

Conversely, if both ends of the span are terminated into dead-end insulator strings, the sags increase. If both ends of the example span are terminated in 2m long insulator strings, with a total mass of 100 kg each, the sag increases from 6.41 m to 6.45 m (i.e. a sag increase of 0.5%). The use of composite insulators would yield a smaller sag increase.

3. **Flexibility of structures** - Changes in conductor tension at angle and dead-end strain structures causes elastic and inelastic structure deflections. If the resulting deflection of a dead-end structure in the preceding example is 1 cm, the sag increases from 6.41 m to 6.49 m, i.e. a change of 1.2%. Pole structures may deflect considerably more than steel lattice.

Other lesser effects, such as survey errors, also occur. In combination with those cited above, such uncertainties yield a typical sag calculation error of 1% to 2% for even the simplest single span line.

As is discussed in Section 7, there are additional errors in sag-tension estimates due to uncertainties regarding the elastic, plastic, and thermal elongation of the bare concentric stranded aluminium conductors typically used in overhead power lines.

## **2.6 Effect of change in conductor loading per unit length**

Overhead power lines, particularly during periods of low electrical current, can accumulate ice and snow under certain atmospheric conditions. This increases the loading per unit length of the bare overhead conductor. Also, wind blowing across the line increases the loading per unit length. Wind forces can occur during times when the conductor is iced and hence the resulting conductor loading is the vector sum of wind force on the iced conductor, the weight of the ice and the weight of the bare conductor.



Figure 9 - Heavy radial ice buildup on a relatively small bare overhead conductor.

If the conductor is inextensible, then the increase in loading per unit length due to ice and wind load would increase the tension but there would be no change in conductor length, thus leaving the sag unchanged. However, bare overhead conductors do elongate under tension load and, depending on the mechanical response characteristics of the conductor, both the tension in the conductor and its length (sag) change during ice accretion and/or high wind events.

## 2.7 Inclined spans

For inclined spans (see Figure 10), if the span is divided into two sections, one to the right and the other to the left of the low point, the catenary equations introduced previously may be used to determine the conductor position and tension. The shape of the catenary, relative to the semi-span position (i.e. low point) is not affected by the difference in suspension point elevation (span inclination),  $h$ .

In each direction (i.e. for  $x_L$  or  $x_R$ ) from the low point of the catenary, the conductor elevation,  $y(x)$ , relative to the low point is given by equation (1):

$$y(x) = \frac{H}{w} \cdot \left[ \cosh\left(\frac{w \cdot x}{H}\right) - 1 \right] \cong \frac{w \cdot x^2}{2 \cdot H}$$

And the sags relative to the supports are:

$$D_L = D_R + h \quad (9)$$



Of course, as shown in Figure 10, the low point is not in the center of the horizontal span as for a level span. In fact the "low point" may even be beyond the end of the span depending on the difference in support elevations or conductor catenary constant.

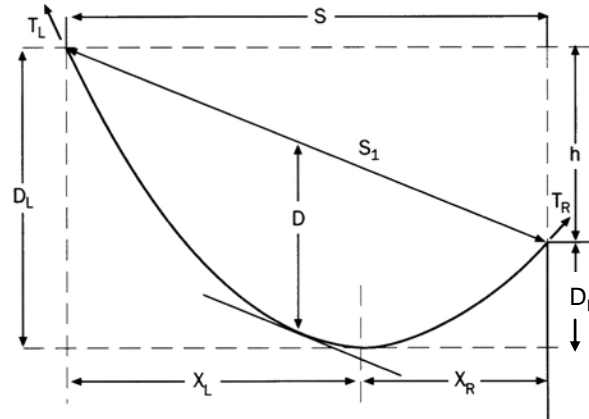


Figure 10 - Sag-tension for inclined spans.

The position of the low point in the inclined span may be calculated exactly by the equation:

$$x_R = \frac{S}{2} - \frac{H}{w} \sinh^{-1} \left[ \frac{h/2}{\frac{H}{w} \sinh \frac{S/2}{H/w}} \right] \quad (10)$$

Consider the following example, where:

$$H = 28 \text{ kN}$$

$$h = 10 \text{ m}$$

$$S = 300 \text{ m}$$

$$w = 15.96 \text{ N/m}$$

$$H/w = 28000/15.96 = 1754 \text{ m}$$

Then the example calculation becomes;

$$x_R = \frac{300}{2} - 1754 \cdot \sinh^{-1} \left[ \frac{10/2}{1754 \sinh \left( \frac{300/2}{1754} \right)} \right] = 91.6 \text{ m}$$

The elevation of any point in the inclined span can be calculated using the basic catenary equation with  $x$  being the horizontal distance from the low point, which for the example is 91.6 m into the span from the right support and 208.4 m from the left.

In the example span, as the difference in support heights increases, the low point of the catenary moves further toward the low support, eventually going beyond it as shown in the following table:

Table 2 - Sag & Vertical force in a 300 m inclined span with Drake ACSR at H = 28000 N.

<i>h</i> [m]	<b>0.00</b>	<b>5.00</b>	<b>10.00</b>	<b>15.00</b>	<b>20.00</b>	<b>25.00</b>	<b>30.00</b>	<b>35.00</b>	<b>40.00</b>
Xr [m]	150.00	120.80	91.60	62.42	33.27	4.15	-24.93	-53.97	<b>-82.95</b>
Xl [m]	150.00	179.20	208.40	237.58	266.73	295.85	324.93	353.97	<b>382.95</b>
Dr [m]	6.42	4.16	2.39	1.11	0.32	0.00	0.18	0.83	<b>1.96</b>
Dl [m]	6.42	9.16	12.39	16.11	20.32	25.00	30.18	35.83	<b>41.96</b>
Vr [N]	2397	1929	1463	996	531	66	-398	-861	<b>-1324</b>
Vl [N]	2397	2865	3334	3803	4273	4744	5216	5688	<b>6161</b>
Tr [N]	28102	28066	28038	28018	28005	28000	28003	28013	<b>28031</b>
<b>TI [N]</b>	<b>28102</b>	<b>28146</b>	<b>28198</b>	<b>28257</b>	<b>28324</b>	<b>28399</b>	<b>28482</b>	<b>28572</b>	<b>28670</b>

With reference to Table 2, notice the following:

- As the difference in elevation increases from 0 to 45m, the vertical force at the left support increases from 2397 N to 6161 N and the downward vertical force on the right support becomes negative (uplift).
- The total tension never exceeds the horizontal component by more than 2.4%.
- When the difference in elevation equals slightly more than 25 m, the low point occurs at the right support point.
- At greater differences in elevation, the low point position of the catenary occurs beyond the right support point.

### 3.0 MODELING MECHANICALLY COUPLED SPANS

Transmission lines are usually comprised of multiple line sections. Each line section is terminated at each end by a strain structure that allows no longitudinal movement of the conductor attachment points as shown in Figure 11. Note that the insulator strings in this structure experience the full tension of the conductor and that the point at the end of the insulator string, where the conductor is attached, is not free to move in the direction of the line.



Figure 11 - Typical strain angle structure used to terminate a transmission line section.

Between such strain structures, tangent suspension structures are used. A typical tangent suspension structure is shown in Figure 12. Here the insulators are free to move both transversely and longitudinally to the line. Any modest difference in conductor tension between adjacent spans would result in a movement of the bottom of the insulator string and an equalization of the tensions between the spans.

Given the free longitudinal movement of the attachment points at each tangent suspension structure, the horizontal component of the conductor tension in all the spans in a line section is approximately equal. This simplifies the sagging of conductor after stringing. Since the horizontal tension is equal in each span, the sag is simply proportional to the square of the tangent span length. Some suspension structure supports allow only free longitudinal movement (V-strings) but restrict movement transversely to the line.

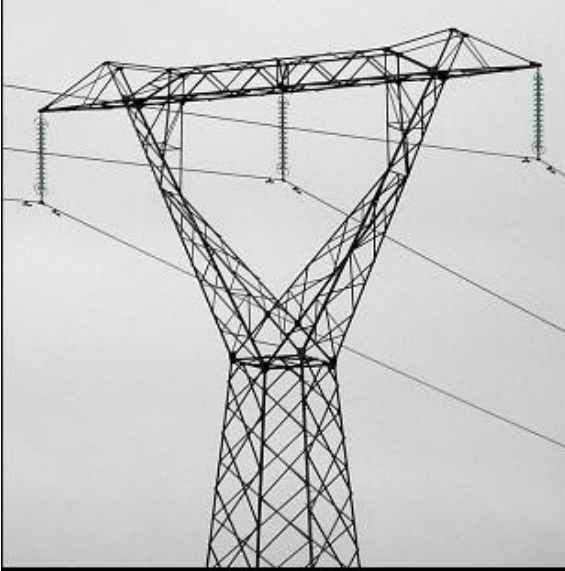


Figure 12 - Typical suspension structure

Post-type insulators only allow limited longitudinal and transverse motion at support points due to flexing of the insulators and of the structures themselves (wood and steel pole structures flex more than steel lattice structures).

### **3.1 Mechanical Equilibrium at Suspension Points**

In a practical transmission line, it is neither possible nor necessary to make all span lengths equal.

During stringing of conductor [10] and subsequent sagging, stringing blocks (pulleys) are attached to the bottom of the suspension insulators. In level terrain, the sagging tension in all spans is approximately equal and sags in each span are simply proportional to the span length squared as shown in equation (2). In uneven terrain, the unequal inclination angle of the conductor at adjacent spans requires the calculation of sag adjustments and clipping offsets.

Once the sag is adjusted, the blocks removed, and the conductor clamped (clipped) to the end of the insulator, changes in conductor temperature or load per unit length will yield different tensions in each span. Small movements of the suspension points, however, equalize the tension between spans. For example, consider Figure 13 which shows the tension difference that develops between an adjacent 250m and 350m span without insulator swing when the tension in each span is equal at 15°C.

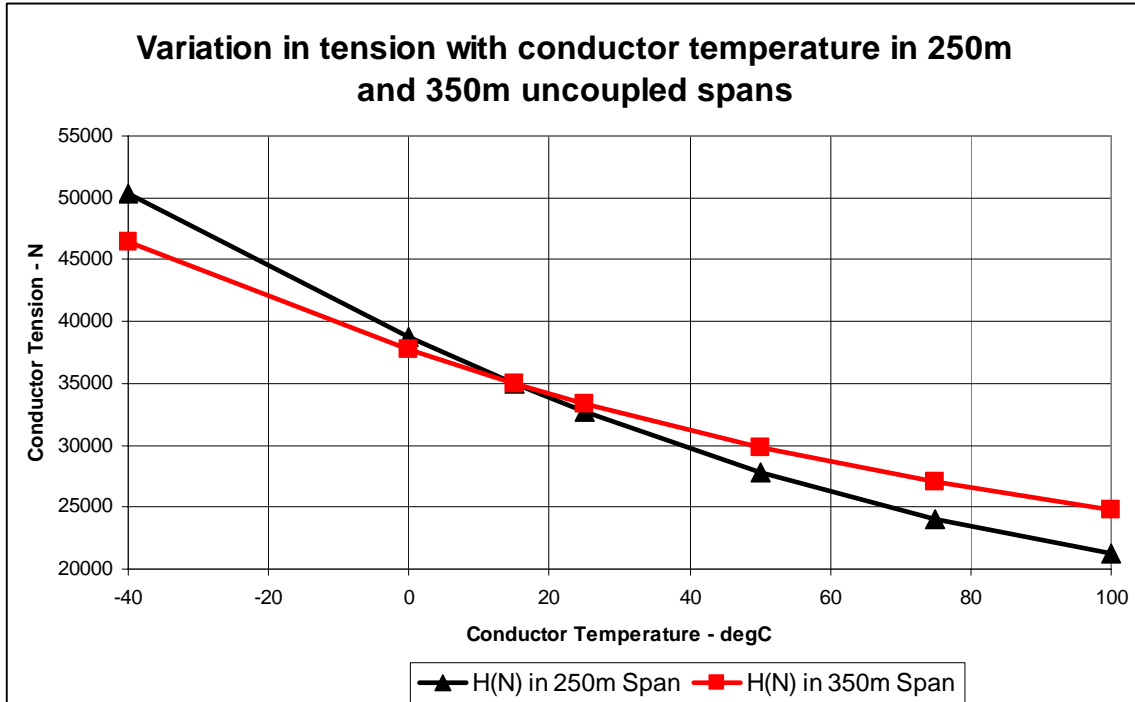


Figure 13 - Conductor Tension Variation with Temperature for 250m and 350m "Dead end" Spans of Drake A1/S1A (ACSR) installed to 35 kN at 15°C.

The longitudinal movement required of the insulator string in order to equalize tension in adjacent spans is usually very small. However, when the spans are sharply inclined or the conductor tension is very low, the typical suspension insulator configuration may not be able to fully equalize tensions. The amount of insulator "tilt" can be calculated by summing the force moments about the insulator attachment point as shown Figure 14.

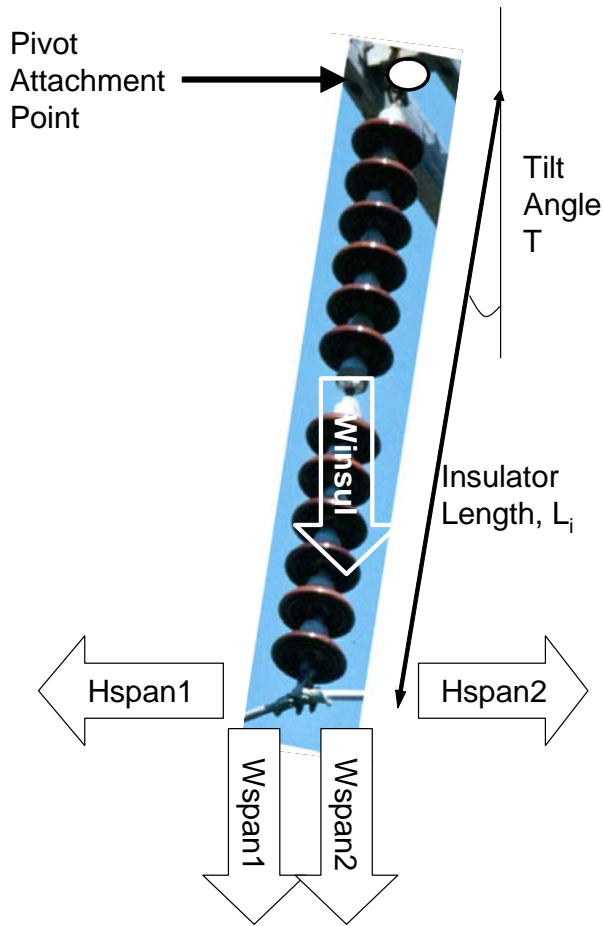


Figure 14 - Moment Forces acting on a ceramic, glass, or composite Insulator Suspension String

Based upon the moment force balance illustrated in Figure 14, for a 1.8 m long insulator string weighing 890 N, with a bare Drake conductor having a total weight span ( $W_{span1} + W_{span2}$ ) of 300m (a vertical conductor weight of 4791 N), Figure 15 shows that only modest force is required to move the insulator string “out of plumb”.

Reading from Figure 15, a horizontal movement of only 20 cm (i.e. a tilt angle of 6.3 degrees) is enough to equalize a span to span conductor tension difference of 580 N.

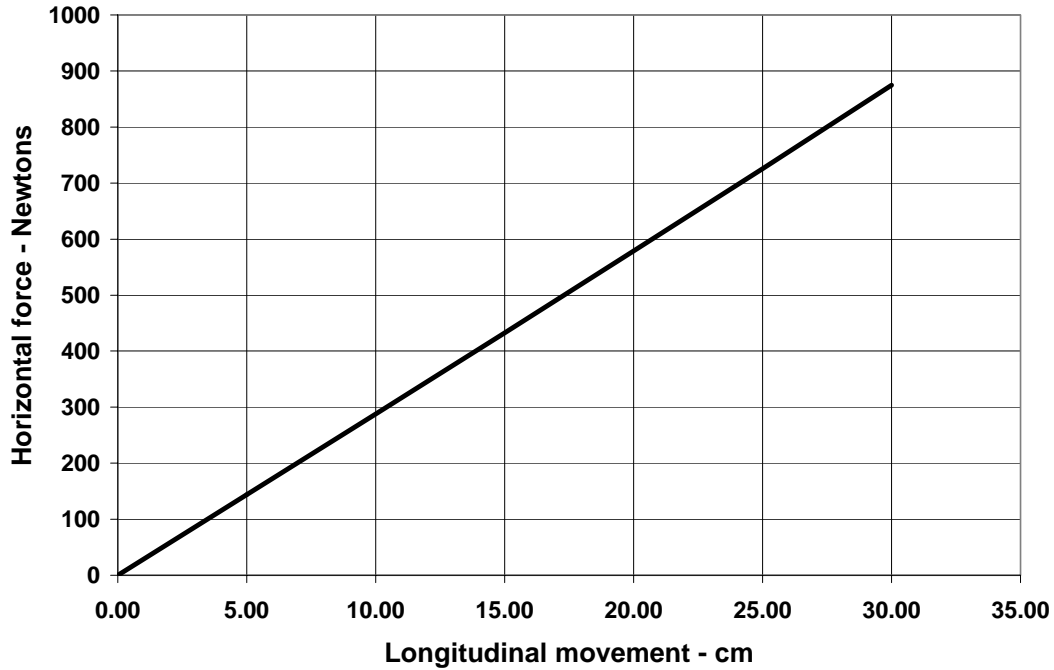


Figure 15 – Unbalanced horizontal tension vs. horizontal deflection for a 1.8m long Insulator String weighing 890N supporting a 300m weight-span of Drake ACSR.

Table 3 (and Figure 13) shows the variation in tension with temperature for 250m and 350m “dead-end” spans of Drake conductor, each strung to an initial tension of 35kN at 15°C. From the top row of Table 3 one can see that, at 100°C, the difference in longitudinal conductor tensions between the 250m and 350m dead-end spans would be approximately 3.5 kN. If the spans are adjacent, and the “dead-end” between them is replaced with the suspension insulator described in Figure 15, a horizontal movement of 68 mm is sufficient to reduce the tension difference from 3500 N to 197 N (see the shaded row of Table 3).

Table 3 – Resultant Force between 250m and 350m dead-end spans of ACSR Drake at 100°C

Longitudinal Swing m	Sag 100C 250m m	Sag 100C 350m m	L-S Slack 250m m	L-S Slack 350m m	Tension @100C 250m N	Tension @100C 350m N	Long. Tension Diff N	Insul Long. Force N
0	5.89	9.91	0.3700	0.7483	21177	24670	-3493	0
0.02	5.73	10.04	0.3500	0.7683	21774	24347	-2573	58
0.04	5.56	10.17	0.3300	0.7883	22424	24036	-1612	116
0.05	5.48	10.24	0.3200	0.7983	22772	23885	-1113	145
0.06	5.39	10.30	0.3100	0.8083	23136	23737	-601	174
0.062	5.37	10.31	0.3080	0.8103	23211	23707	-496	180
0.064	5.36	10.33	0.3060	0.8123	23287	23678	-392	186
0.066	5.34	10.34	0.3040	0.8143	23363	23649	-286	191
0.067	5.33	10.34	0.3030	0.8153	23402	23635	-233	194
<b>0.068</b>	5.32	10.35	0.3020	0.8163	23440	23620	-180	197

Note that when initially plumb, the effect of small insulator swings (e.g. 0.0 to 0.02 m) on the moment due to tension difference (e.g. 3493 N to 2573 N) is much greater than the increase in restoring force due to insulator swing (e.g. 0 to 58 N). Any final residual tension imbalance will be due only to the force provided by the insulator swing.

### 3.2 Ruling Span Sag-tension Calculations

In an overhead line, a typical “line section” can consist of as few as one and as many as 40 or 50 suspension spans (depending on the utility design philosophy) between dead-end strain structures.

If all of the suspension spans were the same length and reasonably level, and all were subject to the same ice and wind loads, then the sag and tension change with ice and wind and conductor temperature would be the same for all spans. Sag-tension calculations for any one of the suspension spans would apply to all, the tension and sag variation in each suspension span would be similar, and there would be little or no movement of the suspension strings between spans.

In most line sections, however, the suspension spans vary in length (though typically not over a large range), the sag and tension variation with ice, wind, and temperature changes in each span is different (e.g. see Figure 13), and the suspension insulators do not remain plumb. To solve this complex coupled mechanical system, sag-tension calculations must be performed for each span, the suspension point supports modeled mechanically, and the sag-tension variation in each span determined by numerical analysis. This exact calculation of sag-tension for multiple, mechanically coupled suspension spans, is certainly possible in this age of digital computers, but it may not always be necessary.

As an alternative to the exact solution for sag-tension in a line section consisting of two or more reasonably level suspension spans, sag-tension calculations can be performed for a single “ruling” span (also called “equivalent” span) [11, 12]. The ruling span method is possible because of the efficient tension equalization that occurs naturally at suspension points, as described in the preceding section of this brochure. The ruling span tension variation with ice and wind loading, time, and conductor temperature is essentially the same as the tension variation for any span of the line section, and the sag variation is proportional to the suspension span over ruling span length squared.

The ruling span is defined by equation (11):

Where:

$$RS = \sqrt{\frac{S_1^3 + S_2^3 + \dots + S_n^3}{S_1 + S_2 + \dots + S_n}} \quad (11)$$

- RS = Ruling span for the line section containing n suspension spans
- S<sub>1</sub> = Span length of first suspension span
- S<sub>2</sub> = Span length of second suspension span



$S_n$  = Span length of nth suspension span

Note from equation (11) that the value of the ruling span is greatly influenced by the longest spans since the numerator depends on the cube of span length.

Since the tension in all of the suspension spans is equal (or nearly so), once the sag and tension for a ruling span has been calculated, the sag in any of the corresponding suspension spans can be calculated as follows:

$$D_i = D_{RS} \cdot \left( \frac{S_i}{S_{RS}} \right)^2 \quad (12)$$

Of course, suspension insulators do not allow complete tension equalization between adjacent spans of different length. However, as shown in Section 3.1, the tension difference is usually acceptably small. The concept works well for the calculation of stringing sags, which permit sag measurements on a few selected spans to be adequate for initial conductor sagging.

Consider two spans where the support between them is rigid or longitudinally flexible. The three cases shown in Table 4 are: (1) The support between the spans is rigid (spans mechanically independent); (2) The support between the spans moves freely in the longitudinal direction (ruling span approach); (3) The support point is at the end of a 1.8 m, 890 N insulator and the tension equalization is calculated exactly, accounting for insulator swing moments.

Table 4 - Comparison of sag-tension for two spans which are mechanically independent, perfectly coupled, and coupled with actual tension inequality.

	Case 1 – Two dead-end spans		Case 2 – Two suspension spans with perfect tension equalization		Case 3 – Two suspension spans with actual tension imbalance at supports	
Span [m]	250	350	250	350	250	350
Sag @100C [m]	7.7	13.0	6.9	13.6	7.0	13.5
Tension @100C [kN]	17.1	19.9	19.0	19.0	18.8	19.0

In Case 3, the insulator string has swung 1.7 degrees toward the longer span at 100°C. Note that the errors in the ruling span approach (perfect tension equalization) are modest.

A recent technical paper [13] provides some guidance concerning line conditions in which sag errors resulting from the ruling span concept may become significant. The conclusion of the reference is that errors are modest except in those line designs where there are relatively large variations in span length and where the conductors are operated at temperatures above 100°C.

## 4.0 CONDUCTOR TENSION LIMITS

Sag-tension calculations, with or without the ruling span approximation, are normally done numerically. Constraints on maximum tension and maximum sag are typically applied for several loading conditions. The user is also allowed to enter multiple ice and wind loading and conductor temperature conditions. The conductor elongation (consisting of thermal, plastic and elastic components) is considered in the calculation. This section of the brochure discusses how tension constraints are selected and why they are an important part of any sag-tension calculations.

### 4.1 Conductor tension limits under high ice and wind loading

Limits on conductor tension can be expressed as a percentage of the conductor’s rated tensile strength ( RTS), as a conductor tension value, or as a catenary constant (H/w). Under high ice and wind loading, the conductor tension increases and, unless constrained by design, the conductors or supporting structures (plus splices and dead-end fittings) may fail.

To avoid failure under high ice and wind loading, the conductor’s initial unloaded tension at the time of construction or reconductoring, is usually limited to a modest value (Table 5).

Table 5 – Sag-tension for maximum ice and wind load and for high temperature shown as a function of initial stringing tension for a 300m span of Drake ACSR.

Initial unloaded tension at 15°C [%RTS]	Max. design tension under ice and wind load [%RTS]	Max. design tension under ice and wind load [kN]	Initial Sag at 15°C [m]	Final Sag at 100°C [m]
10	22.6	31.6	12.9	14.6
15	31.7	44.4	8.6	11.0
20	38.4	53.8	6.4	9.4
25	43.5	61.0	5.1	8.4

Table 5 shows typical results of sag-tension calculations as a function of the initial installed stringing tension. The conductor is 403mm<sup>2</sup>, 26/7 ACSR (403-A1/S1A-26/7) Drake, the ruling span is 300 m, and the ice and wind load conditions are 12.5 mm radial glaze ice with a 380 Pa wind at -20°C. The difference between initial and final sags is estimated on the basis of plastic creep elongation calculations.

The maximum conductor and structure tension loads increase with increasing initial installed tension, while the sag decreases. To avoid conductor tensile failure under high ice and wind loads, the conductor tension under maximum ice and wind is usually limited to 50% - 60% of RTS.

Typical values accepted internationally, as well as in IEC 60826, are as follows:

- 50 to 75% RTS under maximum climatic heavy load conditions;
- 20 to 30% RTS with no ice or wind at 15°C when the conductor is initially installed under tension;

- 15 to 25% RTS with no ice or wind at 15°C the conductor being in its final condition (after the conductor has been exposed to a heavy ice and wind loading event or has been in place for many years.)

Notice that, while limiting the initial unloaded conductor tension limits subsequent maximum conductor and structure loads (e.g. see Table 5), unloaded tension constraints are primarily imposed to limit aeolian vibration to manageable levels. While limiting initial and final unloaded tensions to certain ranges of %RTS is common as a means of vibration control, recent work by CIGRE WG B2.11 suggests that limiting the catenary constant ( $H/w$ ) for the coldest month is better. This is discussed briefly in the following section.

## **4.2 Avoiding Aeolian Vibration Fatigue**

Historically, as noted above, a common design practice used to avoid conductor fatigue, due to aeolian vibration, was to limit the unloaded tension to 15% to 25% of RTS. Specifying an unloaded %RTS value at everyday conditions does not consider the following important fatigue endurance issues:

- The effect of persistency of wind speed and direction relative to the line section;
- Terrain covers of trees, shrubs and buildings and the terrain itself, which can have a marked effect on the degree of wind turbulence;
- Short-span construction with high tensions at low-temperature operation, where significant damage may occur during months of winter temperatures;
- The effect of conductor stranding and the percentage of steel in ACSR, which influences effects on mass and strength.

CIGRE WG B2.11 has suggested a better approach where the tension control parameter is tension-over-weight ( $H/w$ ). The  $H/w$  parameter is more closely related to aluminum stress, and therefore to the self-damping properties of the conductor. Three papers [14, 15, 16] have been published concerning single undamped conductors, damped single conductors, and bundled conductors, respectively. In these papers, the  $H/w$  parameter is justified and other influences such as span length and terrain are considered.

For unprotected round strand, single conductors (no armor rods, dampers, nor AGS clamps), the recommended maximum values of  $H/w$  range from 1000 to 1425 m under initial unloaded low temperature conditions [14]. As can be seen in Table 6, for Drake ACSR in a 300 m span, this acceptable range of  $H/w$  values where dampers are not used, corresponds to an unloaded initial tension of between 10% and 15% RTS at 15C.

If dampers are used, then a higher  $H/w$  level would likely be acceptable, but the WG B2.11 references repeatedly make the point that avoiding conductor fatigue from aeolian vibration over the entire life of an overhead line can be complex. Terrain, span length, annual weather variation, conductor design, and external damping must all be considered. Simply choosing an installed unloaded tension in %RTS is not usually sufficient.

Table 6 - H/w limits on unloaded conductor tension - Drake ACSR in a 300 m span.

Initial, unloaded conductor tension at 15°C [%RTS]	Initial unloaded H/w at average temp. for coldest month) [m]	Tension at - 20°C with max ice and wind load [%RTS]	Tension at max ice and wind load [kN]	Final sag at 100°C [m]
10	900	22.6	31.6	14.6
15	1500	31.7	44.4	11.0
20	2100	38.4	53.8	9.4
25	2700	43.5	61.0	8.4

## 5.0 CONDUCTOR ELONGATION - ELASTIC, PLASTIC, AND THERMAL

As shown in section 2.3, relatively small changes in the length of suspended overhead conductors can cause rather large changes in sag. A change of only 0.1 m in the length of a 300 m long conductor can change the sag by nearly 1 m. Small amounts of elastic, plastic, or thermal elongation yield the same result: a longer conductor, and relatively large changes in sag.

Most power line conductors consist of concentric stranded aluminium wires reinforced with a stranded steel wire core (ACSR or A1/Syz) although all aluminium and all aluminium alloy conductors (AAC and AAAC) are also in common use. In comparing the various methods of “sag-tension” calculation used in countries and utilities around the world, the working group noted large differences in how conductor elongation was calculated for changes in conductor temperature, tension, and time, yet only minor differences in the modeling of catenaries and in the modeling of span coupling of suspension spans.

### 5.1 Overview of Conductor Elongation Models

As explained in Section 6 of this document, the sag and tension of a given span or line section can be calculated as a function of conductor temperature and ice/wind loads by equating the catenary length to the conductor length. This is normally done numerically although it is explained graphically.

At the time of installation, the conductor sag or tension is measured with the conductor unloaded at a known temperature. Sag and tension typically change as: (a) the conductor weight increases due to ice and wind loading; (b) the conductor temperature changes due to changes in air temperature, solar heating and electrical current; and (c) as the conductor’s aluminium layers elongate plastically over time or with design ice and wind loading.

In order to calculate the sag and tension under various loading, temperature, and time conditions, one must be able to model the change in conductor length due to each factor. Once the various conductor elongation models are known, then the tension can be found at which the total conductor length,  $L$ , of loaded conductor equals the sum of the original length (unloaded length) and any plastic, thermal and elastic changes in length due to changes in tension, time, loading, and temperature.

Clearly, the methods of sag-tension calculation are a function of the conductor elongation models. If conductor elongation, due to changes in temperature and tension, is represented by simple linear elongation models, sag-tension can be determined quite simply. If plastic conductor elongation is represented by typical values based on field experience, then the sag-tension calculation method is only marginally more complex, but if plastic conductor elongation is calculated based on non-linear equations which depend on high tension load events and time, then sag-tension calculations become quite complex and must be done graphically or numerically[17].

Although the working group investigated a great variety of sag-tension calculation methods, we were able to classify the different sag-tension calculation methods into one

of three reasonably distinct approaches to modeling conductor elongation. These three approaches are summarized as follows:

- **Linear Elastic (LE) Model** – Overhead conductors are modeled as linear springs with a single elastic modulus and a single coefficient of thermal elongation. An effective elastic modulus and effective coefficient of thermal elongation must be calculated for non-homogeneous conductors (e.g. ACSR). Typical values of modulus and CTE are used.
- **Simplified Plastic Elongation (SPE) Model** – Overhead conductors are modeled as linear springs. Plastic conductor elongation is calculated by adding a typical permanent change in length (usually expressed as an equivalent temperature change). The amount of plastic elongation is based on experience rather than on laboratory tests or design loads.

Normally, the conductor elastic modulus and coefficient of thermal elongation are single valued but for non-homogeneous conductors such as ACSR (A1/S1A), the different tensions in the aluminum layers and steel core can be calculated for the typical plastic elongation but the variation with design loading cannot. For high conductor temperatures, a typical knee-point temperature can be calculated but any dependence on conductor type, design load, and span length cannot.

The excessively high initial loaded tensions that result from ignoring the initial non-linear behavior of the aluminium layers are usually reduced by experienced engineers or used as an additional safety margin in structure design.

- **Experimental Plastic Elongation (EPE) Model** – Overhead conductors are modeled as non-linear springs that elongate elastically as a function of tension, plastically as a function of tension and time, and thermally as a function of temperature. The non-linear behavior of steel core and aluminum layers can be modeled separately for ACSR (A1/SA1). Plastic elongation is calculated based on laboratory tests of stranded conductors. For non-homogeneous conductors, the elongation of each component (e.g. steel and aluminum) is calculated separately. Plastic elongation of the conductor due to “settling”, “creep elongation”, and “permanent elongation due to high tension loads” is calculated for an assumed series of loading events over the life of the line. For A1/Syz conductors at high temperature, the bi-linear thermal elongation and any aluminium compression effects are calculated as a function of assumed loading history.

Clearly, there are many variations on these three elongation models. For example, though the calculation methods differ considerably in detail, both the strain-summation and the Varney graphical calculation methods utilize similar experimental conductor data and thus may be considered to be variations on the EPE model.

Similarly, in estimating typical plastic elongation in the SPE elongation model, the assumed plastic elongation will vary considerably based on the experience and judgment of engineers in different countries, using different line designs, in various types of terrain. Nonetheless, in each application, the plastic elongation is based upon experience and not upon laboratory experiments and loading assumptions.

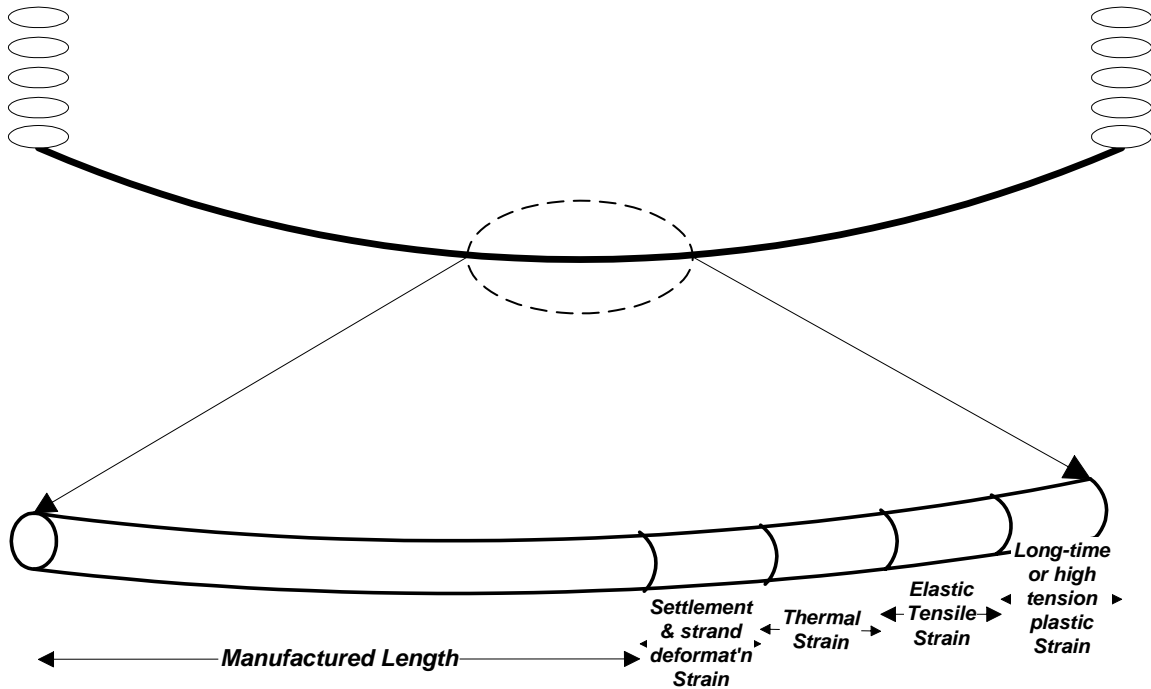


Figure 16 - Elongation diagram of stranded conductor in a catenary.

With reference to Figure 16:

- The LE model ignores “settlement & strand deformation” as well as “long-time or high tension plastic strain” (though such plastic elongation may be allowed for by the use of large clearance buffers).
- The SPE model ignores the settlement and strand deformation that occur during initial tensioning of conductor but account for long-time or high tension creep plastic elongation by using a typical value of plastic conductor elongation (often expressed as a temperature “adder”).
- The EPE elongation model allows the engineer to calculate both settlement & strand deformation and long-time or high tension plastic strain based on laboratory conductor test results and an assumed line design and load sequence. Plastic conductor elongation increases with initial installed tension and decreases the ratio of steel to aluminum crosssectional area.

All three elongation models assume linear elastic elongation under tensile load and linear thermal elongation due to changes in conductor temperature. They differ in the manner in which plastic elongation is calculated.

In North America, EPE models are used almost exclusively. The Varney Graphical method, implemented in a computer program which utilizes experimental conductor test data, is in wide use. Experimental stress-strain and creep data, represented by 4<sup>th</sup> order polynomials, is widely available for all common conductor types and sizes [18].

Conductor test data for use in the SPE and possibly the EPE elongation models can be found in IEC Technical Report 1597 [2]. This report also describes a method whereby the linear modulus of stranded homogeneous and non-homogeneous conductors can be estimated from the cross-sectional area(s), the stranding, and the wire material. The typical plastic elongation of aluminium and A1/Syz (ACSR) conductors, which occurs over extended periods of time, for use with the SPE model, is also to be found in this publication.

## **5.2 Linear Thermal and Elastic Elongation**

The original length of the conductor is assumed to be that produced by the manufacturer (“manufactured length”) at the time that the conductor was stranded and wound on the reel for delivery. On the reel as delivered, the conductor tension is nearly zero. If the conductor has a steel core, then the length of steel core and the aluminium layers wound around it are nearly equal. Rawlins [19] has suggested that there may be residual stresses in the aluminium layers as a result of the stranding process but this is only important when estimating high temperature sag.

In the LE and SPE conductor elongation models, the stranded aluminium conductor is assumed to elongate linearly and reversibly in response to modest changes in tension (Elastic Elongation) and to modest changes in conductor temperature (Linear Thermal Elongation). The linear and reversible change in length (elongation) in response to modest changes in tension and temperature is assumed to behave as was shown in equations (8) and (9). The stranded conductor is represented as a linear “spring” which changes length in response to changes in tension and temperature, returning to its original length when the tension or temperature is returned to their original value.

With the EPE conductor elongation model, the stranded aluminum conductor is assumed to elongate non-linearly with tension when first loaded due to strand deformation and settlement. However, once loaded to a tension  $H_1$ , the conductor behaves linearly at tensions below  $H_1$ . According to the EPE model, if the conductor tension subsequently exceeds  $H_1$ , the conductor again elongates non-linearly as a result of additional strand settlement and deformation up to a new, higher tension  $H_2$ , yet linearly afterward at tensions below  $H_2$ .

Thus, in all three elongation models, the conductor is assumed to behave linearly with tension under all or most field conditions.

### *5.2.1 Linear Elastic Strain - All Aluminium Conductors*

As described in IEC technical brochure 1597, the elastic elongation of a stranded conductor can be represented by the equation:

$$L_H = L_{REF} \left( 1 + \frac{H - H_{REF}}{E \cdot A} \right) \quad (13a)$$



$$\frac{\Delta L}{L} = \varepsilon = \frac{\Delta H}{E \cdot A} \quad (13b)$$

Where:

$L_H$  = Length of conductor under horizontal tension  $H$

$L_{REF}$  = Reference length of conductor under horizontal tension for no ice or wind load at everyday temperature  $H_{REF}$

$E$  = Modulus of elasticity of the conductor

$A$  = Conductor cross-sectional area

$\varepsilon$  = Strain or relative elongation expressed in  $\mu s$  or  $1 \cdot 10^{-6}$

$H/A$  = Stress (tension divided by area)

According to IEC 1597, reasonable values for the modulus of all aluminium stranded conductors, regardless of alloy are shown in Table 7. These values are in rough agreement with other recommendations from the literature.

Table 7 - Typical Linear Elastic Modulus for All Aluminium Conductors

Number of Strands	Elastic Modulus - GPa
7	63.3
19	61.2
37	58.9
61	58.3

According to equation (13), for a 403-A1-37 strand conductor, the elastic strain corresponding to the application of a 12kN (20% of its RTS) tension is 506  $\mu s$  (0.000506 or 0.0506%). For a 300 m length of conductor, the change in length corresponding to application of a tension of 12 kN is only 152 mm.

*Notice that the conductor strain unit “micro-strain” is abbreviated “ $\mu s$ ”. As may be seen in equations (13), the use of GPa for modulus,  $E$ , and mm<sup>2</sup> for the area,  $A$ , yields conductor strain in  $\mu s$ .*

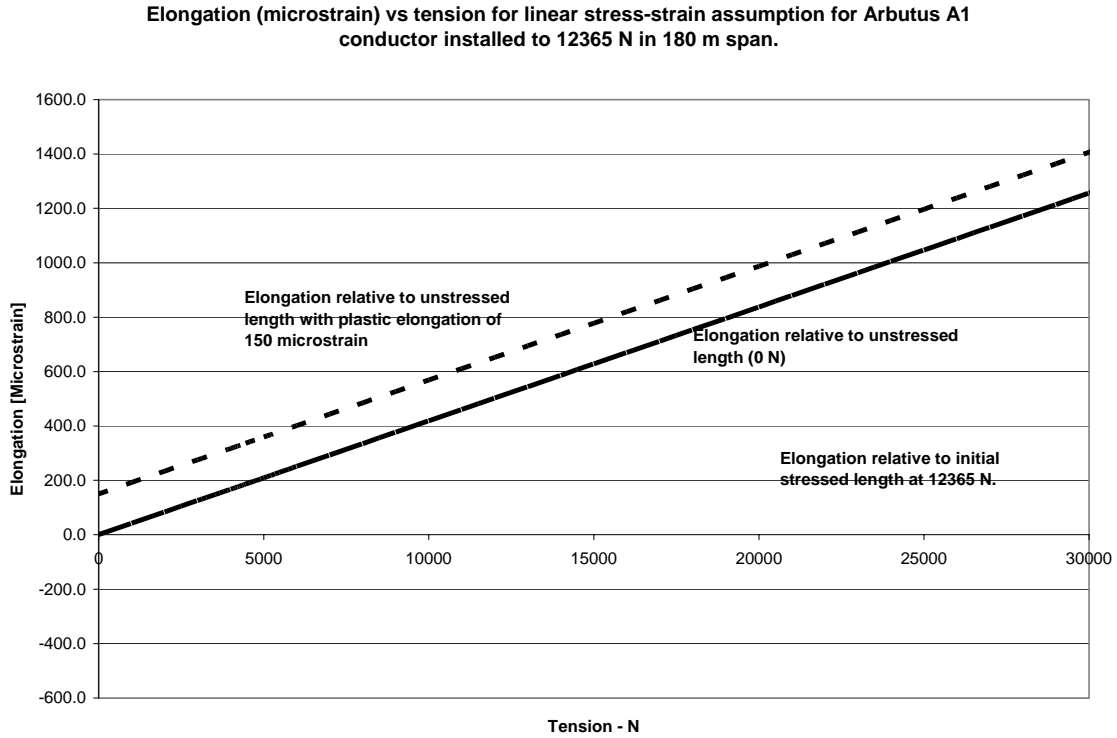


Figure 17 - Assumed linear stress-strain behavior of a 402-A1-37 Arbutus conductor with and without plastic elongation.

The preceding equations (13), the calculation example, and Figure 17 all show how stranded A1 conductors, assumed to have a linear stress-strain characteristic, elongate under load. Notice that the assumption of linear stress-strain behavior does not preclude consideration of unstressed length changes due to “reversible” changes in temperature or to “irreversible” length changes due to plastic elongation. The top curve in Figure 17 illustrates the linear stress-strain behavior of the all aluminium conductor after it has experienced a permanent plastic length increase of 150  $\mu\text{s}$  due to either a temperature change or due to plastic elongation.

### 5.2.2 Linear Thermal Strain – All Aluminium Conductor

For all aluminium (alloy) conductors, the equation for linear thermal elongation is:

$$\frac{\Delta L}{L} = \alpha_A \cdot \Delta T_C \quad (14)$$

Where:

$\alpha_A$  = Aluminium coefficient of linear thermal elongation ( $23 \cdot 10^{-6} \text{ }^\circ\text{C}^{-1}$ )  
 $\Delta T_C$  = change in conductor temperature in  $^\circ\text{C}$

*Notice that equation (14) can be used to convert a change in strain into an equivalent change in conductor temperature. 115  $\mu\text{s}$  is equivalent to a temperature change of  $5^\circ\text{C}$  ( $115 \cdot 10^{-6} / 23 \cdot 10^{-6}$ ) for an all aluminum conductor.*

### 5.2.3 Linear Elastic Strain - Non-Homogeneous ACSR (A1/Syz) Conductors

Approximately 80% of bare overhead stranded conductors used in power lines are ACSR (A1/Syz). With a non-homogeneous stranded conductor such as ACSR, the equation for elastic behavior is more complex than with all aluminum conductors. The composite stiffness (elastic modulus) depends not only on the modulus of each component but also on their relative cross-sectional areas. This section discusses how the composite conductor modulus can be calculated if the component modulus and area is known. Even though the equations in the following refer to A1/S1A conductor, the concept applies equally well to non-homogeneous conductors constructed from other materials.

The total tension,  $H_{AS}$ , in the non-homogeneous conductor is the sum of the tensions in the outer layers,  $H_A$ , and the core,  $H_S$ :

$$H_{AS} = H_A + H_S \quad (15)$$

The strains of the aluminium and steel components must be equal since the two components are bound together at the ends of the conductor:

$$\varepsilon_{AS} = \varepsilon_A = \varepsilon_S \quad (16)$$

Given the link between stress and strain in each component as shown in equations (13), the composite elastic modulus,  $E_{AS}$  of the non-homogeneous conductor can be derived by combining the preceding equations:

$$\varepsilon_{AS} \equiv \frac{H_{AS}}{A_{AS} \cdot E_{AS}} = \frac{H_A}{A_A \cdot E_A} = \frac{H_S}{A_S \cdot E_S} \quad (17)$$

The component tensions are then found by rearranging equations (17):

$$H_A = H_{AS} \cdot \frac{E_A \cdot A_A}{E_{AS} \cdot A_{AS}} \quad (18a) \quad \text{and} \quad H_S = H_{AS} \cdot \frac{E_S \cdot A_S}{E_{AS} \cdot A_{AS}} \quad (18b)$$

Finally, in terms of the modulus of the components, the composite linear modulus is:

$$E_{AS} = E_A \cdot \frac{A_A}{A_{AS}} + E_S \cdot \frac{A_S}{A_{AS}} \quad (19)$$

The two terms on the right hand side of this equation are sometimes referred to as the “virtual modulus” of the outer layers and the core, respectively. Note that a stress-strain plot for ACSR showing the component modulus multiplied by the area fraction can be simply added to find the total modulus.

As noted in Table 8, typical values of  $E_S = 190$  GPa and  $E_A = 55$  GPa are suggested in [2] for stranded steel and aluminium components, respectively.

Table 8 - List of Conductor Final Modulus Values

A1/Syz Stranding	Typical Published Value of Final Modulus - GPa	Steel Core Area Fraction of Total	Calculated Elastic Final Modulus* - GPa
6/1	79.0	14%	74.3
18/1	68.0	6%	62.5
22/7	71.0	9%	67.2
26/7	74.2	14%	73.9
45/7	64.5	6%	63.7
54/7	67.1	11%	70.5
54/19	69.7	11%	70.5
72/7	61.1	4%	60.6
72/19	61.0	4%	60.6
84/7	66.6	8%	65.4
84/19	66.5	8%	65.4

\* - Calculated based on  $E_A = 55\text{GPa}$  and  $E_S = 190\text{GPa}$ .

According to equation (19) and Table 8, even modest steel areas (e.g. 11% of total area) greatly “stiffen” aluminium conductors, increasing the composite modulus from 55 to 68-70 GPa (approximately 25%). Such stiffening reduces the sag increase under heavy ice and wind loads and yields higher maximum tension loads on angle and dead-end structures.

The presence of a steel core also reduces thermal elongation and increases the rated tensile strength of the conductor (e.g. the RTS of 26/7 ACSR is 225% that of an all aluminum conductor with the same electrical resistance).

#### 5.2.4 Linear Thermal Strain - Non-Homogeneous A1/S1x Conductor

For non-homogeneous stranded conductors such as ACSR (A1/Syz), the composite conductor’s rate of linear thermal expansion is less than that of all aluminium conductors because the steel core wires elongate at half the rate of the aluminium layers. The composite coefficient of linear thermal expansion of a non-homogenous conductor such as A1/Syz may be calculated from the following equations:

$$\alpha_{AS} = \alpha_A \left( \frac{E_A}{E_{AS}} \right) \left( \frac{A_A}{A_{AS}} \right) + \alpha_S \left( \frac{E_S}{E_{AS}} \right) \left( \frac{A_S}{A_{AS}} \right) \quad (20)$$

The linear thermal elongation coefficient of aluminium is twice that of steel. Therefore, as the temperature of an A1/Syz conductor increases, while the entire conductor elongates according to the composite coefficient of linear thermal expansion shown above, there is also a transfer of tension from the aluminium strands into the steel strands.

For example, with 403mm<sup>2</sup>, 26/7 ACSR (403-A1/S1A-26/7) “Drake” conductor, the composite modulus and thermal elongation coefficient, according to (19) and (20) are:

$$E_{AS} = 55 \cdot \left( \frac{402.8}{468.6} \right) + 190 \cdot \left( \frac{65.8}{468.6} \right) = 74 \text{ MPa}$$

$$\alpha_{AS} = 23e-6 \cdot \left( \frac{55}{74} \right) \cdot \left( \frac{402.8}{468.6} \right) + 11.5 \cdot 10^{-6} \cdot \left( \frac{190}{74} \right) \cdot \left( \frac{65.8}{468.6} \right) = 18.84 \cdot 10^{-6}$$

### 5.3 Simplified Plastic Elongation (SPE) Model

The preceding equations apply to the elastic elongation of aluminium and steel wires in A1/Syz stranded conductor where both components are under load. But the aluminium wires also elongate plastically under tension. This plastic elongation of aluminium can be divided into three categories (refer to Figure 16):

1. Strand settlement & deformation (Initial Plastic Elongation) – When first loaded to a tension of 15% to 25% of RTS, during the process of stringing and sagging, the aluminium layers of the conductor elongate plastically by an amount which increases with tension.
2. Short-time high-tension plastic elongation (Design Loading Plastic Elongation) – After the conductor has been sagged and clipped, ice and/or wind may raise the tension to much higher levels (e.g. 30% to 80% of RTS) for relatively short times (1 hour to 24 hours). This causes additional plastic elongation of the aluminium layers and lesser plastic elongation of any steel core.
3. Long time “metallurgical” creep elongation (Creep Plastic Elongation) – After the conductor has been sagged and clipped, the aluminium layers will continue to elongate plastically even for moderate “everyday” tensions of 15% to 25% of RTS. Over 10 years or more, the plastic elongation of aluminium layers due to such long-time creep elongation may exceed that associated with high short-time loads. This is especially true in geographical areas not subject to ice or hurricane force winds.

With reference to the Linear Elongation (LE) model defined previously in section 5.2, plastic elongation is completely ignored. In the Simplified Plastic Elongation (SPE) model, plastic elongation of the conductor is represented by a “typical value” based on experience and engineering judgment. Only in the Experimental Plastic Elongation (EPE) model (section 5.4) are the three types of plastic elongation considered separately and the combined resultant plastic elongation calculated as a function of tension, temperature, and time.

In the SPE model, a typical value of plastic elongation is specified to represent the combined effect of strand settlement and deformation, high tension load events, and sustained everyday tension of the life of the line. For a homogeneous conductor (e.g. all aluminum) the “initial” unstressed length of the conductor is simply increased by the amount of plastic elongation and the “final” greater sag and decreased tension are calculated by one of the methods described in section 6. For a non-homogeneous conductor (e.g. ACSR), however, the calculation is more complex because the creep elongation of the steel core wires is normally negligible. As the aluminum wires elongate plastically in ACSR, three things occur: the fraction of composite tension in the aluminum layers decreases; the fraction of composite tension in the steel core increases; and the composite tension decreases while the composite strain (i.e. sag) increases.

For ACSR conductor, neglecting any steel core plastic elongation, the “final” tensions in the steel core,  $H'_S$ , and in the aluminum layers,  $H'_A$ , is a function of the plastic aluminium strand elongation,  $\varepsilon_{CA}$ , as shown in equations (21).

$$\varepsilon = \frac{H'}{A_{AS} \cdot E_{AS}} = \frac{H'_A}{A_A \cdot E_A} + \varepsilon_{CA} = \frac{H'_S}{A_S \cdot E_S} \quad (21a)$$

Rearranging the preceding equations, the fractions of the “final” component tension in the aluminium and steel core can be found as a function of the component areas, the component elastic modulus of aluminium and steel, and the aluminium plastic strain:

$$\frac{H'_A}{H'} = \frac{E_A \cdot A_A}{E \cdot A} \cdot \left(1 - \frac{\varepsilon_{CA} \cdot E \cdot A}{H'}\right) \quad (21b)$$

$$\frac{H'_S}{H'} = \frac{E_S \cdot A_S}{E \cdot A} \cdot \left(1 + \frac{\varepsilon_{CA} \cdot E \cdot A}{H'}\right) \quad (21c)$$

As noted in IEC 1597, one can conclude from these equations that:

1. Plastic elongation in the aluminium strands ( $\varepsilon_{CA}$ ) reduces the fraction of the total conductor tension (see equation 21b) which is carried in the aluminium strands and increases the fraction carried in the steel core strands (equation 21c).
2. The increase in composite conductor length is a result of the increased elastic elongation of the steel core.
3. If the plastic elongation of the aluminum layers is sufficiently large, the tension in the aluminium strands can reach zero and then be negative (i.e. in compression).

Finally, note that the tension shifts described in these equations also occur at increased conductor temperatures because of the higher thermal elongation rate of aluminium as compared to steel. Plastic elongation in the aluminium layers reduces the conductor temperature at which the aluminium tension reaches zero (the “knee-point” temperature) with A1/S1x conductor.

Assuming that a Drake ACSR conductor is recently installed at 28 kN and 15°C, and that the aluminium strand layer plastic elongation due to settling and initial loading is  $\varepsilon_{CA} = 300 \mu\text{s}$ , then according to equations (21b) and (21c), the "initial" tensions in the aluminium layers and steel core are:

$$H_A = \frac{28 \cdot 55 \cdot 402.8}{74 \cdot 468.8} \cdot \left(1 - \frac{300 \cdot 10^{-6} \cdot 74 \cdot 468.6}{28}\right) = 11.2 \text{ kN}$$

$$H_S = 28 - 11.2 = 16.8 \text{ kN}$$

If the conductor temperature then increases to 45°C, the aluminium strands elongate at twice the rate of the steel core which causes an additional strain shift from the aluminium to the steel as follows:

$$\varepsilon = (\alpha_A - \alpha_S) \cdot \Delta T_C = 11.5E - 6 \cdot (45 - 15) = 345 \mu\text{s}$$

Ignoring any reduction in composite tension due to the increased length of the conductor, the tension distribution at 45°C is:

$$H_A = \frac{28 \cdot 55 \cdot 402.8}{74 \cdot 468.6} \cdot \left(1 - \frac{(300 + 345) \cdot 10^{-6} \cdot 74 \cdot 468.6}{28}\right) = 3.6 \text{ kN}$$

$$H_S = 28 - 3.6 = 24.4 \text{ kN}$$

According to equation (21a), this tension shift at constant composite conductor tension can only occur with a composite strain of:

$$\varepsilon = \frac{24.4}{65.8 \cdot 190} = 1952 \mu\text{s}$$

At somewhat higher temperatures, the aluminium tension goes to zero and all the tension is carried by the steel core. Beyond this temperature, the A1/S1x conductor elongates with temperature at the rate of steel. This temperature is commonly referred to as the "knee-point" temperature because it corresponds to the point at which the rate of increase of sag with temperature changes, showing as a "knee" on a plot of sag versus temperature. When the temperature of the conductor decreases, the aluminium strands once again come under tension and the conductor behaves according to the composite modulus and thermal elongation equations above.

For example, Figure 18 depicts 10 years of creep elongation of the aluminium strands which causes the "knee-point" to occur at a lower temperature because the plastic creep elongation has resulted in "stretched" aluminium strands requiring a lower temperature increase to fully unload to the steel core.

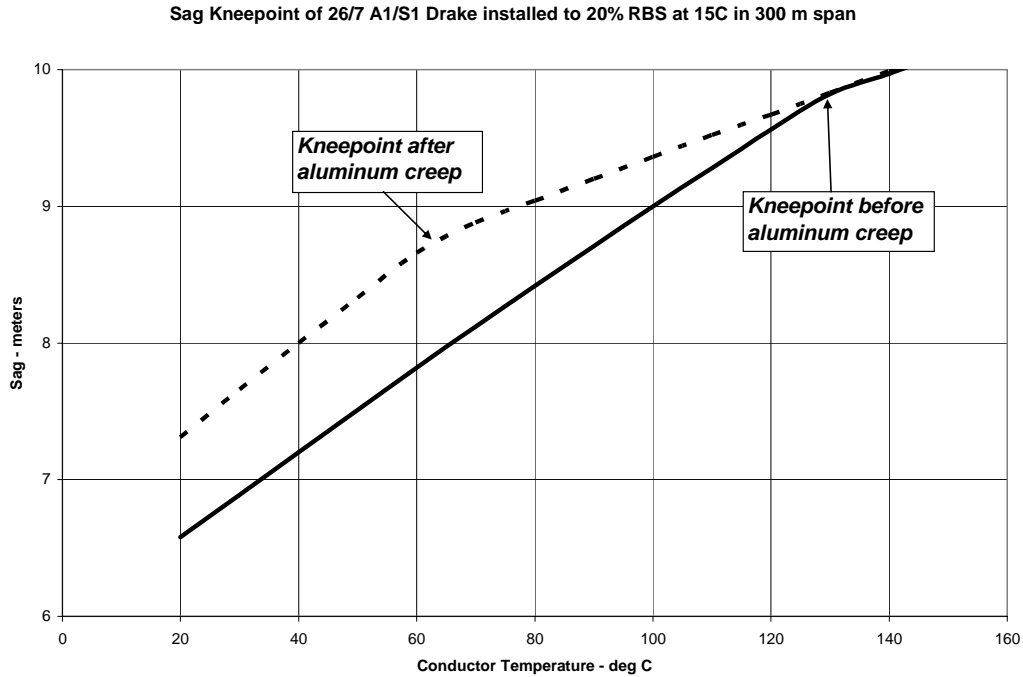


Figure 18 – “Knee-point temperature” as affected by creep elongation of aluminium strands.

Note how the “knee-point temperature” of the example (Drake A1/Syz in a 300 m span) moves from 135°C when the conductor is first installed to 60°C after aluminium creep for 10 years has occurred.

Tests of multi-layer A1/Syz, however, indicate that the “full hard” H19 aluminium layers support a modest level of compression beyond the “knee-point” temperature. Several theories have been proposed to model the composite conductor thermal elongation in this transition region beyond the knee-point temperature.

Rawlins [19] found that the increased sag at temperatures above the kneepoint are due to a combination of residual stress in the aluminium layers (a result of “two-pass” manufacturing stranding process) and interference between the helical layers trying to expand radially (lending the aluminium component layers a small compression modulus). Barrett [20] suggested that the aluminium layers can support up to 10 MPa (1500 psi.) of compression which can be increased by the relatively high radial temperature gradients that can occur at high current densities. Barrett notes a high level of random variation in the observed levels of thermal elongation beyond knee-point. Rawlins’ study found that the compressive aluminum stresses beyond the knee-point temperature to be insignificant. In Barrett’s studies of compression levels in A1/Syz, he found that the aluminium layers supported between 7 and 21 MPa (1000 and 3000 psi.).

Given the variability of sag calculation at high temperatures, and the uncertainty of the details, it seems prudent to take a conservative approach in accounting for aluminium



compression. Recommendations for additional sag due to aluminium compression are summarized in the following table:

Table 1 – Maximum excess sag (m) due to the built-in aluminium stress posited by Rawlins, at temperatures above the kneepoint, as estimated with the Alcoa SAG10 computer program.

A1/Syz Type	Span Length - m		
	<b>200</b>	<b>400</b>	<b>600</b>
Tern – 45/7	0.3	0.3	-
Drake – 26/7	0.5	0.7	1.0
Mallard – 30/19	0.4	0.5	0.7

Of course, direct measurement of sag-tension variation with high temperature could supersede these values.

#### **5.4 Experimentally Measured “Plastic” Elongation of Stranded Conductors**

As discussed previously (and illustrated in **Erreur ! Source du renvoi introuvable.**), concentric stranded aluminium conductors are subject to the following elastic and inelastic strains:

1. Thermal Elongation - reversible linear elongation due to temperature change
2. Elastic Elongation - reversible linear elongation due to tension change
3. Strand Settlement & Deformation (Initial Plastic Elongation) – rapid irreversible plastic elongation under initial loading due to a combination of strand settlement, deformation, and rapid (<1 hour) metallurgical creep of aluminium wires.
4. Short-time, High-Tension Plastic Elongation (Design Loading Plastic Elongation) – rapid irreversible plastic elongation which occurs as the result of high conductor tensions due to wind and ice loads.
5. Long-time “metallurgical” creep elongation (Creep Plastic Elongation) – relatively slow, irreversible plastic elongation which occurs due to persistent moderate tension over the life of a transmission line.

Reversible linear thermal elongation and linear elastic elongation of stranded conductors were described in Section 5.2. This section of the brochure discusses the plastic elongation components.

##### *5.4.1 Stress-strain testing of stranded conductors*

Plastic elongation is readily evident in any laboratory testing of concentric stranded aluminium conductor. The Aluminium Association provides a standard method of stress-strain (and creep) testing of Aluminium and ACSR Conductors. After properly terminating a test length of approximately 13 meters, the conductor is subjected to an initial load equal to approximately 2% of its RTS in order to straighten it. Afterward, the sample is subjected to a series of loads as follows:

1. 30% of RTS for 30 minutes and release to initial load.
2. 50% of RTS for 60 minutes and release to initial load.

3. 70% of RTS for 60 minutes and release to initial load.
4. Increasing load until strand breakage occurs.

Typical results of such a test are shown in Figure 19.

### Stress-Strain Test

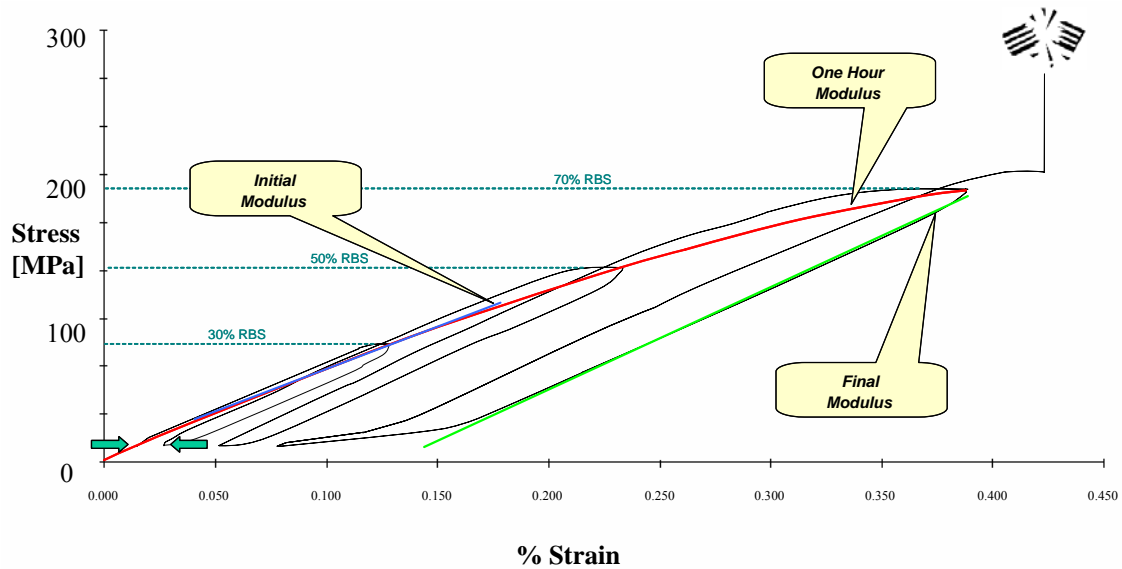


Figure 19 – Typical stress-strain test results with 1-hour initial curve drawn and both initial and final modulus shown.

Note that:

1. The “settlement and 1-hour creep” plastic elongation increases with tension.
2. The curve drawn through the 1-hour hold points is designated as the “initial stress-strain curve”.
3. The slope of the stress-strain curve during unloading and re-loading the conductor after each hold period is the same. This slope is called the “final stress-strain” modulus of the composite conductor.
4. The final modulus is greater than the initial modulus.

If the conductor consists entirely of aluminium wires, then only one stress-strain test is required. As a result of numerous stress-strain tests, with conductors provided by a number of different manufacturers, stress strain curves including both initial and final curves have been made available by the Aluminium Association. Figure 20 shows stress-strain curves for 37-strand, all-aluminium (A1) conductor.

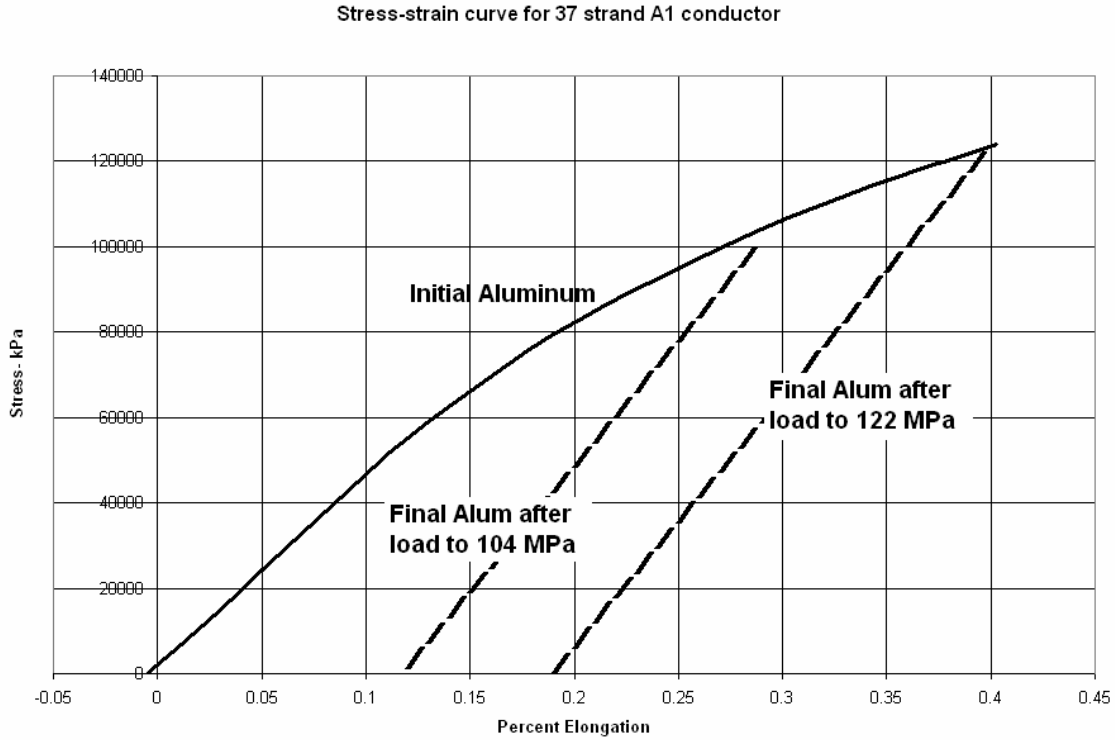


Figure 20- Stress-strain curve for 37 strand A1 conductor.

If the conductor is A1/Syz or another non-homogeneous conductor having components with different thermal elongation coefficients, then two stress-strain tests are required. The first test is performed on the composite conductor as shown in Figure 21.

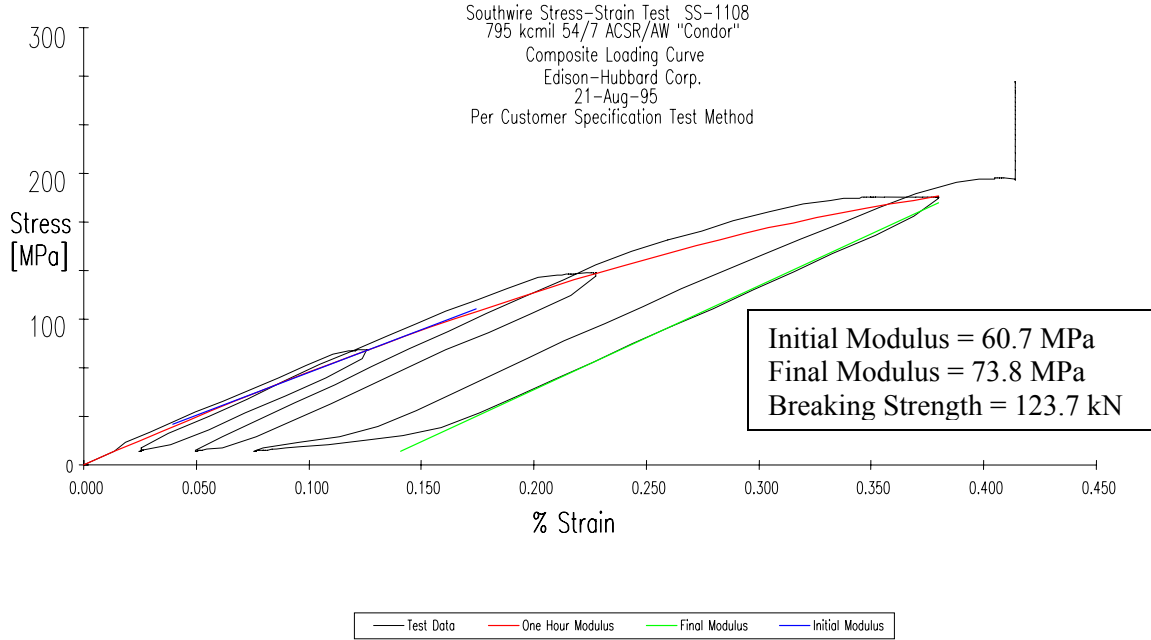


Figure 21 - Raw data from a stress-strain test of A1/Syz conductor

A second test must be performed on the steel core alone. The result of a test on the S1A-7 steel core alone is shown in Figure 22.

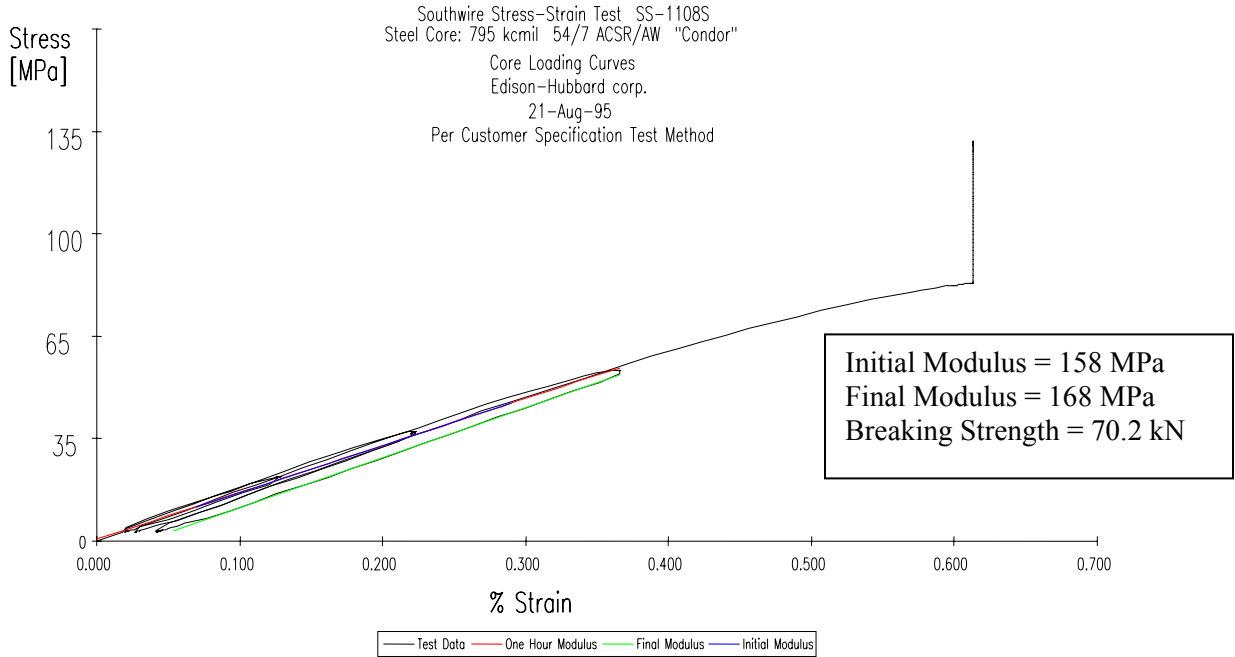


Figure 22 - Raw data for a stress-strain test performed on the steel core alone for the A1/Syz conductor whose composite test results are shown in Figure 21.

Notice that the permanent elongation of the steel core at each of the three hold points is much less than the elongation of the composite conductor. Based on the test results shown in Figure 21 and Figure 22, an "initial stress-strain" curve for the aluminium layers alone can be derived. To do this, note that the total tension,  $H_{AS}$ , in the conductor is the sum of the tension in the aluminum layers,  $H_A$ , and the tension in the steel core,  $H_S$ , and that the stress in the component parts is equal to the component tension divided by the component area. The total stress in the conductor is therefore:

$$\frac{H_{AS}}{A_{AS}} = \sigma_{AS} = \frac{\sigma_A \cdot A_A}{A_{AS}} + \frac{\sigma_S \cdot A_S}{A_{AS}} \quad (22)$$

Where  $\sigma_{AS}$  is the ordinate of Figure 21 and  $\sigma_S$  is the ordinate of Figure 22.

In Figure 21, the percent strain at which the final stress-strain curve of the composite conductor intersects the horizontal axis, depends on the maximum tension to which the stranded conductor has been exposed, however the slope of the curve (the conductor modulus) does not. Therefore, the higher the stress experienced by the conductor, the greater the plastic elongation the conductor experiences as a result of the maximum loading event.

#### 5.4.2 *Plastic elongation under initial high loading*

The experimental stress-strain curves can be used to calculate the initial conductor plastic strain as a function of the maximum tension as shown in Figure 23. The plastic elongation due to strand settlement and deformation during initial tension loading is equal to the difference in strain between the linear behavior (indicated by the final curve drawn through the origin) and the initial 1-hour hold curve. No attempt is made in this document to draw a distinction between settlement strain and short time creep elongation at high tension levels.

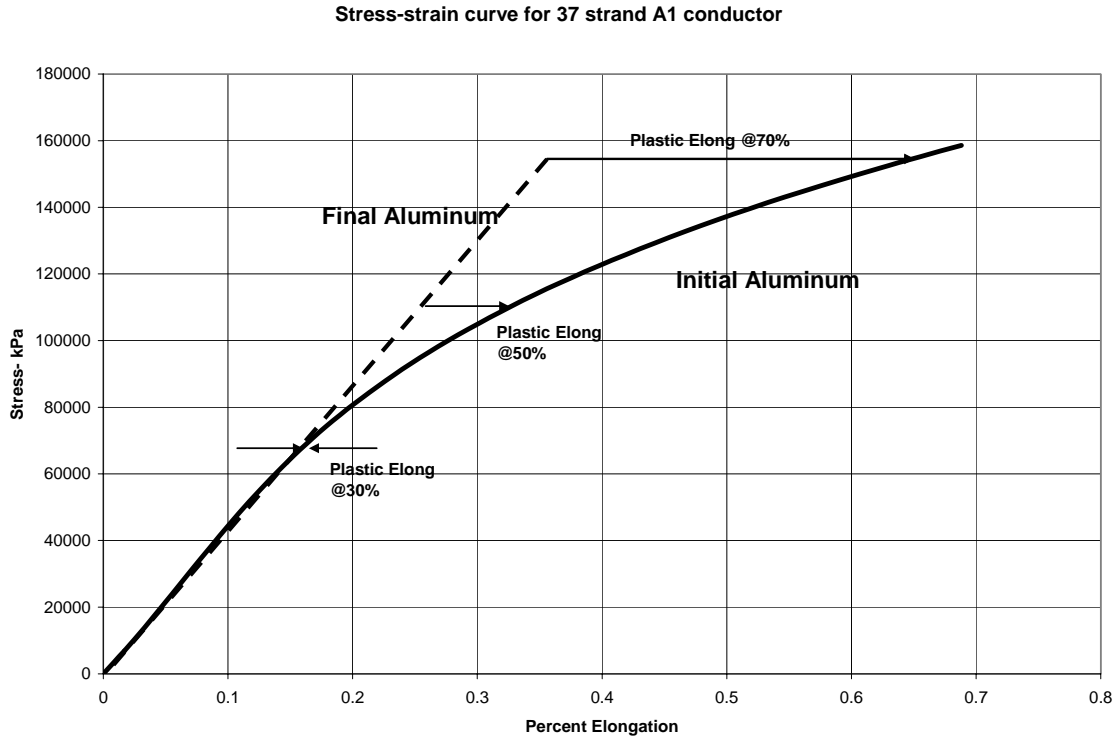


Figure 23 - Initial plastic strain as a function of tension.

Harvey and Larson [21, 22, 23] reviewed data from a large series of stress-strain tests to determine the initial settling and strand deformation values of plastic elongation shown in Figure 23 for various types of aluminum conductor. They noted that there was considerable random variation between test samples but that the values shown in Table 10 were generally consistent with the tests they reviewed. They also noted that these values were not dependent on the rod source (continuous-cast or rolled aluminum rod) or, for A1/Syz, on the stranding.

Table 10 - Initial settling and one-hour creep strain as a function of conductor type and stress from Harvey & Larson.

<b>Conductor Type</b>	<b>%Plastic Strain [<math>\mu</math>s]</b>		
	<b>30% RTS</b>	<b>50% RTS</b>	<b>70% RTS</b>
A1	240	570	1180
A1/Syz	370	830	1760
A2	260	500	1120
A1/A2	200	580	1530

Similar data is presented in Table 3 of IEC 1597 [2] but the IEC data indicates a discernable difference as a function of ACSR stranding. Table 11, below, summarizes the IEC data.

The plastic elongation due to initial settlement and strand deformation as a function of tension can be derived from the values given in Table 11.

Table 11 - Stress-strain data from IEC 1597 Table 3

Type	Stranding	$E_{final}$ -GPa	Plastic Settlement & 1-hour creep as a function of stress [ $\mu$ s]				
			25MPa	50MPa	75MPa	100MPa	125MPa
A1 or A2	7 strand	63.3	105	310	515	1020	1925
A1 or A2	19 strand	61.2	92	283	575	1066	2058
A1 or A2	37 strand	58.9	76	251	527	1002	1978
A1 or A2	61 strand	58.3	71	342	714	1285	2256
A1/S1	6/1	79.0	84	167	151	234	418
A1/S1	18/1	68.0	132	265	397	629	862
A1/S1	22/7	71.0	148	196	444	592	739
A1/S1	26/7	74.2	163	226	389	452	615
A1/S1	45/7	64.5	212	325	437	650	962
A1/S1	54/7	67.1	127	255	382	510	737
A1/S1	54/19	69.7	141	183	324	465	707
A1/S1	72/7	61.1	291	382	573	763	1054
A1/S1	72/19	61.0	290	380	570	761	1151
A1/S1	84/7	66.6	125	149	374	598	923
A1/S1	84/19	66.5	124	148	272	496	820

Plastic elongation due to settlement and strand deformation may be estimated by interpolating linearly between the table values or by using the table values to derive a polynomial equation such as the following for 37-strand A1:

$$\epsilon_{Ci} = 0.001333598 \cdot \sigma^3 - 0.08566234 \cdot \sigma^2 + 5.602464 \cdot \sigma$$

Where  $\epsilon_{Ci}$  is the conductor strain in  $\mu$ s and  $\sigma$  is the conductor stress in MPa.

The final elongation curve for 37 strand A1 conductor is given by:

$$\epsilon_{Cf} = 0.01698 \cdot \sigma$$

#### 5.4.3 Long-time “Metallurgical” Creep - Plastic Elongation for Persistent Moderate Loading

As can be seen from the test results in the previous section, the initial plastic elongation at moderate tension loading is quite small (e.g. less than 200  $\mu$ s at 20% RTS). However,

as described in two excellent Electra articles [24, 25], aluminium strands also undergo significant plastic elongation when even moderate tensions are applied for extended periods of time.

This long-time plastic elongation of aluminium at moderate tension levels is commonly referred to as metallurgical creep or simply creep plastic elongation. Since bare overhead conductors are typically installed to tensions on the order of 20% RTS, and sag increases with conductor length, the accurate calculation of conductor creep plastic elongation over the life of the line is an important factor in maintaining electrical clearances.

As for stress-strain testing, there is a standard method for measuring the creep plastic elongation of concentric stranded bare overhead conductors [26, 27]. The preferred test length is the same as for stress-strain tests – 12.5 m. When tested at room temperature, the conductor specimen is allowed to stabilize to room temperature. After the test tension is applied, the specimen length is measured at one hour and at subsequent time intervals up to 1000 hours.

For a series of such creep elongation tests (each with a different new sample of conductor) the data can be plotted on "log-log" giving a series of "creep" curves as shown in Figure 24.

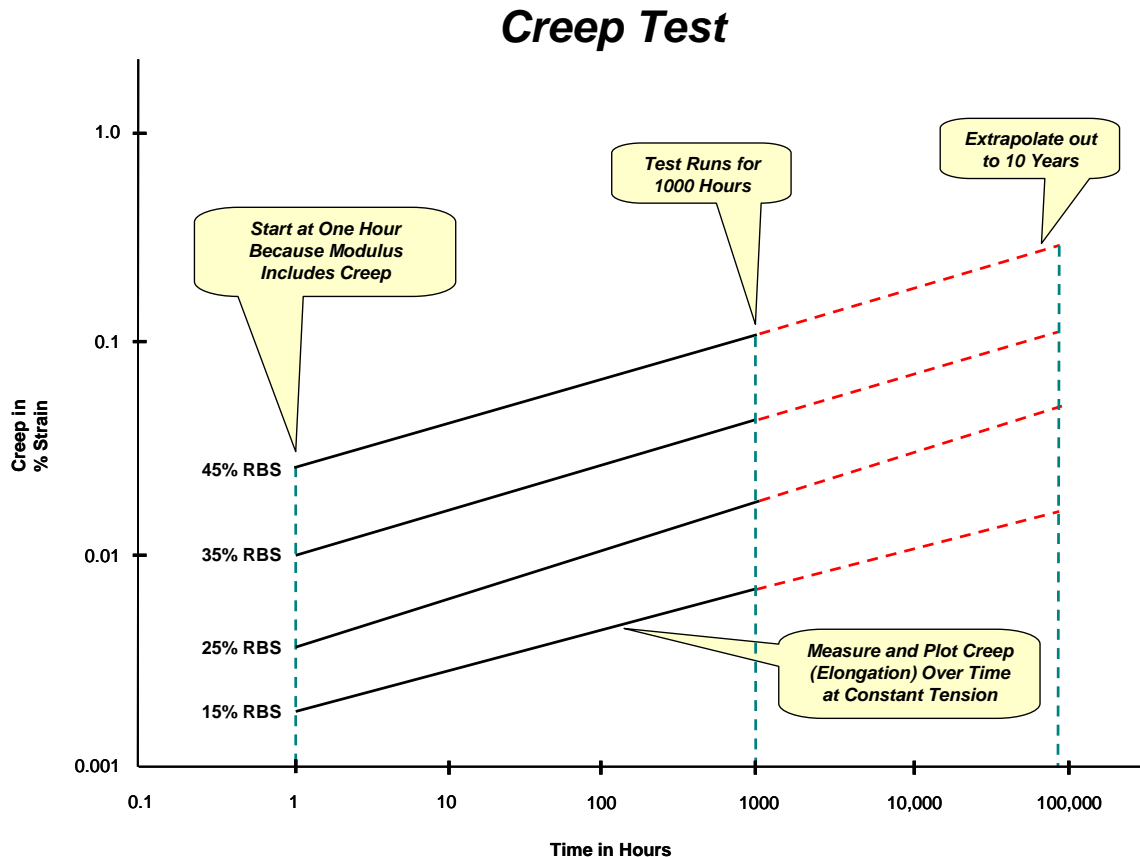


Figure 24 - Creep elongation curves resulting from a series of tests at different tension levels, all at room temperature.



These curves do not allow estimate of creep plastic elongation at times less than 1 hour. For such short times, the plastic elongation is estimated from the stress-strain measurements. Also, the straight lines on log-log paper indicate the decreasing rate of creep elongation with time. In general, the increase in elongation between 10 and 100 hours is the same as the change between 100 and 1000 hours. The rate of creep elongation decreases by a factor of 10 as the time increases by a factor of 10.

The data shown in Figure 24 can be represented algebraically. Harvey & Larson suggest the following equations for plastic creep elongation of A1 stranded conductor at everyday temperatures:

$$\epsilon_c = 1.23 \cdot [\sigma(MPa)]^{1.3} \cdot [t(hrs)]^{0.16} \text{ microstrain}$$

The aluminium source is assumed to be rolled-rod aluminum, and t is the elapsed time in hours. Thus the plastic creep elongation of our example Arbutus A1 conductor at 20% of its RTS (RTS = 61 800 N), expressed as stress (H/A = 0.2\*61 800/403.8 = 30.6 MPa) applied for 10 years (87 600 h) is:

$$\epsilon_c = 1.23 \cdot (30.6)^{1.3} \cdot 87600^{0.16} = 649 \text{ microstrain}$$

These algebraic equations are one way of summarizing the test data for creep plastic elongation in stranded conductors. An equally valid method, used in the load-strain sag-tension method, is to summarize the data graphically as shown in Figure 25.

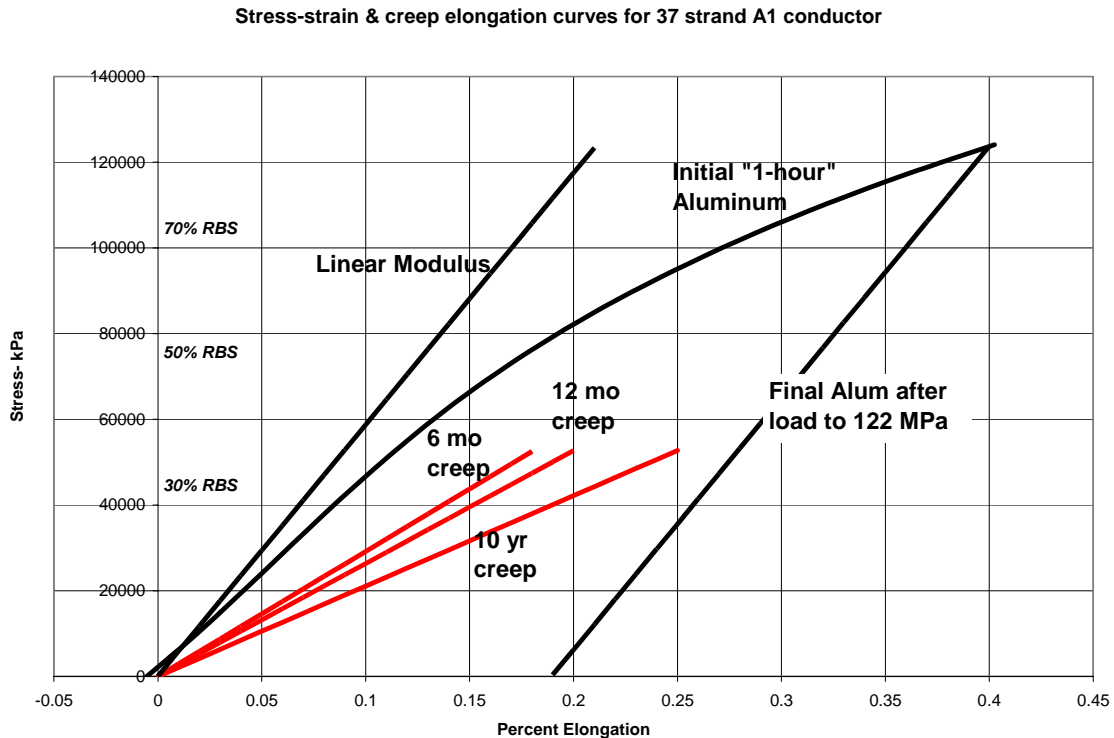


Figure 25 - Creep elongation curves for A3 stranded conductor.

For example, the creep elongation of this 37 strand all aluminium stranded conductor can be calculated for an elapsed time of 10 years at a stress of 30.6 MPa. Re-plotting Figure 25 into Figure 26, we can see that the total conductor creep over 10 years, including initial settling strain, is approximately 0.09% or 900  $\mu$ s.

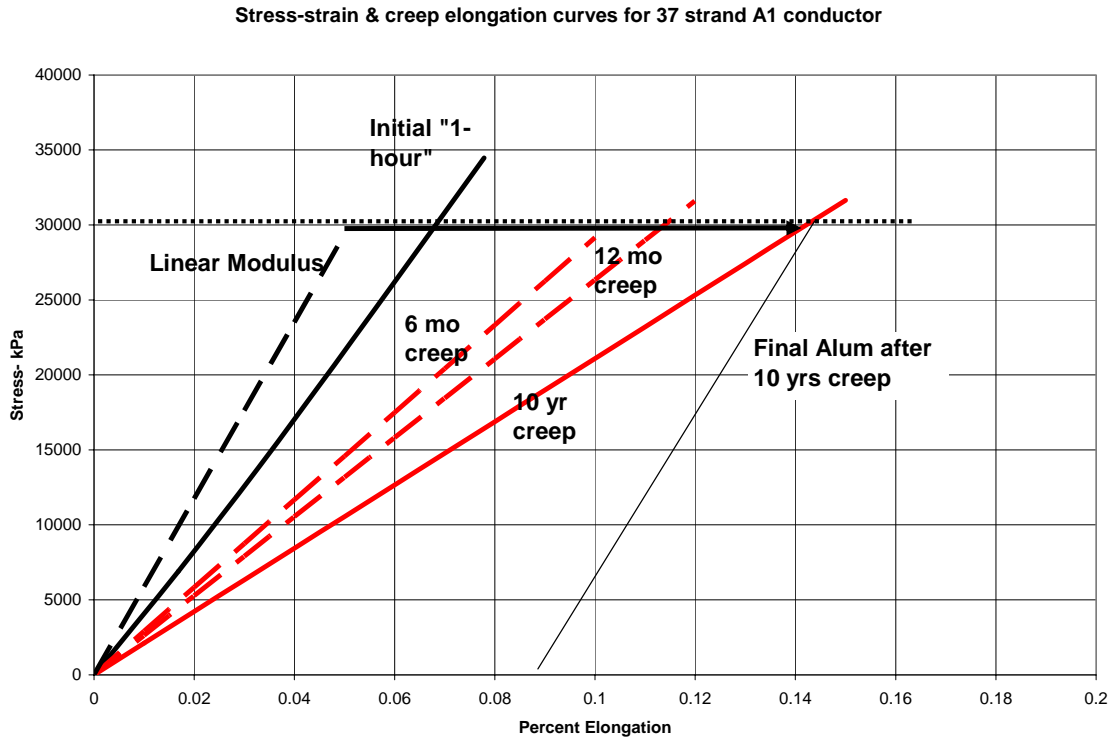


Figure 26 - Graphical determination of creep elongation for a 37 strand all aluminium stranded conductor at a constant tension equal to 20% of the RTS over 10 years.

Permanent increase in conductor length due to heavy load occurrences cannot be predicted at the time a line is built. The reason for this unpredictability is that the occurrence of heavy ice and wind loads is random. A heavy ice storm may occur the day after the line is built or may never occur over the life of the line. This uncertainty is normally handled by assuming a conservative load sequence.

The plastic conductor elongation, caused by strand deformation and settling at high tension due to heavy ice and wind loads, may not simply be added to the plastic elongation due to metallurgical creep at everyday tensions. Instead, "final" sag-tensions are calculated based on everyday conductor stress over an extended period of time (e.g. 10 years) and based on an assumed heavy ice and wind load. The final sag and tension values for the two cases are compared and final sags and tensions are based on the case which gives the largest permanent elongation (i.e. greatest change in sag).

#### *5.4.4 Long-time Creep Plastic Elongation with non-homogeneous stranded conductors*

The creep test data for non-homogeneous conductors can be applied in much the same manner as for homogeneous conductors. The permanent elongation due to creep at moderate tension levels leads to an increase in sag and a corresponding decrease in tension over the life of the line. For example, IEC 1597 suggests that the long term creep plastic elongation of A1/S1A and A1 can be represented by an equivalent temperature increase of 30°C and 35°C, respectively. This simple approach to accounting for creep elongation in A1/Sxy ignores the fact that only the aluminium layers are permanently elongating while the steel core is elongating due to increased tension.

For A1/S1A conductors, plastic elongation of the composite conductor amounts to a permanent elongation of the unstressed length of the aluminium layers and an increase in the tension applied to the steel core. Thus given creep test data such as that shown in Figure 24, one must separate the permanent elongation of the aluminium layers from the composite length change.

In brief, the increase in stress of the steel core is determined by multiplying the long-time creep elongation found under test by the steel core final modulus. The increase in length of the aluminium layers is then found by subtracting the reduced elastic elongation from the creep elongation.

The method of dealing with non-homogeneous conductors is described in more detail in section 6 of this brochure.

#### *5.4.5 Summing Plastic Elongation*

In the preceding sections of this brochure, two distinct types of plastic elongation have been considered. One occurs due to high tension loads which persist for short times, typical of ice storms or periods of extremely high wind. The second occurs at moderate tension levels sustained for long periods of time. The two types of plastic elongation may not be added to find the total elongation. That is, the total plastic strain experienced by the conductors in an overhead line is not the sum of the strains due to high load events and sustained everyday tension.

In fact, a well-known method of preventing moderate tension long-time creep from occurring during the stringing and sagging process is to “pre-stress” the conductor. In pre-stressing, the conductor is tensioned to a relatively high tension for a short period of time (e.g. 30% to 50% of RTS for 4 to 24 hours) after which the conductor does not plastically elongate until well after installation is completed.

## 6.0 SAG-TENSION CALCULATION METHODS

There are many sag-tension calculation methods in use around the world. Each is somewhat unique and presumably gives acceptable results based on the experience of the transmission line designer. In almost every case, such calculations are done numerically but differ in how conductor elongation in response to changes in tension, temperature and time. As shown in Section 5, the various methods of calculation largely differ in how the conductor elongation is represented. It is suggested that the various approaches can be grouped into one of three conductor elongation models: (1) Linear Elongation (LE); (2) Simplified Plastic Elongation (SPE); or (3) Experimental Plastic Elongation (EPE) models.

Whatever the elongation model used, sag-tension calculations normally produce calculated sags and corresponding tensions for a series of loading cases (ice and wind load plus conductor temperature) under one or more constraints on tension or sag at particular loading conditions. In most calculation methods, where plastic conductor elongation is considered, sag-tension calculations are performed for a set of loading cases corresponding to the "initial" conductor state at the time of construction and one or more "final" states corresponding to a time-line of 10 years or more.

As an example, using the EPE elongation model, sag-tension calculations are shown in Table 12 as generated by the SAG10 program, which is widely used in North America. The difference in sag and tension between the loading cases is due to differences in conductor temperature and weight per unit length. The difference in initial and final sag-tensions is the result of plastic conductor elongation that results from design tension loading events and metallurgical creep over time. Notice that the initial and final sag-tension is equal in the first row. This occurs because the maximum plastic elongation of the conductor occurs as a result of this loading condition, rather than being the result of metallurgical creep at everyday conditions.

Table 12 - Typical Sag-tension Calculation Results where the permanent elongation of the aluminum strands is determined by the maximum wind and ice load rather than by metallurgical creep at everyday temperature.

Conductor DRAKE 26/7 ACSR									
Area = 468.6 sq. mm. OD = 28.14 mm Bare Wt = 15.96 N/m									
Span = 300 m RTS = 140119 N									
Loading Case				Final			Initial		
Temp °C	Ice mm	Wind N/m <sup>2</sup>	Weight N/m	Sag m	Tension N	RTS %	Sag m	Tension N	RTS %
-20	12.5	380	36.377	9.26	44386	31.7	9.26	44386	31.7
-40	0	0	15.966	7.25	24818	17.7	6.92	25996	18.6
0	0	0	15.966	8.61	20938	14.9	8.13	22146	15.8
15	0	0	15.966	9.08	19847	14.2	8.57	21018	15.0*
25	0	0	15.966	9.39	19200	13.7	8.86	20340	14.5
50	0	0	15.966	10.13	17805	12.7	9.56	18864	13.5
75	0	0	15.966	10.62	17001	12.1	10.23	17636	12.6
100	0	0	15.966	10.99	16425	11.7	10.88	16601	11.8

Even though the sag-tension calculations in Table 12 were generated by a specific calculation method, the tabular result showing both initial and final sag-tension values is typical of any sag-tension calculation method except one in which plastic elongation of the conductor is ignored. If the LE elongation model is used in sag-tension calculations, the initial and final values would be the same (no plastic elongation).

Not only are the results of calculation similar for the various sag-tension calculation programs, but the numerical methods used to find the solutions for each loading case are usually similar. The numerical method follows a process similar to the following:

1. For the span,  $S$ , and bare installed conductor weight,  $w_0$ , the conductor sag,  $D_0$ , and conductor length,  $L_0$ , are determined for the initial installed loading condition tension,  $H_0$ , and temperature,  $T_0$  (e.g. 15% RTS at 15°C in a 300 m span). This condition is indicated by the asterisk in Table 12.
2. For Loading Condition #1, the conductor weight,  $w_1$ , per unit length is determined from the conductor bare weight and any ice and wind loads specified in loading condition #1.
3. For the Loading Condition #1, the conductor length is adjusted to  $L_1$ , based on the difference in conductor temperature using equation (9).
4. Given the weight,  $w_1$ , and the conductor length,  $L_1$ , the conductor tension,  $H_{11}$ , is calculated according to equation (5).
5. Based on the initial estimate of conductor tension,  $H_{11}$ , the conductor length for loading condition #1 can be estimated by adjusting for the change in tension ( $H_0 - H_{11}$ ) using equation 8 (or a non-linear experimental curve).
6. A new estimate of conductor length for loading case #1 is then  $L_{12}$ .
7. Using  $L_{12}$ , the conductor tension is recalculated using equation (9), etc., until the conductor lengths and the conductor tensions are equal.

From the preceding discussion, it is clear that the difference in the calculation methods centers on modeling and manipulating conductor elongation data, rather than how the sag-tension values are calculated in determining the simultaneous solution of catenary and conductor elongation equations.

None of the contributors to this brochure could identify a power transmission company that used the simplest linear model for sag-tension behavior, where plastic elongation is ignored. However, the simplicity of this elongation model allows certain physical insights that the more complex elongation models do not.

The basic intention of any sag-tension calculation method is to determine the variation in sag and tension with (1) changes in conductor weight due to ice and wind, (2) changes in conductor length due to temperature variation, and (3) the effects of plastic elongation (if any) as a function of time and high mechanical loads.

Sag-tension calculations utilizing the three elongation models will be demonstrated with two typical transmission conductors:

- 37 strand, 403 mm<sup>2</sup>, 26.1 mm diameter Arbutus A1 conductor installed in a 300 meter span.
- 26/7, 468 mm<sup>2</sup>, 28.1 mm diameter Drake A1/S1A installed in a 300 and a 180 m span.

The initial catenary conditions can be calculated based on the exact catenary equations described in Section 2 of this brochure:

Table 13 - Characteristics of 37-strand A1 and 26/7 strand A1/Sxy

<i>Sag-tension Case</i>	<i>Example #1</i>	<i>Example #2</i>
Conductor Name (IEC)	403-A1-37	<b>403-A1/S1A-26/7</b>
Conductor Common Name	403 mm <sup>2</sup> 37 AAC	<b>403 mm<sup>2</sup> 26/7 ACSR</b>
Span Length [m]	300	<b>180 or 300</b>
Outside Diameter [mm]	26.1	<b>28.1</b>
Bare Wt. per unit length [N/m]	10.89	<b>15.97</b>
Rated Tensile Strength [kN]	61.8	<b>140.1</b>
Final Elastic Modulus [MPa]	58.9	<b>73.9</b>
Total Area [mm <sup>2</sup> ]	402.9	<b>468.6</b>
Steel Area [mm <sup>2</sup> ]	-	<b>65.8</b>

Sag-tension calculations are necessary in order to determine:

- Installation (“stringing”) sags for other span lengths and conductor temperatures.
- Sags at the line’s maximum allowable (“design”) conductor temperature to assure adequate electrical clearance.
- Sag and tension under maximum ice and wind load to define maximum structure conductor tension loads and to ensure that minimum electrical clearances are met.
- Predict uplift problems and allow clipping offsets to be determined in mountainous regions.

### **6.1 Sag-tension for A1 Conductor with LE (Linear Elongation) Model**

As the conductor weight per unit length, *w*, increases with the addition of ice or wind pressure, the conductor tension increases. If the conductor is inextensible, then the increase in tension is simply proportional to the increase in weight per unit length. Any elongation of the conductor reduces the increase in tension but increases both the catenary length and sag.

The linear elongation model has the advantage of simplicity, allowing a rather simple yet exact sag-tension calculation process. If the conductor elongates linearly as a result of the increase in tension, the change in conductor length is given by the following simple equation (13a) presented previously in section 5.2.1:

$$\frac{L_H - L_{REF}}{L_{REF}} = \frac{H - H_{REF}}{E \cdot A}$$

With the bare A1 conductor installed at 15.33 kN (25% RTS) in a 300 m span, the initial sag at 15°C is 8.0 m according to equation (2). If, after being installed, the conductor is subjected to a wind pressure of 430 MPa at 15C, the conductor weight per unit length increases from 10.89 N/m (bare) to the vector sum of the bare conductor weight (10.89 N/m) and the horizontal wind force ( $430 \cdot 0.0261 = 11.2$  N/m) or 15.6 N/m.

If the conductor were completely inelastic, then the sag of the bare conductor (8.0 m) would be unchanged, and the new conductor weight per unit length of 15.6 N/m would yield a conductor tension of 22 kN ( $15.33 \cdot (15.6/10.89) = 22.0$ ).

But the conductor is assumed to elongate linearly (LE model) with tension so the conductor length and sag will increase and the conductor tension will be somewhat less than if it were inelastic. To determine the new sag-tension value under this high wind loading, the catenary equations and the elastic elongation equation can be solved iteratively. This is conveniently done by searching for a tension value at which the increase in conductor strain due to the increased conductor tension is equal to the increase in catenary strain ( $(L-S)/S$ ) due to the increased weight per unit length and tension.

The increase in conductor strain under tension is given by a form of equation (8) with the final or elastic modulus of the Arbutus A1 conductor as 58.9 GPa:

$$\Delta \varepsilon_H = \frac{L - 300.5682}{300.5682} = \left[ \frac{H(N) - 15.33 \cdot 10^3}{58.9 \cdot 10^9 \cdot 403 \cdot 10^{-6}} \right]$$

The increase in catenary strain under increased conductor weight and the corresponding increase in tension are given by a rearrangement of equation (4):

$$\Delta L_{CAT} = \frac{L - 300.5682}{300.5682} = \left( \frac{2 \cdot H[N]}{300.5682 \cdot 15.6} \right) \cdot \sinh\left( \frac{300 \cdot 15.6}{2 \cdot H[N]} \right) - 1$$

Setting the increases in conductor strain equal, we have the following equation which can be solved for the new tension, H:

$$\left[ \frac{H - 15330}{58.9 \cdot 10^9 \cdot 402.9 \cdot 10^{-6}} \right] = \left( \frac{2 \cdot H}{300.5682 \cdot 15.6} \right) \cdot \sinh\left( \frac{300 \cdot 15.6}{2 \cdot H} \right) - 1$$

The horizontal component of tension which satisfies the equation is:

$$H = 20745 \text{ N}$$

From equation (2), the corresponding sag is:

$$D = \frac{H}{w} \cdot \left\{ \cosh\left( \frac{w \cdot S}{2 \cdot H} \right) - 1 \right\} = \frac{20745}{15.6} \cdot \left\{ \cosh\left( \frac{15.6 \cdot 300}{2 \cdot 20745} \right) - 1 \right\} = 8.5 \text{ m}$$

The resulting conductor tension under this wind load (i.e. 20.75 kN) is higher than when initially installed (i.e. 15.33 kN) but less than if the conductor did not elongate (i.e. 21.94 kN). At the equilibrium tension, the tension has increased by 5415 N, the sag has increased by 0.5 m, and the conductor strain has increased by 228  $\mu$ s.

The preceding calculation can be illustrated graphically as shown in Figure 27. The slope of the linear stress-strain curve is equal to the conductor elastic modulus. The intersection of the stress-strain curve (at "A") with the bare conductor catenary curve occurs at a conductor stress of 38 MPa (15.33 kN divided by 402.9 mm<sup>2</sup>).

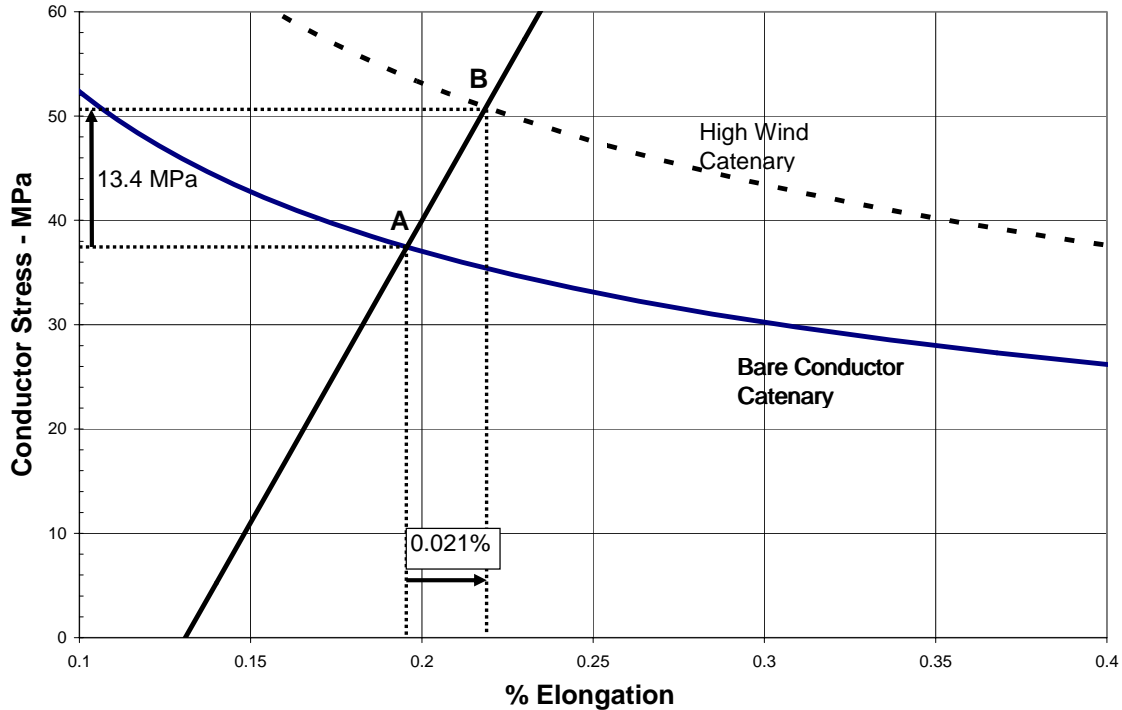


Figure 27 - Sag-tension calculation for A1 conductor with High wind loading.

The solution for sag-tension at the high wind load condition is shown in Figure 27 at "B", the intersection of the linear stress-strain curve and the high wind catenary curve. It can be seen that the stress has increased to about 51 MPa and the elongation increased by about 0.021% (210 micro-strain) which compares favorably with the exact value of 228  $\mu$ s.

## 6.2 Sag-tension for A1/S1A Conductor at high temperature with Simplified Plastic Elongation (SPE) Model

Using the Simplified Plastic Elongation (SPE) model, the sag-tension of A1/S1A Drake conductor at high temperature can be solved using the algebraic plastic elongation methods explained in Section 5 and illustrated with use of a stress-%elongation diagram.



In the SPE conductor model, plastic elongation is assumed equal to a typical value based on historical experience and the tension induced elongation is assumed elastic.

With a steel-cored aluminum conductor, plastic elongation occurs primarily in the outer layers of aluminum strands. Unlike all-aluminum conductors, since there is little or no permanent elongation in the steel core, any plastic elongation of the composite ACSR is limited by the core.

For example, with 795kcmil-26/7 Drake ACSR conductor, the composite modulus and thermal elongation coefficient, according to (19) and (21) are:

$$E_{AS} = 8.6 \cdot \left( \frac{0.6247}{0.7264} \right) + 27.0 \cdot \left( \frac{0.1017}{0.7264} \right) = 11.2 \text{ Mpsi}$$

This equation applies to the ACSR conductor as long as both the steel core and the aluminum layers are in tension.

Since we are only interested in calculating the high temperature sag of this conductor, for which the conductor weight per unit length remains the same, only the bare conductor catenary curve is shown in Figure 28. Since we are using the SPE conductor model, the stress-strain behavior of the conductor is assumed to be simply linear and the plastic elongation is equal to a fixed, typical value, based on experience and engineering judgment.

The calculation begins with the bare conductor installed initially to a stress of 48 MPa at 15°C as shown at point “A” in Figure 28. The unstressed initial elongation of the conductor is found from the intersection of the elastic modulus (starting at “A”) with the zero stress abscissa.

To calculate the “final” unloaded tension at 100°C, one must account for plastic elongation over the life of the line and for thermal elongation in going from the conductor temperature when installed (i.e. 15°C) to the higher value (100°C). Since we are using the SPE elongation model, it can be assumed that a typical plastic elongation of the conductor has been established based on field investigations or a conservative engineering estimate. We will assume that this typical plastic elongation is 600 micro-strain (or 0.06%).

With reference to Figure 28, the initial “unstressed” conductor elongation at 15°C is found by moving from point “A” to point “B” (Notice that the elongation is reduced by approximately 0.065%). The typical plastic elongation of 0.060% is represented in this diagram by moving from point “B” to point “C”. The increased conductor sag at 15°C due to this plastic elongation is found by following the linear modulus from point “C” to point “D” where the elastic modulus intersects the bare catenary curve. At point “D”, the stress is 43 MPa and the elongation is 0.0245%.

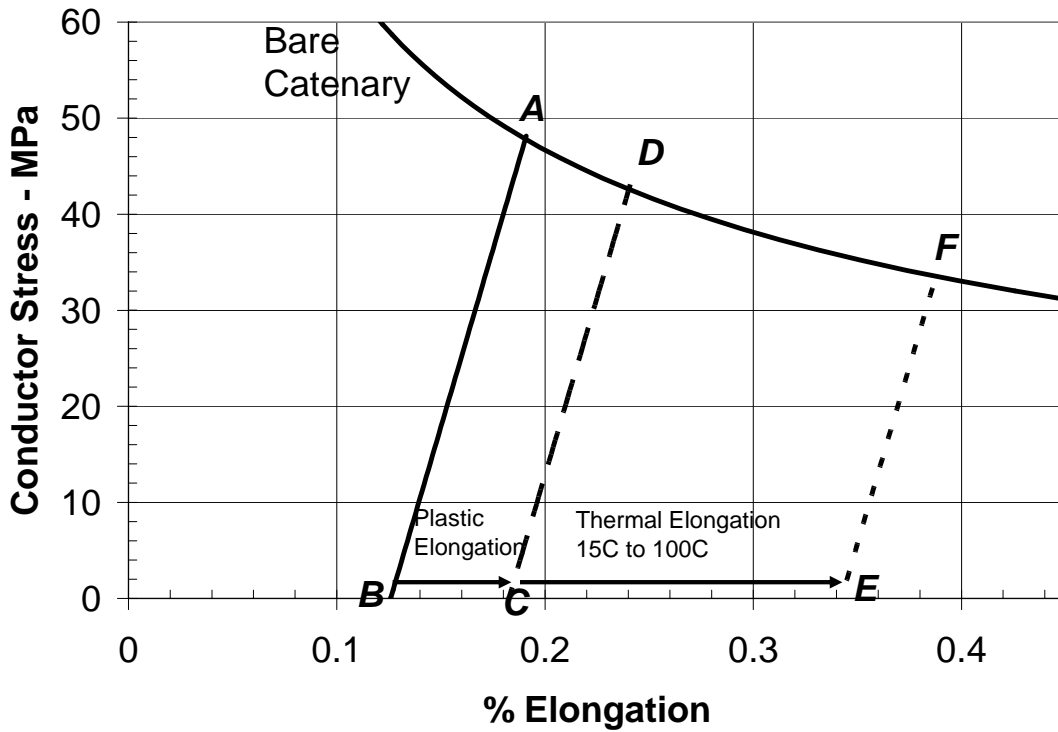


Figure 28 - Sag-tension at High Temperature with SPE model for Drake ACSR in 300 m span.

Converting this stress and elongation to “final” tension and sag at 15°C, we get:

$$H = 43\text{MPa} \cdot 468.6 = 20.1\text{kN}$$

$$D = \frac{20,100}{15.97} \cdot \left\{ \cosh\left(\frac{15.97 \cdot 300}{2 \cdot 20100}\right) - 1 \right\} = 8.95\text{m}$$

Under “final” conditions, the initial installed tension has decreased from 28.0 kN to 20.1 kN and the initial installed sag of 8.0 m has increased to 8.95 m.

The “final” sag-tension condition at 100°C is found by shifting the intersection of the elastic modulus curve and the zero stress axis to the right (“C” to “E”) by the change in %elongation corresponding to the conductor temperature change from 15 to 100°C (i.e. 0.160% or 1600 micro-strain).

The final sag-tension condition at 100°C is then found by moving up the elastic modulus curve from “E” to “F” where the elastic modulus intersects the bare catenary curve. The final sag and tension values at 100°C are found to be 15.9 kN (34 MPa) and 11.3 m (0.39%).

### **6.3 Sag-tension Calculation with Experimental Plastic Elongation (EPE) Model**

In doing sag-tension calculations using non-linear, experimental conductor elongation data, the curves are typically represented by 4<sup>th</sup> order polynomials. Normally, such calculations are done by computer but the explanation of calculations is clearer when described graphically. In this section, we will illustrate sag-tension calculation methods which utilize the Experimental Plastic Elongation (EPE) model by using graphs of catenary and conductor elongation data. While such graphical solutions are reminiscent of the Varney graphical method, the calculation methods actually illustrate the main points of any sag-tension method that utilizes an EPE model for conductor.

The graphical sag-tension calculation utilizing EPE conductor data will be limited to a 180 m ruling span with 403 mm<sup>2</sup> 26/7 Drake ACSR, installed to an initial tension of 28 kN (20% of its RTS) at 15°C. The ruling span is assumed to be subject to occasional ice and wind loadings of 12.5 mm radial glaze ice combined with a wind pressure of 383 Pascals.

While a normal “sag-tension” calculation considers a series of loading and conductor temperature conditions, for the sake of clarity, we’ll confine ourselves to one loading condition at a time in this section.

#### *6.3.1 Maximum conductor tension with the EPE model*

Strain structures are designed to withstand the calculated maximum conductor tension loads under high wind and ice conditions. Accounting for the plastic elongation of 1350-H19 aluminum strands, due to settling and strand deformation during initial high tension loading, yields a reduced estimate of maximum conductor tension.

Figure 29 illustrates how the use of an experimental plastic elongation (EPE) model results in a lower estimate of maximum conductor tension than either the Linear Elongation (LE) or Simplified Plastic Elongation (SPE) models, both of which assume that the conductor elongates linearly with tension. Notice that the vertical axis is the composite stress of the conductor and has the units of MPa.

In Figure 29, letter A indicates the starting point for this description. At A, the bare Drake conductor is initially installed in a 180 m span with the bare conductor at a tension of 28kN and a conductor temperature of 15°C. Given the total composite conductor cross-sectional area of 468.6 mm<sup>2</sup>, 28 KN corresponds to a composite stress of 59.8 MPa, which we will round off to 60 MPa on the graph.

The letters E and F indicate solution points on the “loaded” catenary curve (the catenary curve which corresponds to a conductor temperature of -18°C and a conductor weight of 32.2 N/m due to the ice and wind loading) for the LE/SPE methods and for the EPE elongation model, respectively. The difference (about 9%) in conductor stress between these two points indicates the difference in maximum structure tension load obtained by the linear and experimental conductor elongation models.

**468 mm<sup>2</sup>, 26/7 Drake ACSR (with EPE model) in 180 m span  
with 12.5 mm glaze ice and 383 Pa wind loading.**

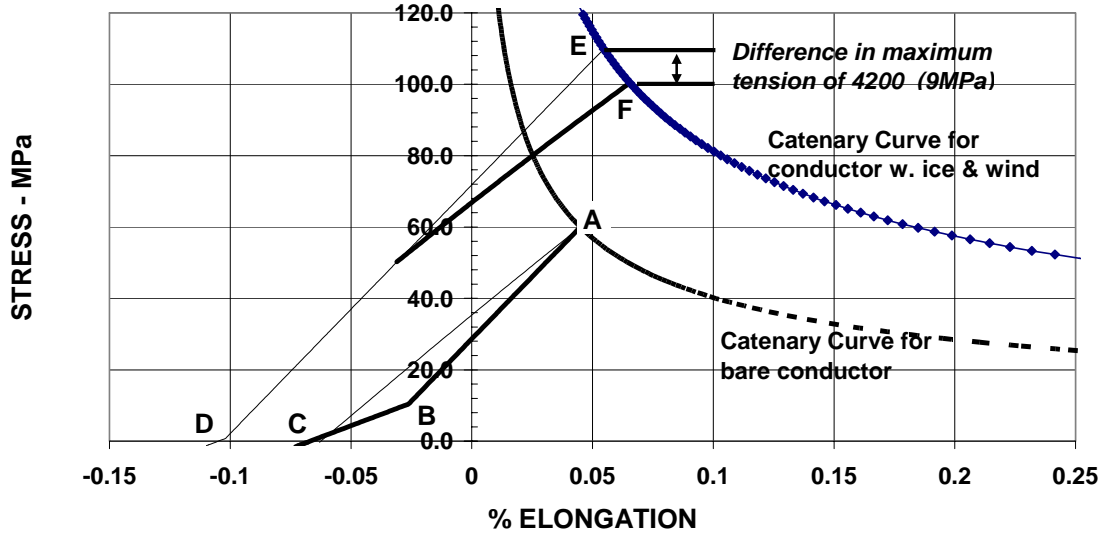


Figure 29 - Sag-tension calculations of maximum, loaded conductor tension illustrating the effect of plastic elongation

Though not shown in Figure 29, the sag of the conductor can be found for any %elongation by application of equation (8) or from the stress (tension) and conductor weight according to equation (2). For example, at point A, where the bare conductor is initially installed, the sag is:

$$D = \frac{H}{w} \cdot \left\{ \cosh\left(\frac{w \cdot S}{2 \cdot H}\right) - 1 \right\} = \frac{60 \cdot 468.6}{15.97} \cdot \left\{ \cosh\left(\frac{15.97 \cdot 180}{2 \cdot 60 \cdot 468.6}\right) - 1 \right\} = 2.3m$$

Since the ice and wind loading occurs at -18°C, the unstressed lengths of the steel core and the aluminum layers must be reduced, moving the unstressed %elongations to the left, from C to D. Since the aluminum layers contract twice as much as the steel core, the zero-tension lengths of the steel core and the aluminum layers for the EPE model are nearly equal at the reduced temperature. Also, in this particular case, the %elongation shift for the linear LE/SPE model at -18°C yields nearly the same zero tension length at point D.

Starting at the % elongation which corresponds to the unstressed length of the conductor at -18°C, both the linear LE/SPE and the non-linear EPE stress-strain curves are traced to their intersection with the “loaded” catenary at points E and F. Above the initial installed stress of 60 MPa, with the EPE model, further strand deformation and settling occurs.

Since the LE/SPE models are linear, this additional plastic elongation of the aluminum layers is ignored. The additional plastic elongation predicted by the EPE model results in a lower estimate of maximum conductor tension (point F) than that predicted by the LE or SPE models (point E).

Notice that the more realistic EPE elongation model gives both a more realistic estimate of maximum structure tension loading and that the difference between the linear estimate and the non-linear estimate will be larger in severe ice and wind load areas.

The use of the EPE model makes it possible to calculate the plastic elongation of the aluminum layers as a function of realistic high mechanical loading events rather than ignoring it in the LE model or using a typical value in the SPE model. In addition, the plastic elongation of the aluminum layers due to deformation and settling during high tension load events can be compared to metallurgical creep plastic elongation to obtain a more accurate estimate of actual plastic elongation. This, in turn, yields a better estimate of final sags under high conductor temperatures as demonstrated in Section 6.3.3.

### 6.3.2 Final sag-tension accounting for aluminum creep with the EPE model

One of the very basic limitations of the linear elongation (LE) and Simplified Plastic Elongation (SPE) conductor models is that, for non-homogeneous conductors, the changes in component tensions which result from aluminum creep and the higher thermal elongation rate of aluminum are usually ignored. Even with the SPE model, where a typical plastic elongation of the aluminum layers could be selected, the selected plastic elongation value would not be a function of loading events or time.

In contrast, Figure 30 shows how the EPE model allows one to keep track of the component tension levels in aluminum layers and steel core for ACSR. In developing Figure 30, the ACSR conductor is assumed to be installed (sagged and clipped) initially to a total conductor tension of 60 MPa (28 kN) at 15°C. In applying this initial tension to the previously unstressed, non-homogeneous conductor, the composite conductor is elongated by about 0.105% as the conductor elongates along the AL-I + ST curve from A to B.

The component stresses in the aluminum layers and the steel core can be plotted on the same figure by noting equation (19) from section 5.2.3:

$$E_{AS} = E_A \cdot \frac{A_A}{A_{AS}} + E_S \cdot \frac{A_S}{A_{AS}} \quad (19)$$

The component stress-strain curves shown in Figure 30 are the actual stress-strain curves multiplied by the ratio of the component area to the total area. The composite stress is then simply the sum of the component stresses shown in the figure in accordance with equation (19).

**486 mm<sup>2</sup> 26/7 Drake ACSR in 180 m span showing initial installed conditions prior to creep**

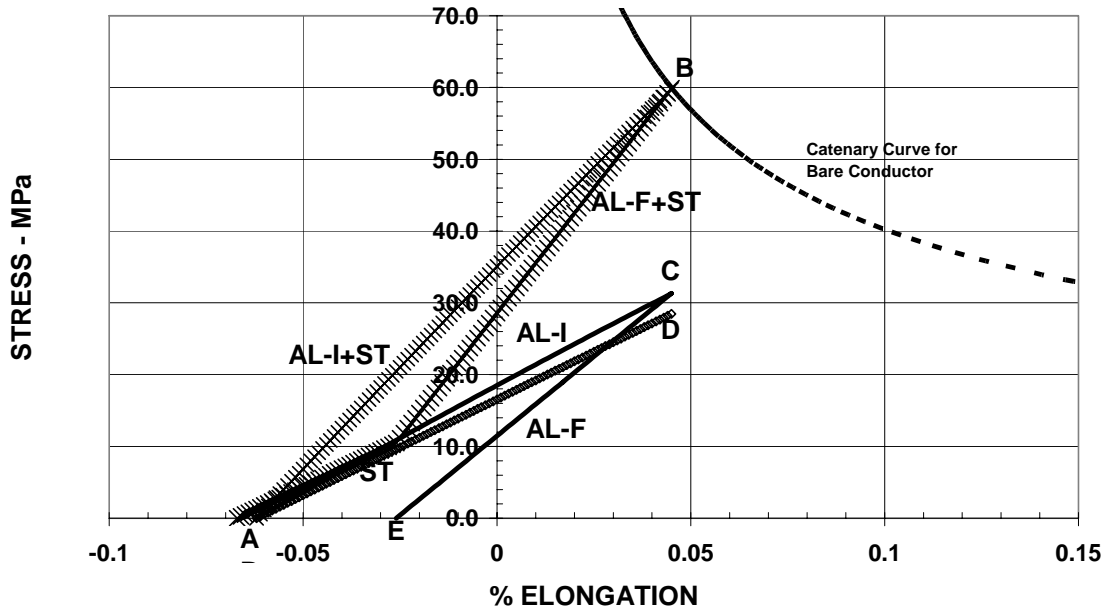


Figure 30 – Application of Experimental Plastic Elongation method in calculating aluminum and steel core component stresses for initial installation of Drake ACSR at 20%RTS and 15°C.

From the component stress-strain curves shown in Figure 30, the initial component tensions in the aluminum and steel core can be seen at the points marked “C” (31 MPa) and “D” (29 MPa), respectively. Even though during the initial loading process, the aluminum layers and the steel core are elongated equally, the strand settlement and deformation in the aluminum layers during initial sagging, permanently lengthens the aluminum strand layers but not the steel core. This can be seen by reducing the total conductor tension. The aluminum layer elongation decreases along the “final” stress-strain curve “AL-F” and the steel core elongation decreases along the same “ST” stress-strain curve which it followed initially (no plastic elongation of the steel core).

The composite conductor elongation decreases along the total curve “AL-F+ST” reaching a composite elongation of approximately -0.025% when the aluminum stress becomes zero. At this point, the composite conductor curve changes suddenly to that of the steel core alone (if we ignore the possibility of compressive forces in the aluminum layers).

If the Drake conductor, initially installed at a tension of 60 MPa, remains in place without high ice and wind loads for 10 years, the aluminum layers will elongate plastically due to metallurgical creep but the steel core will not. This is demonstrated in Figure 31.

The permanent creep elongation of the aluminum layers due to metallurgical creep over 10 years yields the following results:

- The composite conductor tension is reduced from 60 to approximately 49 MPa as may be seen by following the bare conductor catenary curve from A to A'.
- The composite conductor elongation increases from 0.045% to 0.065%.
- The aluminum layer tension is reduced from 31 to 17 MPa (B to B')
- The steel core tension increases from 29 MPa to 32 MPa even though the composite conductor tension decreases.

**486 mm<sup>2</sup> 26/7 Drake ACSR in 180 m span showing final component tensions after 10 years of creep at 15C**

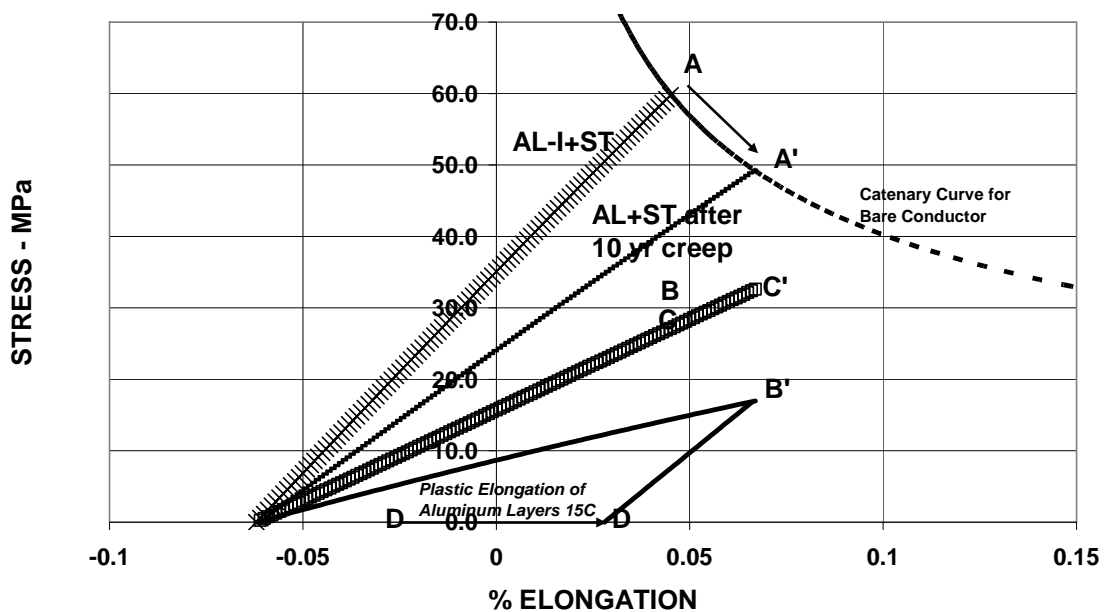


Figure 31 - Application of Experimental Plastic Elongation method in calculating aluminum and steel core component stresses after 10 years of creep elongation at 15°C for Drake ACSR initially installed at 20%RTS.

As is typical of creep in ACSR conductor, the plastic elongation of the aluminum layers yields an increase in the elastic elongation of the steel core.

### 6.3.3 Calculating Final sag-tension at high temperature with EPE model

Another advantage of EPE model becomes apparent at high conductor temperatures. Figure 32 illustrates how the experimental plastic elongation (EPE) conductor model allows one to calculate sag-tension at a high conductor temperature (100°C) accounting for permanent creep elongation of the aluminum layers over 10 years at 15°C .

**486 mm<sup>2</sup> 26/7 Drake ACSR in 180 m span showing tension at 100C after 10 years of creep at 15C.**

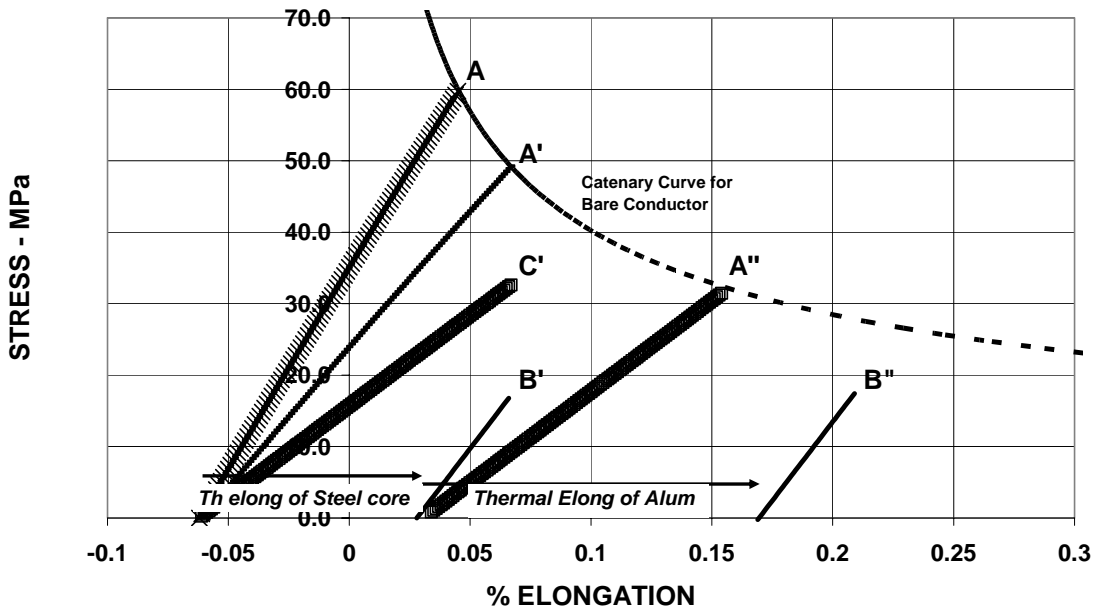


Figure 32 - Conductor Sag-tension calculation for high temperature after 10yr creep elongation at 15C.

The thermal elongation of the aluminium layers of the Drake ACSR (A1/S1A) conductor is twice as much as the steel core per degree increase in temperature. The zero-tension %elongation of the aluminum layers at 15°C (after 10 years of creep elongation) is 0.03%. It increases to 0.022% when the conductor temperature increases to 100°C. The zero-tension %elongation of the steel core at 15°C is -0.06%. It increases to +0.04% as the core temperature increases to 100°C. As a result of the difference in thermal elongation rate of the aluminum layers and the steel core, and the permanent creep elongation of the aluminum layers, the tension at 100°C is entirely in the steel core and any further increase in sag at higher temperatures occurs at the thermal elongation rate of the steel core alone.

For this ACSR conductor, in this span, the knee-point temperature is found to be 90°C. Thus under these final conditions, the ACSR conductor is supported entirely by the steel core at temperatures at 90°C. For ACSR conductors with a single layer of aluminum strands, the aluminum layers cannot support significant aluminum compression force at temperatures above the kneepoint but ACSR with multiple layers of aluminum wires can support some modest amount of compression. Thus with multiple aluminum layer ACSR, the compressive force in the aluminum layers increases the tension in the steel core causes more

The "kneepoint temperature" also depends upon the span length and upon the relative area of steel and aluminium in the A1/S1 conductor. Generally, as is shown in Table 14,



taken from Technical Brochure 244, the "kneepoint temperature" is lower for A1/S1 conductors with a high percentage of steel and for short spans.

Table 14 - "Knee-point temperatures" of A1/S1 (ACSR) as a function of stranding and span length determined by the Alcoa graphical method. All conductors have an aluminium strand area of 403 mm<sup>2</sup>.

A1/S1		Steel mm <sup>2</sup>	Span m	Kneepoint Temp [°C]	
Name	Stranding			No Alum Compression	20 MPa of Alum Compression
Tern	45/7	28	300	150	156
Condor	54/7	53	300	100	112
Drake	26/7	66	300	70	88
Mallard	30/7	92	300	32	52
Drake	26/7	66	450	74	100
Drake	26/7	66	300	70	88
Drake	26/7	66	200	55	71
Drake	26/7	66	100	42	50

Table 14 lists the kneepoint temperatures for these conductor spans under final conditions, that is, they include the plastic elongation of the aluminium strands that occurs as a result of tension loading over time. When first installed, the kneepoint temperatures are higher.

## 7.0 CONDUCTOR PARAMETER STUDIES

Clearly there is quite a range of sag-tension calculation methods in use in the industry. A detailed comparison of the three major ones is made in Section 6.4, using two different examples. But, perhaps, even more important than the method used are the differences in how a conductor's elastic, plastic, and thermal elongation are modeled.

In this section a sensitivity study of the different parameters involved in the calculation methods is carried out, in order to see how they affect final results. The study is based upon the case discussed earlier in this document: a 468 mm<sup>2</sup> conductor, 26/7 A1/S1 Drake, in a 300 m span, with an initial tension of 28.02 kN at 15° C. The method used in this example is the Load-Strain Method, but it can be proved that other methods would lead to similar results. In Table 15 there is a summary of sensitivities for the different calculation parameters.

Other factors, which may cause significant errors in calculated sag-tension values that are not considered here, include imperfect tension equalization in adjacent spans due to extremely high conductor temperatures or unequal ice loads, flexibility of strain structures, temperature difference between strands, and other factors such as those discussed in section 2.4.

### 7.1 Conductor Weight

As pointed out in Section 2.4, conductor weight usually exceeds the nominal value by 0.2% to 0.6%. Also, during the life of an overhead line, the conductor's mass can be greater due to tarnishing effects, humidity or pollution, which can lead to greater sags and tensions than expected.

However, this slight increase in weight normally does not significantly affect final sags due to its small quantity. In this example, an increase of 3% in the conductor weight has been considered, and sag increments at any temperature are not greater than 0.19 m (see Table 15). These increments are very constant with temperature. In general, for the same Ax/Sxy conductor the kneepoint temperature shifts upward as conductor weight increases.

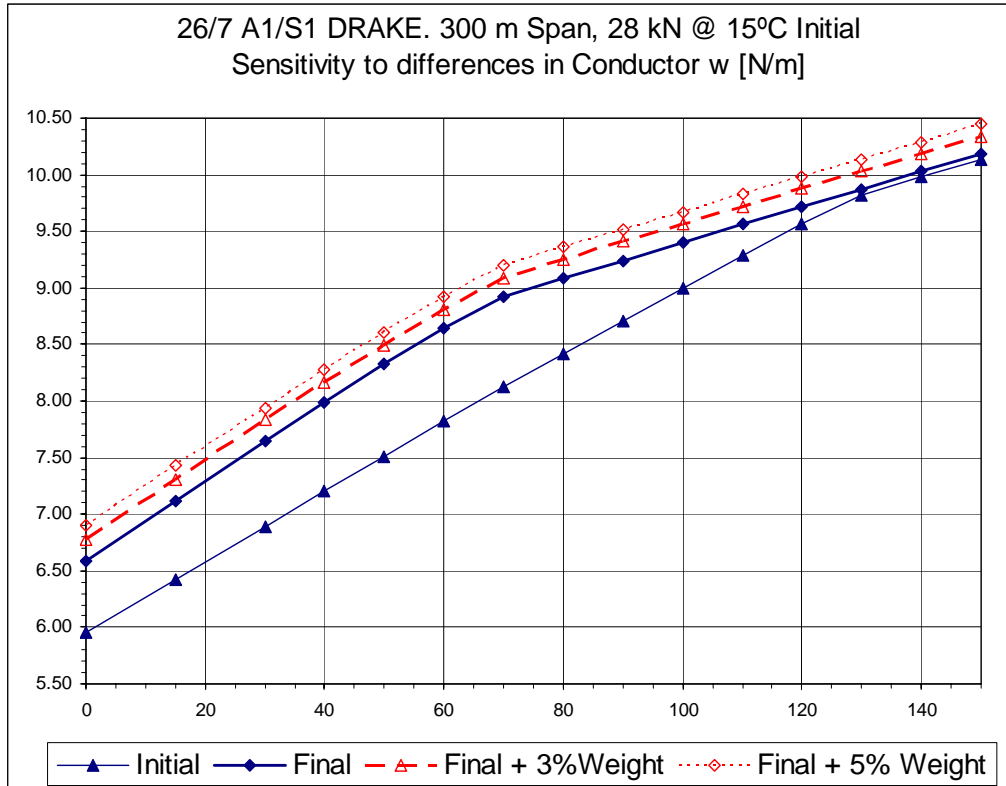


Figure 33 - Sensitivity of Sag-tension calculations to variation in conductor weight per unit length.

Tensions at low temperatures, which can have importance due to aeolian vibrations, are minimally affected. For this case, an increase of 3% in conductor weight produces an increment of only 0.1 kN on the final tension at 15°C.

In the improbable case that the weight of the conductor would increase considerably (say by 5%) the sags would also increase by 0.3m with respect to the nominal calculation values.

## 7.2 Elastic Elongation

All of the sag-tension calculation methods recognize that the stress-strain behavior of stranded conductors is essentially linear for short times and moderate stress levels once the conductor has been installed. This can be seen from the final curve of the load-strain method, whose slope is the final modulus of the conductor. But in reality the elastic modulus of the materials used for overhead conductors are a function of temperature and exact values are not always correct.

Variations of elastic modulus of either steel or aluminium change the final value of the conductor's coefficient of thermal expansion. Also, when considering composite conductors, variations in elasticity directly affects the kneepoint temperature, resulting in sag differences.

Nevertheless, variations in the conductor's elastic modulus do not greatly affect sag-tension values. For example, an increment of 10% of the value of both the aluminium and steel elastic modulus can cause a sag decrement of only 0.02m at 60°C, and 0.04m at 120°C.

At low temperatures, there are also no significant differences in tensions, so elastic modulus has minimal effect on aeolian vibration risks.

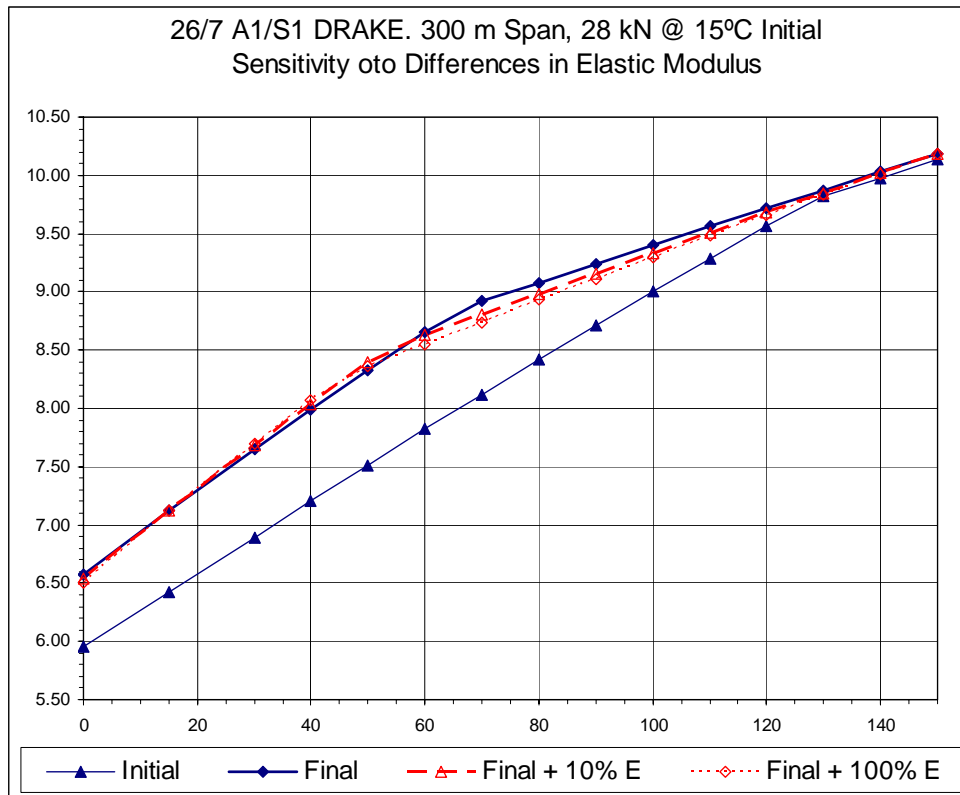


Figure 34 - Sensitivity of Sag-tension calculations to variation in conductor elastic modulus.

### 7.3 Plastic Elongation

The accurate determination of a conductor's plastic elongation, either due to long time periods at modest tension levels (creep) or short time periods at high stress (design loading), is very important with regard to maintaining adequate electrical clearances along the line during its lifetime. As described in Sections 5 and 6, Load-Strain and Strain Summation Methods use experimental data to model the long-term creep elongation in aluminium strands, and the plastic elongation due to high load events. Conversely, linear methods approximate these plastic elongations by general formulae or typical values, as described in IEC Technical Report 1597. For example, a typical value of 0.05 % is given for A1/Sxy conductors.

The different ways in which permanent plastic elongation is modeled may lead to significant differences in sag, even (or specially) at moderate temperatures. Additionally,

the conductor stress-strain model under high stress events has an influence on the maximum conductor tension transmitted to the towers. In order to simplify and evaluate only the value sensitivity, rather than the method, the creep and the permanent elongation due to high loads have been combined as plastic elongation, in the same way as the Linear Methods approximates these effects. Again, in this case the kneepoint temperature is significantly affected. As plastic elongation increases, the kneepoint temperature decreases, causing sag differences at low temperatures only, assuming no creep of the steel core. On the other hand, for homogeneous All Aluminium Conductors this is not an issue, but plastic elongation is much more critical.

The results for this example are shown in Table 15, where it can be seen that for moderate conductor temperatures the difference between considering a plastic elongation of 0.03% (equivalent temperature shift of approximately 20°C) or 0.05% (equivalent temperature shift of approximately 33°C) can cause a sag difference of about 0.44m. These differences come to zero above the kneepoint temperature. If we consider 0.06 % plastic elongation (equivalent temperature shift of approximately 40°C), the sag difference can reach 0.72m at 15°C.

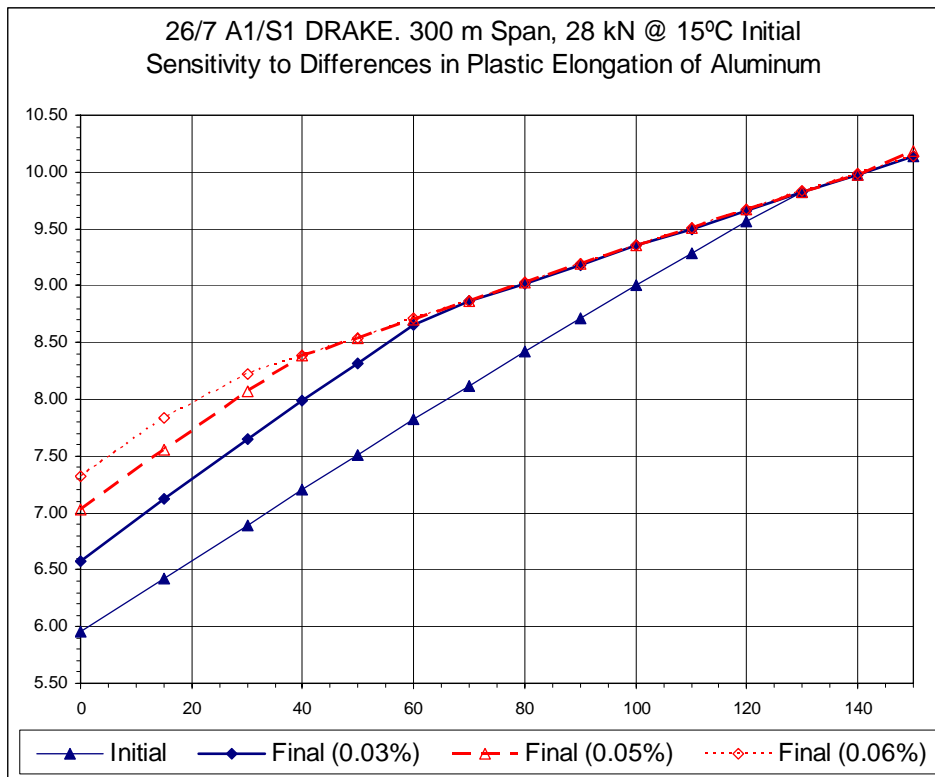


Figure 35 - Sensitivity of Sag-tension calculations to variation in plastic elongation of Aluminum.

#### 7.4 Thermal elongation

As with plastic elongation, thermal elongation variations translate directly into sag clearance variations and can have an influence when determining sags at elevated operating temperatures. On the other hand, thermal contraction at low temperature affects the tension attained during periods when aeolian vibration is most damaging.

Although most calculation methods assume that the coefficient of thermal expansion is constant, in reality it is a function of the stress and the elastic modulus [29]. The values used for aluminium and steel strands are usually  $23 \cdot 10^{-6}$  and  $11.5 \cdot 10^{-6}$  per  $^{\circ}\text{C}$ , respectively, and the composite coefficient is determined as described in Section 5.2.

The variations in coefficient of thermal expansion can cause relevant changes in calculated sags at elevated temperatures. An increase of 10% of both aluminium and steel thermal expansion coefficients (i.e. an increase in 10% of composite coefficient) causes an increase in sag of 0.18m at  $90^{\circ}\text{C}$  and 0.22m at  $120^{\circ}\text{C}$ . This sag variation can reach 0.56m at  $120^{\circ}\text{C}$  for an increase of 30% of both aluminium and steel thermal expansion coefficients.

It can be noted in this case again that the knee-point temperature decreases as thermal expansion coefficient increases.

For low temperatures, increments of thermal expansion coefficient cause decrements of sag and increments of tension. For a 10% increment of both aluminium and steel thermal expansion coefficients we obtain a tension increment of 0.22kN at  $0^{\circ}\text{C}$  and for a 30% increment we obtain a tension increment of 0.67kN at  $0^{\circ}\text{C}$ .

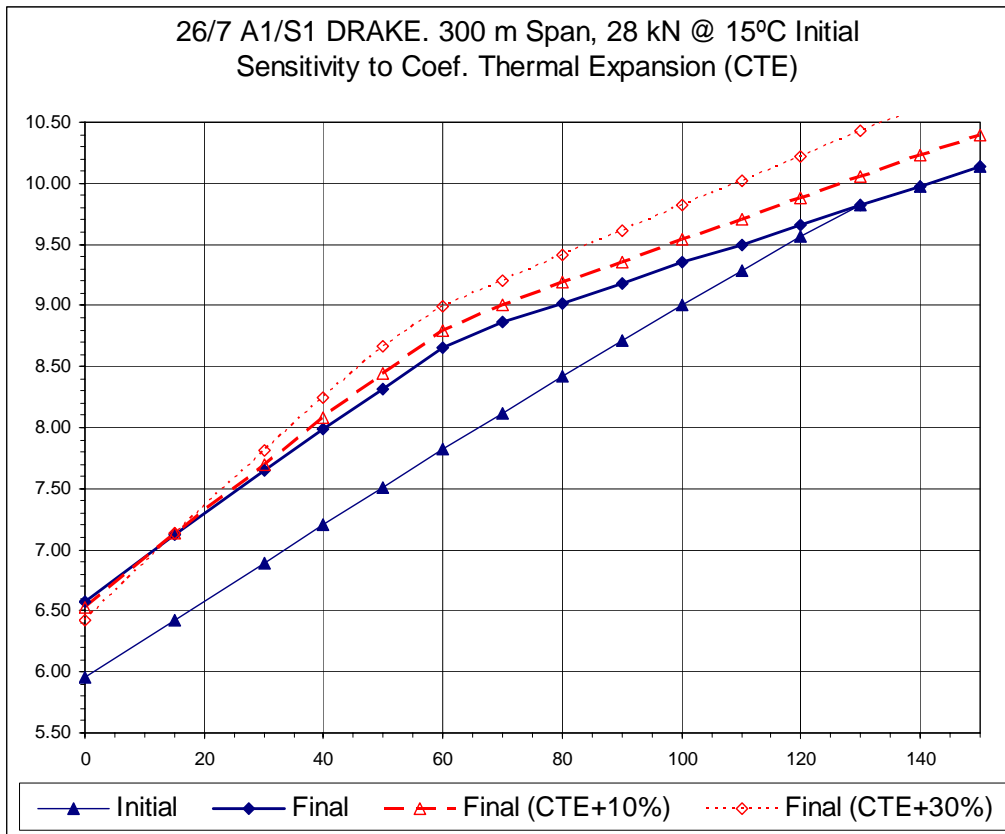


Figure 36 - Sensitivity of Sag-tension calculations to variation in thermal elongation rate.

Table 15 shows some values, demonstrating some of the sensitivity of the different parameters involved in the sag-tension calculation in the example case given in section 2.1.

Table 15 - Table of Basic Sag-tension Sensitivities

26/7 A1/S1 DRAKE. 300 m Span. 28,02 kN @ 15°C Initial				
Sag in m				
	15°C	60°C	90°C	120°C
Initial Condition	6.42	7.82	8.71	9.57
Final Condition (0.03% plastic elongation)	7.12	8.65	9.24	9.72
Sag variation (in m) with respect to Final Condition (0.03% plastic elongation)				
	15°C	60°C	90°C	120°C
3% Increment in Conductor Weight	+0.19	+0.16	+0.17	+0.16
5% Increment in Conductor Weight	+0.31	+0.27	+0.28	+0.26
10% Increment in Elastic Modulus	+0.00	-0.02	-0.08	-0.04
100% Increment in Elastic Modulus	+0.00	-0.10	-0.13	-0.06
Consider 0.05% Plastic Elongation	+0.44	+0.05	+0.01	+0.01
Consider 0.06% Plastic Elongation	+0.72	+0.06	+0.01	+0.01
10% Increment in Thermal Coefficient	+0.00	+0.15	+0.18	+0.22
30% Increment in Thermal Coefficient	+0.00	+0.34	+0.43	+0.56

### 7.5 Errors at elevated temperature

As with plastic elongation, thermal elongation errors translate directly into sag clearance errors and can have an important influence on the public safety. Given the increasing tendency to operate transmission lines close to their thermal limits, there is a genuine concern that minimum electrical clearances may not be adequately maintained.

Technical Brochure 244 contains a thorough discussion of the various sources of sag error at high temperature. Table 2 from that brochure summarizes the most important sources of sag error at high temperature:

Table 16 - Various high temperature sag errors.

#### Typical error magnitudes in high temperature sag calculations

	<u>ACSR Drake</u>	<u>ACSR Condor</u>	<u>ACSR Tern</u>
Aluminium area (strands)	403 mm <sup>2</sup> (26)	403 mm <sup>2</sup> (54)	403 mm <sup>2</sup> (45)
Steel area (strands)	66 mm <sup>2</sup> (7)	53 mm <sup>2</sup> (7)	28 mm <sup>2</sup> (7)
Final tension at 20°C	25 800 N	23 150 N	19 100 N
Equivalent span length	250 m	250 m	250 m
Sag at 20°C	4.84 m	5.06 m	5.36 m

#### Effect of calculation methods on final 120 °C sag:

Calculation assuming constant modulus	7.76 m	7.78 m	8.53 m
Graphical method with no Al compression	7.00 m	7.53 m	8.53 m
Graphical method with typical 20 MPa maximum compression	7.32 m	7.73 m	8.53 m

Additional sag errors at 120 °C :

Temperature difference core/surface	+0.03 m	+0.05 m	+0.06 m
Change of elastic modulus vs. temperature	+0.15 m	+0.11 m	+0.06 m
High temperature creep	0	0	+0.50 m
Multiple span effects	+0.6 to -1.0	+0.5 to -0.9 m	+0.5 to -0.8 m
Effect of core magnetization losses	0	+ 0.07 m	+0.05 m
Effect of manufacturing temperature	+/- 0.14	+/- 0.12	0

Table 16 lists the sag errors produced by different knee-point assumptions. It also includes estimates of sag errors due to other relatively "minor" sources of calculation error including consideration of radial temperature differences between the steel core and outside of the conductor, changes in elastic modulus with temperature, non-ideal ruling span effects, etc. Note that the errors due to non-ideal ruling span effects are generally larger than those due to the other factors. Sags are usually greater than predicted in the shortest spans and less than predicted for relatively long spans.

### **7.6 Thermal elongation at low temperature.**

Thermal contraction at low temperature affects the tension attained during periods when aeolian vibration is most damaging. Sag-tension calculation errors are unlikely to be large enough to be important in estimating aeolian vibration levels given the variation and uncertainty in other factors such as terrain and air temperature.



## 8.0 References

Documents listed in the Reference Section are specifically referred to in the brochure.

- 
- 1 IEC 1089, "Round wire concentric lay overhead electrical stranded conductors", First Edition, 1991.
  - 2 IEC 1597, "Overhead electrical conductors – Calculation methods for stranded bare conductors", First Edition, 1995.
  - 3 Aluminum Association, "Aluminium Electrical Conductor Handbook", Second Edition 1982, New York.
  - 4 Barrett, JS, Dutta S., and Nigol, O., "A New Computer Model of A1/S1A (ACSR) Conductors", IEEE Trans., Vol. PAS-102, No. 3, March 1983, pp 614-621.
  - 5 Dwight H.B., "Sag Calculations for Transmission Lines", AIEE Transactions, May, 1926, pp.796-805.
  - 6 Ehrenburg, D.O., "Transmission Line Catenary Calculations," AIEE Paper, Committee on Power Transmission & Distribution, July 1935.
  - 7 Lummis J., Ficher H.D., "Practical application of sag and tension calculations to transmission line design", AIEE Transactions, paper 54-501
  - 8 Martin J.S., "Sag calculations by the use of Martin's Table" (book), Copperweld Steel Co., Pa, 1031
  - 9 Southwire Company, Overhead Conductor Manual, 1994.
  - 10 IEEE Subcommittee 15.11, "IEEE Guide to the Installation of Overhead Transmission Line Conductors," IEEE Standard 524-1993, Published by IEEE, New York, NY.
  - 11 Thayer, E.S., "Computing tensions in transmission lines", Electrical World, Vol.84, no.2, July 12, 1924
  - 12 Healy, E.S., Wright, A.J., "Unbalanced conductor tensions", AIEE Transactions, Sept. 1926, pp.1064-1070
  - 13 IEEE Subcommittee 15.11, "Limitations of the Ruling Span Method for Overhead Line Conductors at High Operating Temperatures". Report of IEEE WG on Thermal Aspects of Conductors, IEEE WPM 1998, Tampa, FL, Feb. 3, 1998
  - 14 CIGRE SC22/WG11.04 "Safe design tension with respect to aeolian vibrations. - Part I: Single unprotected conductors", ELECTRA, no.186, October 1999, pp. 53-87.

- 15 CIGRE SC22/WG11.04 "Safe design tensions with respect to aeolian vibrations. – Part II: – Damped single conductors with dampers" *Electra* Vol 198, Oct 2001.
- 16 CIGRE SCB2/WG 11.04 "Overhead conductor safe design tension with respect to aeolian vibrations" with Part III: "Bundled conductor lines", *ELECTRA*, no.220, June 2005, pp 48-59. Technical Brochure No. 273, 2005.
- 17 Varney T., Aluminium Company of America, "Graphic Method for Sag Tension Calculations for A1/S1A (ACSR) and Other Conductors.", Pittsburg, 1927
- 18 Aluminium Association, "Stress-Strain-Creep Curves for Aluminium Overhead Electrical Conductors," Published 7/15/74.
- 19 Rawlins, C.B., "Some Effects of Mill Practice on the Stress-Strain Behavior of ACSR", IEEE WPM 1998, Tampa, FL, Feb. 1998.
- 20 Barrett, JS, and Nigol, O., "Characteristics of A1/S1A (ACSR) Conductors as High Temperatures and Stresses", IEEE Trans., Vol. PAS-100, No. 2, February 1981, pp 485-493
- 21 Harvey, JR and Larson RE. "Use of Elevated Temperature Creep Data in Sag-Tension Calculations". IEEE Trans., Vol. PAS-89, No. 3, pp. 380-386, March 1970
- 22 Harvey, JR and Larson, RE. "Creep Equations of Conductors for Sag-Tension Calculations". IEEE Paper C72 190-2
- 23 Harvey, JR. Creep of Transmission Line Conductors. IEEE Trans., Vol. PAS-88, No. 4, pp. 281-285, April 1969
- 24 CIGRE WG 22.05, "A Practical Method of Conductor Creep Determination" *Electra*, No. 24, pp. 105-137, October 1972.
- 25 CIGRE WG 22.05 (12), "Permanent Elongation of Conductors. Predictor Equations and Evaluation Methods", *Electra*, No. 75, pp. 63-98, March 1981.
- 26 Aluminium Association, "A Method of Stress-Strain Testing of Aluminium Conductor and ACSR" and "A Test Method for Determining the Long Time Tensile Creep of Aluminium Conductors in Overhead Lines", January, 1999, The Aluminium Association, Washington, DC 20006, USA.
- 27 IEC 61395, "Overhead electrical conductors – Creep test procedures for stranded conductors", First Edition, 1998.